AWARD NUMBER: W81XWH-17-1-0168

TITLE: Development of a New, More Effective Live-Attenuated Influenza Vaccine: An Essential Platform for Future Pandemic Protection

PRINCIPAL INVESTIGATOR: Stephen Dewhurst, PhD

CONTRACTING ORGANIZATION: University of Rochester

REPORT DATE: DECEMBER 2021

TYPE OF REPORT: Final Technical Report

PREPARED FOR: U.S. Army Medical Research and Development Command
Fort Detrick, Maryland 21702-5012

DISTRIBUTION STATEMENT: Approved for Public Release;
Distribution Unlimited

The views, opinions and/or findings contained in this report are those of the author(s) and should not be construed as an official Department of the Army position, policy or decision unless so designated by other documentation.

REPORT DOCUMENTATION PAGE

Form Approved
OMB No. 0704-0188

Public reporting burden for this collection of information is estimated to average 1 hour per response, including the time for reviewing instructions, searching existing data sources, gathering and maintaining the data needed, and completing and reviewing this collection of information. Send comments regarding this burden estimate or any other aspect of this collection of information, including suggestions for reducing this burden to Department of Defense, Washington Headquarters Services, Directorate for Information Operations and Reports (0704-0188), 1215 Jefferson Davis Highway, Suite 1204, Arlington, VA 22202-4302. Respondents should be aware that notwithstanding any other provision of law, no person shall be subject to any penalty for failing to comply with a collection of information if it does not display a currently valid OMB control number. **PLEASE DO NOT RETURN YOUR FORM TO THE ABOVE ADDRESS.**

1. REPORT DATE	2. REPORT TYPE	3. DATES COVERED
DECEMBER 2021	Final Report	1 Sep 2017 – 31 Aug 2021

4. TITLE AND SUBTITLE

Development of a New, More Effective Live-Attenuated Influenza Vaccine: An Essential Platform for Future Pandemic Protection

5a. CONTRACT NUMBER
W81XWH-17-1-0168

5b. GRANT NUMBER

5c. PROGRAM ELEMENT NUMBER

6. AUTHOR(S)
Stephen Dewhurst, PhD

E-Mail: Stephen_Dewhurst@urmc.rochester.edu

5d. PROJECT NUMBER

5e. TASK NUMBER

5f. WORK UNIT NUMBER

7. PERFORMING ORGANIZATION NAME(S) AND ADDRESS(ES)
University of Rochester, 601 Elmwood Ave, Rochester NY 14642-0001

Icahn School of Medicine at Mt. Sinai, 1 Gustave L. Levy Pl, New York, NY 10029

Texas Biomedical Research Institute, 8715 W. Military Dr, San Antonio, TX 78227

Emory University, 1648 Pierce Dr NE, Atlanta, GA 30307

8. PERFORMING ORGANIZATION REPORT NUMBER

9. SPONSORING / MONITORING AGENCY NAME(S) AND ADDRESS(ES)

U.S. Army Medical Research and Development Command
Fort Detrick, Maryland 21702-5012

10. SPONSOR/MONITOR'S ACRONYM(S)

11. SPONSOR/MONITOR'S REPORT NUMBER(S)

12. DISTRIBUTION / AVAILABILITY STATEMENT

Approved for Public Release; Distribution Unlimited

13. SUPPLEMENTARY NOTES

14. ABSTRACT

Vaccination is the most cost-effective approach by which the spread of a pandemic influenza virus could be prevented, and severe disease reduced. However, current influenza vaccines have had poor efficacy. Thus, it is very important to develop a new and more effective live-attenuated influenza vaccine (LAIV). We hypothesize that by understanding the molecular basis for the temperature sensitive (ts) and attenuated (att) phenotypes of LAIV, it will be possible to develop a new, more effective live-attenuated influenza vaccine that leverages LAIV's superior ability to protect against infection by diverse influenza viruses. Our goal is to develop a new and improved LAIV that has enhanced safety and efficacy, due to (1) a greater temperature sensitivity than current LAIVs, resulting in viral replication only in the lower temperatures of the nasal cavity and extreme upper airway and (2) high levels of virus gene expression but poor replication – resulting in abundant protein expression (and immunogenicity) but minimal production of infectious progeny virus.

15. SUBJECT TERMS

Influenza, vaccine, pandemic, LAIV, live-attenuated, live-attenuated influenza vaccine

16. SECURITY CLASSIFICATION OF:			17. LIMITATION OF ABSTRACT	18. NUMBER OF PAGES	19a. NAME OF RESPONSIBLE PERSON
a. REPORT	b. ABSTRACT	c. THIS PAGE			USAMRDC
Unclassified	Unclassified	Unclassified	Unclassified	66	19b. TELEPHONE NUMBER *(include area code)*

Standard Form 298 (Rev. 8-98)
Prescribed by ANSI Std. Z39.18

TABLE OF CONTENTS

	Page
1. Introduction	4
2. Keywords	4
3. Accomplishments	4
4. Impact	22
5. Changes/Problems	22
6. Products	23
7. Participants & Other Collaborating Organizations	23
8. Special Reporting Requirements	32
9. Appendices	32

FINAL REPORT

PROPOSAL TITLE: Development of a New, More Effective Live-Attenuated Influenza Vaccine: An Essential Platform for Future Pandemic Protection

AWARD NUMBER: W81XWH-17-1-0168

PI: Stephen Dewhurst, Ph.D.

1. INTRODUCTION

Vaccination is the most cost-effective approach by which the spread of a pandemic influenza virus could be prevented, and severe disease reduced. However, current influenza vaccines have had poor efficacy. Thus, it is very important to develop a new and more effective live-attenuated influenza vaccine (LAIV). We hypothesize that by understanding the molecular basis for the temperature sensitive (ts) and attenuated (att) phenotypes of LAIV, it will be possible to develop a new, more effective live-attenuated influenza vaccine that leverages LAIV's superior ability to protect against infection by diverse influenza viruses. Our goal is to develop a new and improved LAIV that has enhanced safety and efficacy, due to (1) a greater temperature sensitivity than current LAIVs, resulting in viral replication only in the lower temperatures of the nasal cavity and extreme upper airway and (2) high levels of virus gene expression but poor replication – resulting in abundant protein expression (and immunogenicity) but minimal production of infectious progeny virus.

2. KEY WORDS

Influenza, vaccine, pandemic, LAIV, live-attenuated, live-attenuated influenza vaccine

3. ACCOMPLISHMENTS

3A: Major project goals

NC: Not completed

AIM/TASK	Timeline	Responsible Site	Status
SPECIFIC AIM 1 To identify the mechanisms by which the current LAIV mutations affect viral polymerase function			
Major Task 1 To study the effects of the LAIV mutations on the biochemical activity of the purified viral polymerase	Months		
Subtasks: Purification of polymerase proteins; Functional analysis of pol proteins	1-12	Emory	Completed
Milestone(s) Achieved: Identification of biochemical correlates of LAIV polymerase temperature sensitivity	12	Emory	Completed

Major Task 2 To study the effects of the LAIV mutations, both alone and in combination, on genomic replication versus transcription by the viral polymerase			
Subtasks: Construction of minigenome plasmids; Performance of cell-based minigenome assays	1-12	UR	Completed
Milestone(s) Achieved: Identification of LAIV mutations associated with increased temperature sensitivity in minigenome assays	12	UR	Completed
Major Task 3 To study the effects of the LAIV mutations, both alone and in combination, on intracellular trafficking of the viral polymerase			
Subtasks: Construction of viral mutants; Analysis of viral mutants	9-20	UR	NC; see below
Milestone(s) Achieved: Identification of LAIV mutations associated with temperature sensitive changes in nuclear/cytoplasmic trafficking of the viral polymerase	20	UR	NC. We de-prioritized studies on intracellular trafficking of the polymerase in favor of studies on the temperature sensitivity of viral replication (Task 4). Our rationale was that temperature sensitivity of replication is more predictive of attenuation and more directly on the critical path for vaccine discovery & development.
Major Task 4 To study the effects of the LAIV mutations, both alone and in combination, on the temperature sensitivity of viral replication			
Subtasks: Construction of viral mutants; Analysis of viral mutants	5-12	UR	Completed
Milestone(s) Achieved: Identification of LAIV mutations associated with temperature sensitive changes in virus replication	12	UR	Completed
SPECIFIC AIM 2 To identify the mechanisms by which other polymerase mutations associated with *ts* and *att* phenotypes affect viral polymerase function			
Major Task 5 To study the effects of the other polymerase mutations on the biochemical activity of the purified viral polymerase	Months		

Subtasks: Purification of polymerase proteins; Functional analysis of pol proteins	13-24	Emory	Completed
Milestone(s) Achieved: Identification of biochemical correlates of polymerase temperature sensitivity	24	Emory	Completed
Major Task 6 To study the effects of the other polymerase mutations, both alone and in combination, on genomic replication versus transcription by the viral polymerase			
Subtasks: Construction of minigenome plasmids; Performance of cell-based minigenome assays	13-24	UR	NC; see below
Milestone(s) Achieved: Identification of pol mutations associated with increased temperature sensitivity in minigenome assays	24	UR	NC. We de-prioritized studies on intracellular trafficking of the polymerase in favor of studies on the temperature sensitivity of viral replication (Task 4). Our rationale was that temperature sensitivity of replication is more predictive of attenuation and more directly on the critical path for vaccine discovery & development.
Major Task 7 To study the effects of the other polymerase mutations, both alone and in combination, on intracellular trafficking of the viral polymerase			
Subtasks: Construction of viral mutants; Analysis of viral mutants	24-36	UR	NC; see below
Milestone(s) Achieved: Identification of pol mutations associated with temperature sensitive changes in nuclear/cytoplasmic trafficking of the viral polymerase	36	UR	NC. We de-prioritized studies on intracellular trafficking of the polymerase in favor of studies on the temperature sensitivity of viral replication (Task 4). Our rationale was that temperature sensitivity of replication is more predictive of attenuation and more directly on the critical path for vaccine discovery & development.
Major Task 8 To study the effects of the other polymerase mutations, both alone and in combination, on the temperature sensitivity of viral replication			
Subtasks: Construction of viral mutants; Analysis of viral mutants	13-20	UR	Completed

Milestone(s) Achieved: Identification of pol mutations associated with temperature sensitive changes in virus replication	20	UR	Completed
SPECIFIC AIM 3 To evaluate the in vivo replicative capacity, safety and protective efficacy of novel LAIVs containing rationally designed combinations of mutations			
Major Task 9 To identify the relative contribution of LAIV mutations to viral attenuation in mice			
Local IACUC Approval	13	UR	Approval obtained
Subtasks: Assess viral virulence and replication in mice; Assess lung damage/pathology in infected mice	14-18	UR	Completed
Milestone(s) Achieved: Identification of novel LAIVs with greater *in vivo* attenuation than the unmodified U.S. and Russian LAIVs	18	UR	Completed
Major Task 10 To test whether enhanced LAIVs retain immunogenicity and protective efficacy in mice			
Local IACUC Approval	13	UR	Approval obtained
Subtask: Assess immunogenicity and protective efficacy of novel LAIVs in mice	19-24	UR	Completed
Milestone(s) Achieved: Identification of novel, enhanced LAIVs that retain immunogenicity and protective efficacy in mice	24	UR	Completed
Major Task 11 To confirm that mutations that enhance the safety of LAIV in mice also do so in a ferret model			
Local IACUC Approval	13	Mt Sinai	Approval obtained
Subtasks: Analysis of virus replication and histopathology; Analysis of pulmonary safety; immunization/challenge studies	15-36	Mt Sinai	Completed
Milestone(s) Achieved: Identification of new and more effective LAIVs for future development as candidate universal influenza vaccines.	36	Mt Sinai	Completed

3A. What was accomplished under these goals?

3A1. Contribution of mutations in the American and Russian live-attenuated influenza vaccine in virus attenuation, immunogenicity and protection efficacy.

Summary

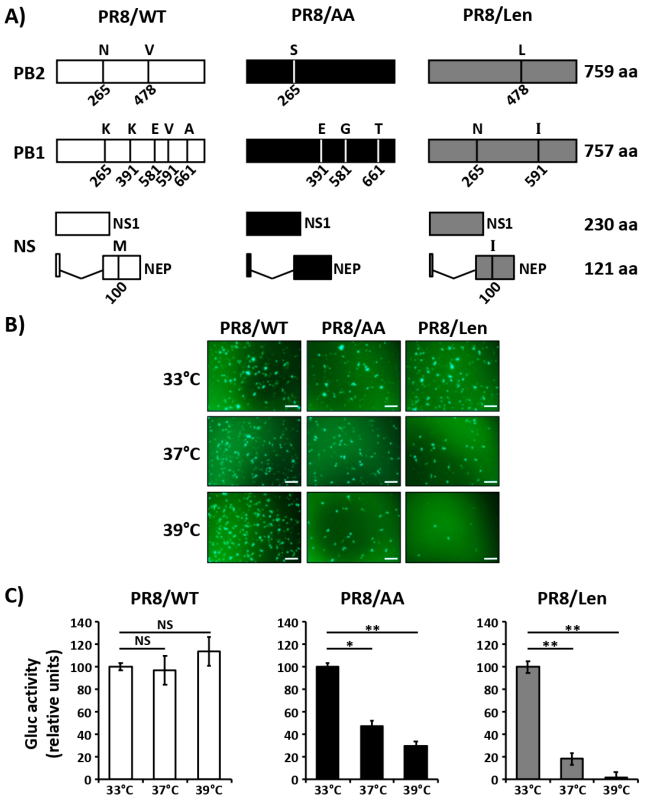
Influenza viruses cause annual, seasonal infection across the globe. Vaccination represents the most effective strategy to prevent such infections and/or to reduce viral disease. Two major types of influenza vaccines are

approved for human use: inactivated influenza vaccines (IIVs) and live attenuated influenza vaccines (LAIVs). Two Master Donor Virus (MDV) backbones have been used to create LAIVs against influenza A virus (IAV): the United States (US) A/Ann Arbor/6/60 (AA) and the Russian A/Leningrad/134/17/57 (Len) H2N2 viruses. The mutations responsible for the temperature sensitive (ts), cold-adapted (ca) and attenuated (att) phenotypes of the two MDVs have been previously identified and genetically mapped. However, a direct comparison of the contribution of these residues to viral attenuation, immunogenicity and protection efficacy has not been conducted. Here, we compared the *in vitro* and *in vivo* phenotype of recombinant influenza A/Puerto Rico/8/34 H1N1 (PR8) viruses containing the *ts, ca* and *att* mutations of the US (PR8/AA) and the Russian (PR8/Len) MDVs. Our results show that PR8/Len is more attenuated *in vivo* than PR8/AA, although both viruses induced similar levels of humoral and cellular responses, and protection against homologous and heterologous viral challenges. Our findings support the feasibility of using a different virus backbone as MDV for the development of improved LAIVs for the prevention of IAV infections, and of combining different mutations from the AA and Len LAIVs in order to produce a more effective LAIV.

Mutations of the US AA MDV and Russian Len MDV Confer Different Levels of Temperature Sensitivity to the Polymerase of PR8

To evaluate if the *ts, ca* and *att* mutations of the Russian Len MDV confer a temperature sensitive phenotype on the well studied influenza A virus, A/PR/8/34 (hereafter referred to as "PR8"), we introduced the amino acid substitutions into PR8′s PB2 (V478L), PB1 (K265N and V591I) and NEP (M100I) (**Figure 1A**) and tested them in a minigenome assay (**Figure 1B,C**). Green Fluorescence Protein (GFP) and Gaussia luciferase (Gluc) expression levels induced by PR8/WT polymerase were similar at the three temperatures assayed (33 °C, 37 °C and 39 °C). In the case of cells transfected with the PR8/AA polymerase complex, GFP and Gluc expression were reduced at 37 °C and, more notably, at 39 °C in comparison with the expression levels at 33 °C (~ 50% and ~ 70% reduction, respectively). Likewise, GFP and Gluc expression levels in cells transfected with the PR8/Len polymerase were highly reduced at 37 °C and almost undetectable at 39 °C as compared to the levels observed at 33 °C. These results demonstrate that the mutations of the Russian Len MDV induce a more robust temperature sensitive phenotype than the mutations of the US AA MDV in the context of the viral polymerase complex of PR8.

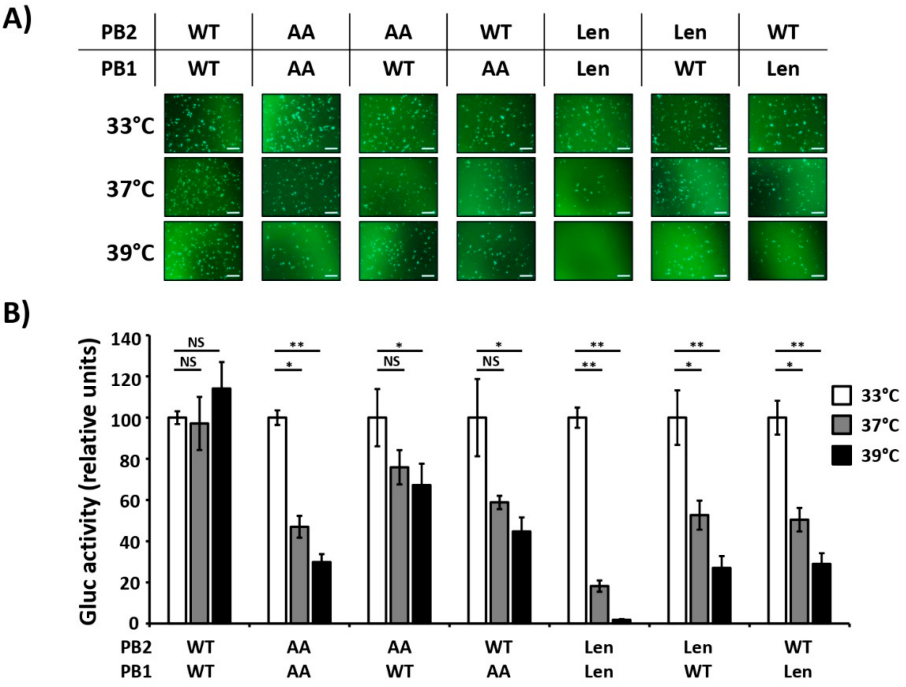
Figure 1. Effect of temperature on the polymerase activity of PR8/AA and PR8/Len.



LEGEND. (A) Schematic representation of segments 1 (PB2), 2 (PB1) and 8 (NS) of PR8/WT (white, left), PR8/AA (black, middle) and PR8/Len (grey, right). Amino acid substitutions to generate PR8/AA and PR8/Len are indicated. **(B-C)** Minigenome activity: HEK293T cells (12-well plate format, 4×10^5 cells/well, triplicates) were transiently co-transfected with 250 ng of ambisense pDZ expression plasmids encoding the minimal requirements for viral genome replication and gene transcription (PB2, PB1, PA, and NP) together with 500 ng of a vRNA-like expression plasmid encoding GFP (B) or Gluc (C) under the control of the human polymerase I promoter (hPol-I-GFP and -Gluc, respectively), and 100 ng of an SV40 Cluc expressing plasmid to normalize transfection efficiencies. After transfection, cells were placed at 33°C, 37 °C, or 39 °C, and viral replication and transcription was evaluated 24 h later by GFP (B) and luciferase (C) expression. Gluc activity was normalized to that of Cluc. Data represent means and SDs of the triplicates. Normalized reporter expression is relative to that obtained in the absence of pDZ NP. Data were represented as relative activity considering the activity of each polymerase complex at 33°C as 100%. *, $P < 0.05$; **, $P < 0.01$; NS, no statistical differences (Student t test). Scale bars, 200 μm.

Both of the commercial/licensed lineages of LAIV (AA and Len) have mutations in the PB2 and PB1 viral segments. Thus, we next evaluated which of the viral segments has a more significant impact on the temperature sensitive phenotype in PR8. Using the same minigenome approach and different combinations of PB2 and PB1 viral segments of PR8/WT, PR8/AA or PR8/Len, GFP (**Figure 2A**) and Gluc (**Figure 2B**) expression levels were evaluated. PR8/WT polymerase activity was similar at the three tested temperatures (33 °C, 37 °C and 39 °C), while reporter gene expression by PR8/AA and PR8/Len polymerase complexes was reduced at 37 °C and, more markedly, at 39 °C, similar to our initial minigenome studies (**Figure 1**). When PR8/AA PB2 or PB1 were combined with PR8/WT PB1 and PB2, respectively, we observed reduced GFP and Gluc expression levels at 37 °C and 39 °C as compared to those at 33 °C (**Figure 2A,B**). However, the AA PB1 mutations conferred a stronger ts phenotype effect than the AA PB2 mutations. In the case of PR8/Len, both the PB1 and PB2 segments induced a similar decrease in GFP and Gluc expression at 37 °C and 39 °C (**Figure 2A,B**). Remarkably, the combinations that contain only one of the viral segments (PB2 or PB1) with the LAIV mutations (AA or Len) had an accentuated *ts* phenotype in our minigenome assays. These results demonstrate that mutations in both PB2 and PB1 segments are responsible for the *ts* phenotype of AA and Len MDV and an additive effect in the polymerase activity at high temperatures is observed when both viral proteins (PB2 and PB1) have the aforementioned mutations.

Figure 2. Contribution of PB2 and PB1 mutations of PR8/AA and PR8/Len in the viral polymerase activity at different temperatures.



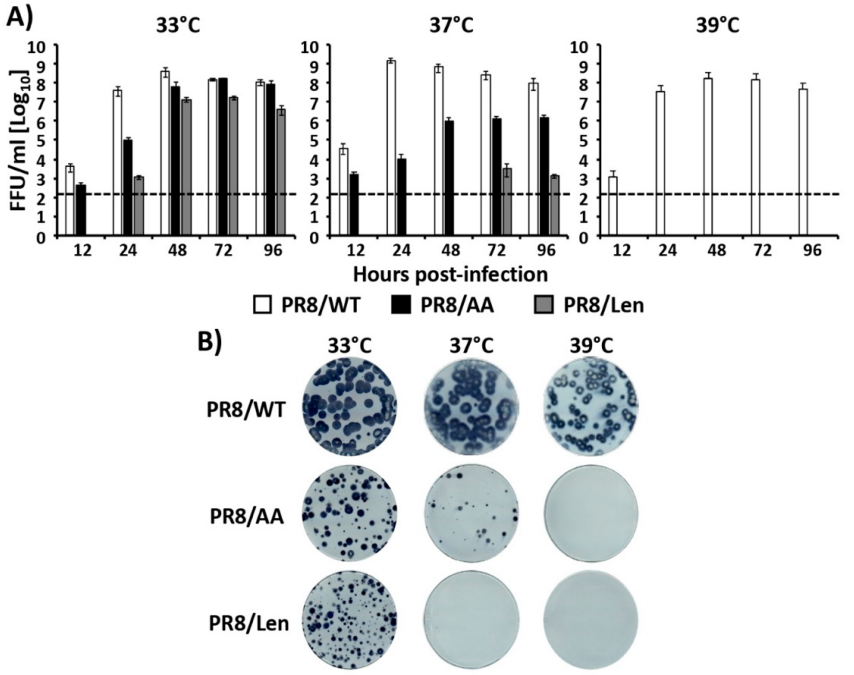
LEGEND. HEK293T cells (12-well plate format, 4×10^5 cells/well, triplicates) were transiently co-transfected with 250 ng of the indicated combinations of ambisense pDZ expression plasmids encoding the PB2 and PB1 from PR8/WT, PR8/AA and PR8/Len together with the pDZ encoding PA and NP PR8/WT proteins; together with 500 ng of the hPol-I-GFP (A) and -Gluc (B), and 100 ng of SV40 Cluc to normalize transfection efficiencies. After transfection, cells were placed at 33 °C, 37 °C, or 39 °C, and reporter gene expression was evaluated 24 h later by GFP imaging (A) and Gluc expression (B). Gluc activity was normalized to that of

Cluc. Data represent means and SDs of the triplicates. Normalized reporter expression is relative to that in the absence of pDZ NP plasmid. Data were represented as relative activity considering the activity of each polymerase complex at 33 °C as 100%. *, P < 0.05; **, P < 0.01; NS, no statistical differences (Student t test). Scale bars, 200 μm.

Recombinant PR8/Len is More Temperature Sensitive than PR8/AA

Based on the minigenome results using transfected cells in which Len MDV mutations induced a stronger reduction in the PR8 polymerase activity at high temperatures (37 °C and 39 °C) than those induced by the AA MDV mutations (**Figure 1 and Figure 2**), we next evaluated the impact of the AA and Len MDV mutations in the context of PR8 viral infections. To that end, we used reverse genetics to rescue a PR8/Len virus and then evaluated and compared the viral replication kinetics (**Figure 3A**) and plaque phenotype (**Figure 3B**) of PR8/Len with those of PR8/WT and our previously described PR8/AA [35] at different temperatures (33 °C, 37 °C and 39 °C). At 33 °C, PR8/WT reached higher viral titers than PR8/AA and PR8/Len viruses at early times (12 h and 24 h) post-infection (p.i.), but at 72 h p.i. the three viruses reached similar viral titers (**Figure 3A**). Replication of PR8/WT at 37 °C and 39 °C was similar to that observed at 33 °C. However, PR8/AA replication was reduced at 37 °C, and abolished at 39 °C. In the case of PR8/Len, replication was only detected at the latest time p.i. (72 h) at 37 °C, and virus was not detected at 39 °C. Likewise, the plaque phenotype of PR8/WT was similar at 33 °C and 37 °C and slightly reduced at 39 °C (**Figure 3B**), in agreement with the results of the growth kinetic studies (**Figure 3A**). In the case of PR8/AA, both the number and the size of the plaques were reduced (37 °C), or not detected (39 °C), when compared to 33 °C. PR8/Len could only generate plaques at 33 °C, corroborating the growth kinetics results (**Figure 3A**). Taken together, these results demonstrate that the mutations of the Russian Len MDV induce a more clear temperature sensitive phenotype in the backbone of PR8 than the mutations of the US AA MDV.

Figure 3*. In vitro* characterization of PR8/AA and PR8/Len viruses

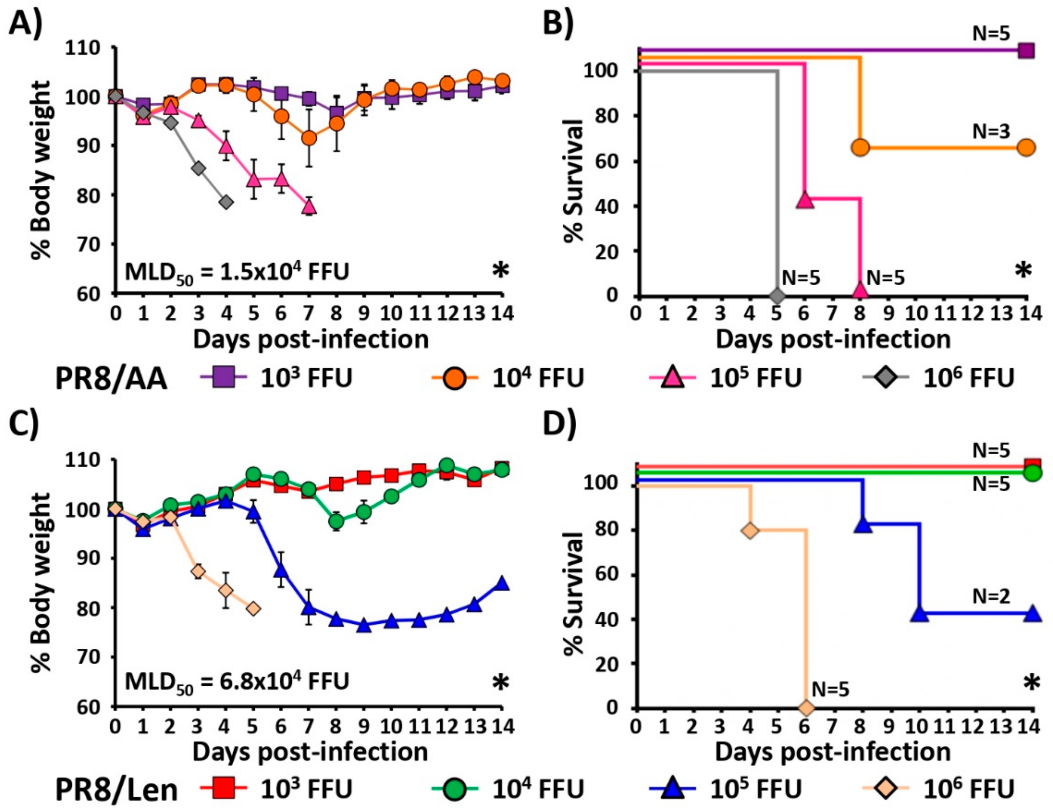


LEGEND. (A) Multicycle growth kinetics: MDCK cells (12-well plate format, 4×10^5 cells/well, triplicates) were infected at low MOI (0.001) with PR8/WT (white bars), PR8/AA (black bars) and PR8/Len (grey bars) viruses and placed at 33 °C, 37 °C, or 39 °C. Tissue culture supernatants were recovered at the indicated times post-infection (p.i.) and viral titers were determined by immunofocus assay (FFU/mL) using an anti-NP mAb (HB-65). Data represent the means and SDs of the results determined from triplicate wells. Dotted black lines indicate the limit of detection (200 FFU/mL). **(B)** Plaque assays: MDCK cells (6-well plate format, 1 × 106 cells/well) were infected with PR8/WT, PR8/AA or PR8/Len viruses and incubated at 33 °C, 37 °C, or 39 °C for 3 days. Plaque phenotype was assessed by immunostaining with the HB-65 anti-NP mAb.

Attenuation of PR8/Len and PR8/AA in a Mouse Model of Influenza Infection

In our next set of experiments, we compared the virulence of both PR8 LAIVs *in vivo* (**Figure 4**). To that end, groups of C57BL/6 mice (N = 5) were infected with 10^3, 10^4, 10^5 and 10^6 fluorescent forming units (FFU) of PR8/AA (**Figure 4A,B**) or PR8/Len (**Figure 4C,D**) and monitored over 14 days p.i. for body weight loss (Figure 4A,C) and survival (**Figure 4,D**). Mice infected with 10^5 and 10^6 FFU of PR8/AA showed a dramatic weight loss at early times p.i. (**Figure 4A**), resulting in a rate of mortality of 100% at days 5 and 8 p.i., respectively (**Figure 4B**). Two mice (40%) infected with 10^4 FFU of PR8/AA lost weight and died at day 8 p.i., while mice infected with 10^3 FFU of PR8/AA virus did not show noticeable weight loss and all of them survived infection, resulting in a theoretical 50% mouse lethal dose (MLD50) of ~1.5×10^4 FFU]. In the case of PR8/Len (**Figure 4C,D**), all mice infected with 10^6 FFU died at day 6 p.i., 40% of mice survived infection with 10^5 FFU and those infected with 10^4 and 10^3 FFU did not show body weight loss and all survived viral infection, resulting in a calculated MLD50 of ~6.8×10^4 FFU (i.e., ~5 fold greater attenuation than PR8/AA).

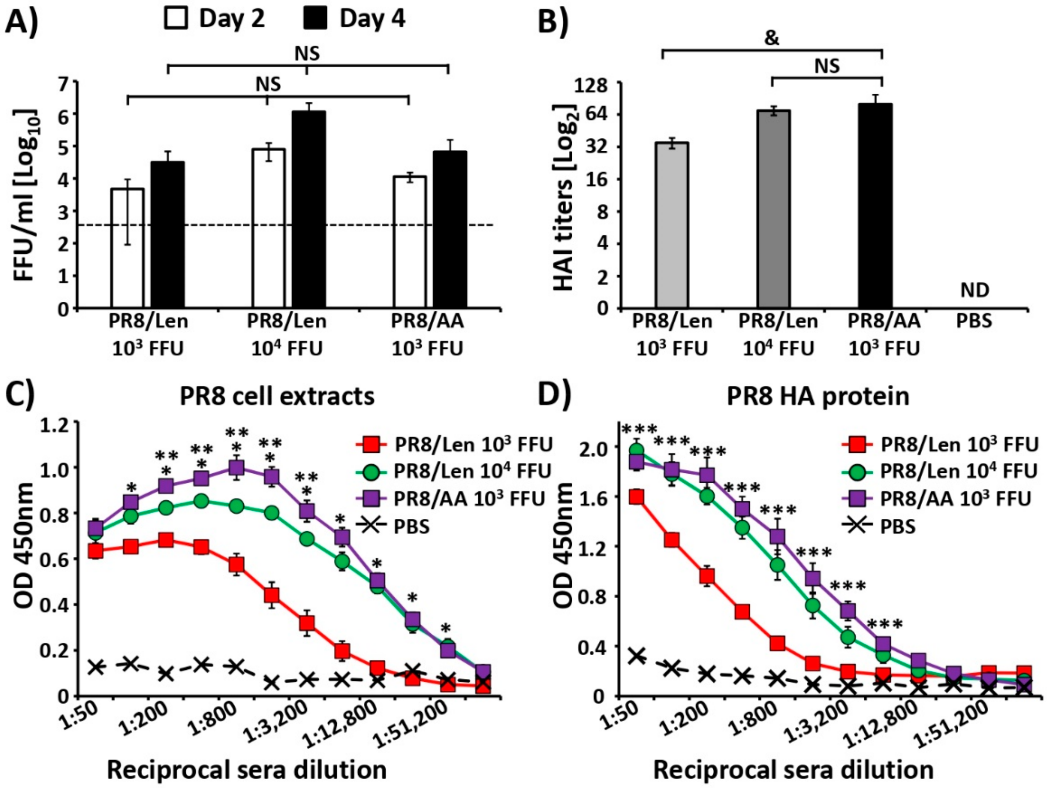
Figure 4. Attenuation of PR8/AA and PR8/Len viruses *in vivo*.



LEGEND. Six-to-8-week-old female C57BL/6 mice (n = 5) were infected intranasally (i.n.) with the indicated FFU of PR8/AA (A,B) or PR8/Len (C,D) viruses and then monitored daily for 2 weeks for body weight loss (**A,C**) and survival (**B,D**). Mice that lost 25% of their initial body weight were sacrificed. Data represent the means and SDs of the results determined for individual mice (n = 5). The viral 50% mouse lethal dose (MLD50) for PR8/AA and PR8/Len were calculated based on survival data using the method of Reed and Muench. (**A,C**) Statistical analysis was performed using one-way ANOVA test comparing % body weight loss between groups (* $P < 0.0001$). (**B,D**) Statistical analysis was performed using log-rank (Mantel-Cox) test (* $P < 0.0001$).

We also evaluated viral replication in the lungs of mice infected with PR8/Len and PR8/AA. To that end, groups of C57BL/6 mice (N = 6) were infected with 10^3 and 10^4 FFU of PR8/Len or 103 FFU of PR8/AA (doses that resulted in 100% survival, **Figure 4**) and viral replication was evaluated at days 2 (N = 3) and 4 (N = 3) p.i. (**Figure 5A**). No statistically significant differences were observed in lung viral titers in animals infected with PR8/Len or PR8/AA, although higher viral titers were detected in the lungs of mice infected with 10^4 FFU of PR8/Len.

Figure 5. Replication of PR8/AA and PR8/Len viruses in mice and induction of humoral immune responses.



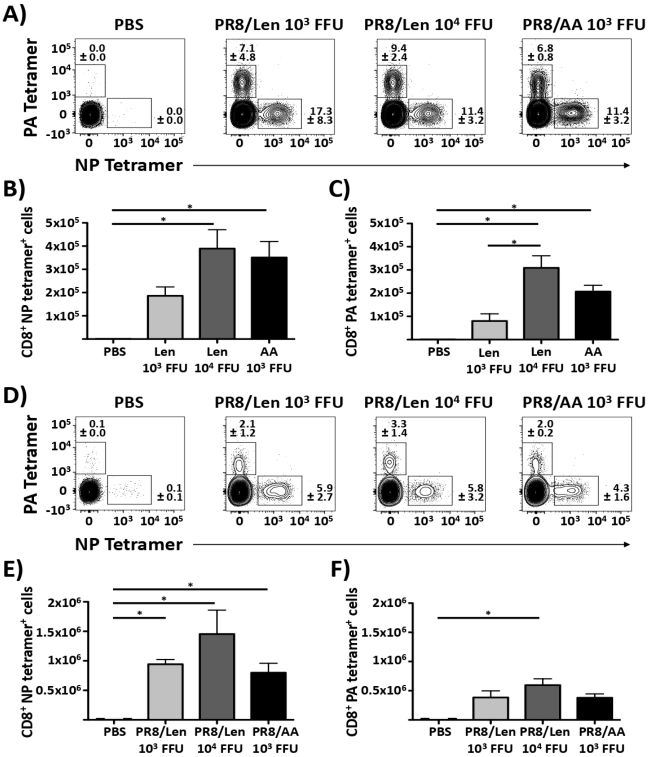
LEGEND. (A) Lung viral titers: Six-to-eight-week-old female C57BL/6 mice (n = 6) were infected i.n. with 10^3 and 10^4 FFU of PR8/Len and 103 FFU of PR8/AA viruses. Viral titer in lungs of infected mice was evaluated at days 2 and 4 p.i. (n = 3) by immunofocus assay (FFU/mL) in MDCK at 33 °C using an anti-NP mAb (HB-65). Data represent the means and SDs of the results determined from each group of mice (n = 3). Dotted black line represents the limit of detection of the assay (200 FFU/mL). NS, no statistical differences (Student t test). **(B–D)** Humoral immune responses: Six-to-eight-week-old female C57BL/6 mice (n = 5) were infected i.n. with 10^3 and 10^4 FFU of PR8/Len and 10^3 FFU of PR8/AA viruses, or mock-infected (PBS). At 14 days p.i., mice were bled and sera were collected and evaluated individually by HAI assay for hemagglutination inhibiting antibodies **(B)** and by ELISA for IgG Abs against total influenza viral proteins using cell extracts of MDCK cells infected with PR8/WT **(C)** or against recombinant purified PR8 HA protein **(D). (B)** HAI titers: ND, not detected. &, $p < 0.05$ (PR8/Len 10^3 FFU vs PR8/AA 10^4 FFU) (Student t test); NS, no statistical differences (Student t test). **(C,D)** ELISAs: OD, optical density. Data represent the means and SDs of the results for five individual mice. *, $p < 0.001$ (PR8/Len 10^3 FFU vs.PR8/AA 10^3 FFU); **, $p < 0.05$ (PR8/Len 10^4 FFU vs.PR8/AA 10^3 FFU); ***, $p < 0.01$ (PR8/Len 10^3 FFU vs.PR8/AA 10^3 FFU) (Student t test).

Immune Responses and Protection Efficacy of PR8/Len and PR8/AA in Mice against a Homologous Viral Challenge

We next evaluated and compared immune responses induced by PR8/Len and PR8/AA viruses (**Figure 5B,D**). Groups of C57BL/6 mice (N = 5) were immunized with the same non-lethal doses of PR8/Len (10^3/10^4 FFU) and PR8/AA (10^3 FFU) (Figure 4), or mock infected with PBS. Hemagglutination inhibition (HAI) assay results revealed a higher titer of hemagglutination inhibiting antibodies in mice vaccinated with 10^3 FFU of PR8/AA than those vaccinated with 10^3 FFU of PR8/Len, while no statistical differences were observed between the sera of mice immunized with 10^3 FFU of PR8/AA and 10^4 FFU of PR8/Len (**Figure 5B**). Humoral immune responses were also evaluated by ELISA using cell extracts from MDCK cells infected with PR8/WT virus (**Figure 5C**) or purified PR8 HA protein (**Figure 5D**). Sera from all virus-vaccinated mice showed antibodies against total PR8 viral proteins and against the viral HA (**Figure 5C,D**, respectively). Interestingly, sera from mice vaccinated with 10^3 FFU of PR8/AA showed a significantly higher titer of antibodies than sera from mice immunized with 10^3 FFU of PR8/Len, while comparable antibody responses were detected in the sera from mice immunized with 10^3 FFU of PR8/AA and 10^4 FFU of PR8/Len.

To have a more complete analysis of immune responses, we also evaluated and compared the induction of CD8 T cell responses by PR8/AA and PR8/Len (**Figure 6**). To that end, groups of C57BL/6 mice (N = 5) were immunized with 10^3 or 10^4 FFU of PR8/Len, 10^3 FFU PR8/AA, or mock-vaccinated (PBS). At 10 days p.i., lungs and spleens were recovered and processed to collect CD8 T cells. The results showed that vaccination with both PR8 LAIVs induced NP- and PA-specific CD8 T cells in the lungs (**Figure 6A,C**) and the spleen (**Figure 6D,F**). Although no statistical differences were observed when comparing the responses induced by PR8/Len versus PR8/AA (with the exception of the levels of PA-specific CD8 T cells in the lungs of mice vaccinated with 10^3 and 10^4 FFU of PR8/Len, **Figure 6C**), the number of CD8 T cells in the lungs and spleen tended to be greater after vaccination with 10^4 FFU of PR8/Len and 10^3 FFU of PR8/AA than with 10^3 FFU PR8/Len. These results suggest that vaccination with both LAIVs elicits a robust virus-specific CD8 T cell response in the spleen and lung.

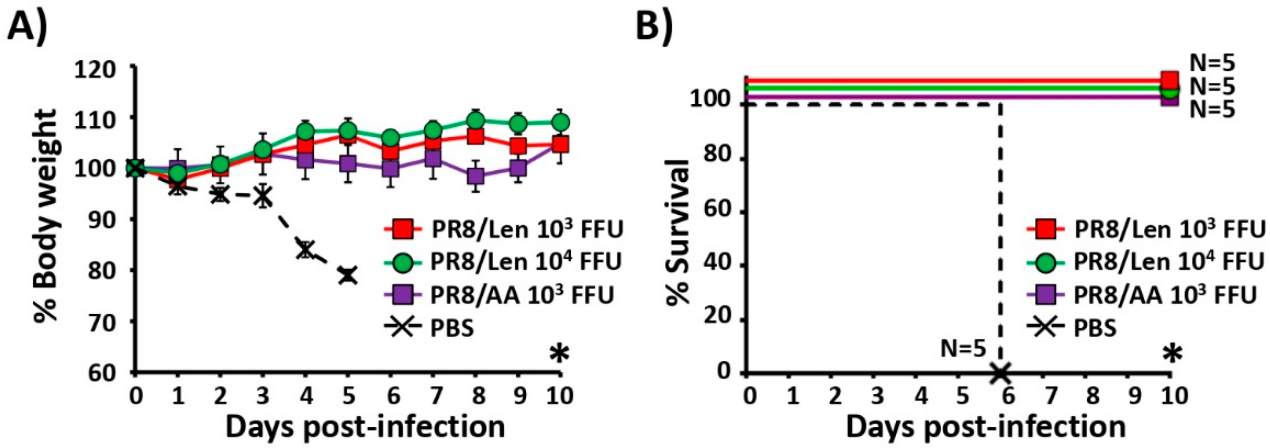
Figure 6. Induction of CD8 T cell responses by PR8/AA and PR8/Len viruses



LEGEND. Female six-to-eight-week-old C57BL/6 mice (n = 5) were infected (i.n.) with 10^3 and 10^4 FFU of PR8/Len and 10^3 FFU of PR8/AA viruses. Mice were also mock (PBS) infected as an internal control. Ten days p.i., lungs (**A–C**) and spleens (**D–F**) were collected and resident cells were prepared for flow cytometry. Live CD8 T cells specific for NP (**B,E**) or PA (**C,F**) tetramers were counted. Data represent the means +/– SDs of the results for 5 individual mice. *, $p < 0.001$ for the indicated pair wise comparisons (Student t test).

Having confirmed the immunogenicity of both LAIVs, we proceeded with challenge experiments, initially focusing on a homologous viral challenge (**Figure 7**). Groups of C57BL/6 mice (N = 5) were vaccinated with the same PR8 LAIVs doses used in the immunogenicity studies, or mock (PBS) vaccinated (**Figure 6**). At day 15 post-vaccination, mice were challenged with 1000× MLD50 of PR8/WT and monitored over 10 days for body weight loss (**Figure 7A**) and survival (**Figure 7B**). All mice mock vaccinated lost weight quickly and died at day 6 post-challenge. All mice vaccinated with PR8/Len (independently of the dose) and PR8/AA survived without body weight loss. These results indicate that although PR8/Len is more attenuated than PR8/AA (**Figure 4**), it is able to confer protection against a homologous PR8 viral challenge with the same viral dose (10^3 FFU). Since all mice survived the challenge with PR8/WT, we cannot conclude which one of the two LAIVs (PR8/AA or PR8/Len) is more protective.

Figure 7. Protection efficacy of PR8/AA and PR8/Len against homologous viral challenge

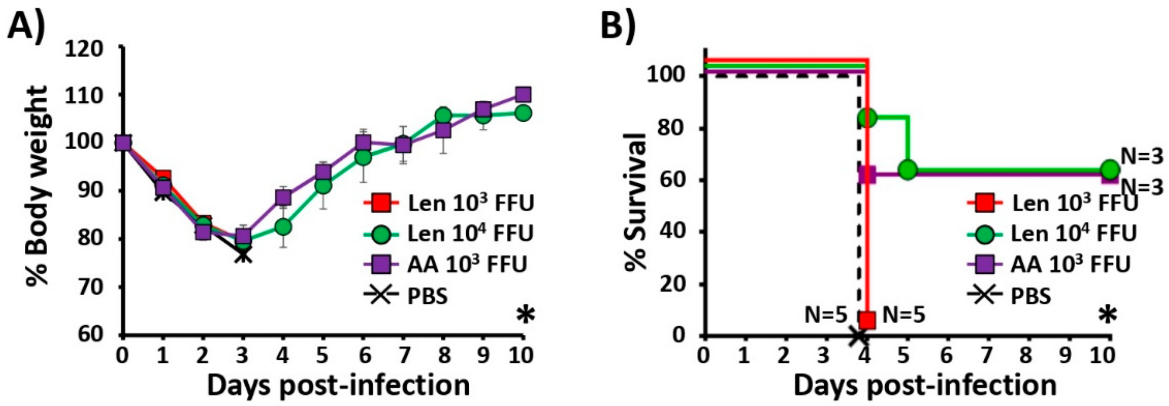


LEGEND. Six-to-eight-week-old female C57BL/6 mice (n = 5) were infected i.n. with 10^3 and 10^4 FFU of PR8/Len and 10^3 FFU of PR8/AA viruses, or mock vaccinated (PBS). At 15 days p.i., mice were challenged i.n. with 1,000 MLD50 of PR8/WT and monitored daily over 10 days for body weight loss **(A)** and survival **(B).** Mice that lost 25% of their initial body weight were sacrificed. Data represent the means and SDs of the results determined for individual mice (n = 5). Statistical analysis was performed using one-way ANOVA **(A)** and Dunnett's **(B)** tests comparing the PBS group to the other groups (* $P < 0.0001$).

Immune Responses and Protection Efficacy of PR8/Len and PR8/AA Against a Heterologous Viral Challenge

We next examined the humoral immune responses and the protection efficacy of PR8/Len and PR8/AA against a heterologous challenge with X31 (H3N2) (**Figure 8**). Groups of C57BL/6 mice (N = 5) were vaccinated with the same PR8/Len and PR8/AA viral doses used in the homologous challenge studies (**Figure 7**). Fourteen days post-vaccination, mice were bled and the presence of total antibodies against X31 were analyzed by ELISA. Sera from mice immunized with 10^3 FFU of PR8/AA showed significantly higher antibody titers than sera from mice vaccinated with 10^3 FFU of PR8/Len and, to a lower extent, than mice vaccinated with 10^4 FFU of PR8/Len. It is worth mentioning that X31 is a PR8 virus containing the HA and NA of A/Hong Kong/68 H3N2. Contrarily, the PR8 LAIVs (both AA and Len) contain their respective H1N1 glycoproteins and, therefore, the antibodies detected in the ELISA are mainly directed against internal PR8 viral proteins, which are the same in all viruses.

Figure 8. Protection efficacy induced by PR8/AA and PR8/Len against heterologous virus challenge.



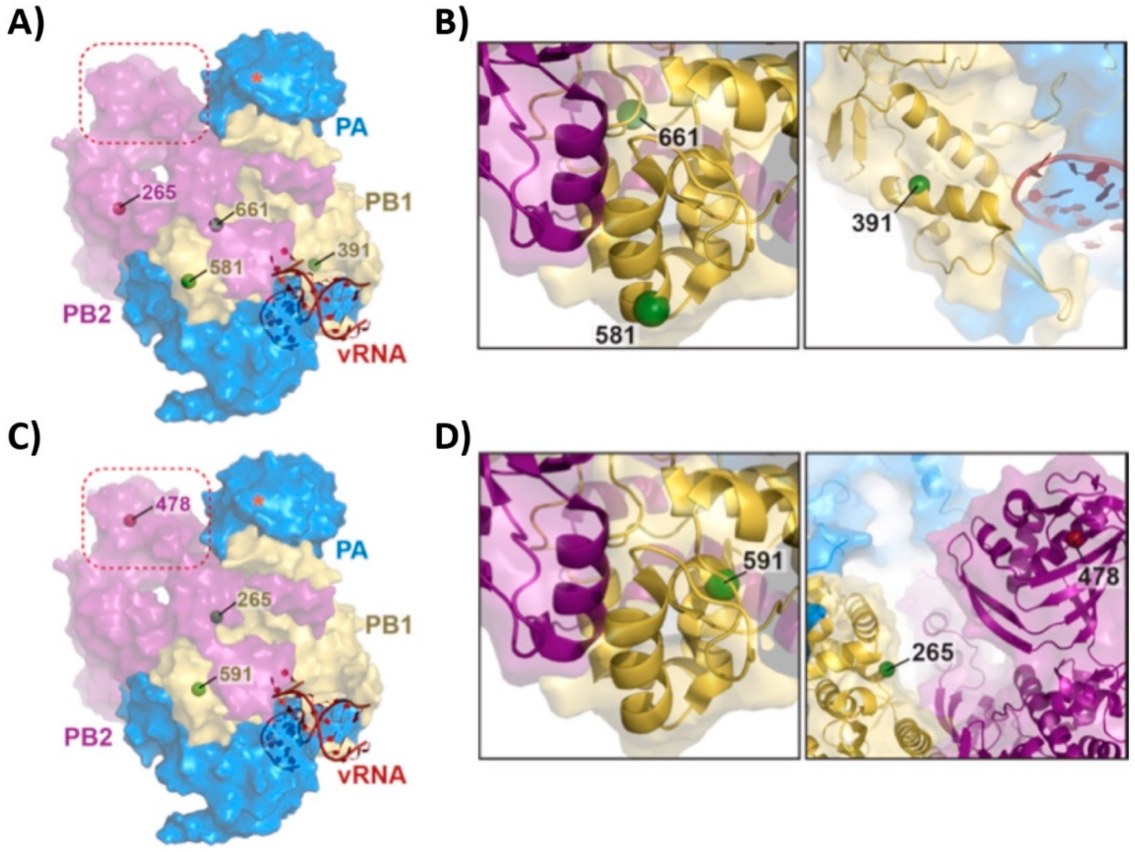
LEGEND. Six-to-eight-week-old female C57BL/6 mice (n = 5) were infected i.n. with 10^3 and 10^4 FFU of PR8/Len or 10^3 FFU of PR8/AA viruses, or mock-infected (PBS). At 15 days p.i., mice were challenged i.n. with 50 MLD50 of X-31 and then monitored daily over 10 days for body weight loss **(A)** and survival **(B).** Mice that lost 25% of their initial body weight were sacrificed. Data represent the means and SDs of the results determined for individual mice (n = 5). Statistical analysis was performed using one-way ANOVA **(A)** and Dunnett's **(B)** tests comparing the PBS group to the other groups (* P < 0.0001).

Then, fifteen days post-vaccination, mice were challenged with 50× MLD50 of X31 H3N2 and monitored daily over 10 days for body weight loss (**Figure 8A**) and survival (**Figure 8B**). Mock-vaccinated mice and mice vaccinated with 10^3 FFU of PR8/Len lost weight and all succumbed to viral challenge with X31 at day 4 post-challenge (**Figure 8A,B**). Mice vaccinated with 10^3 FFU of PR8/AA and 10^4 FFU of PR8/Len also lost weight (**Figure 8A**) but 60% of them (in both groups) recovered and survived the X31 lethal challenge (**Figure 8B**). These results indicate that, at the same dose, PR8/AA induces stronger immune responses and protection against a heterologous viral challenge than PR8/Len. However, induction of immune responses and protection efficacy with 10^4 FFU of PR8/Len is equivalent to that induced with 10^3 FFU of PR8/AA. Altogether, these results indicate that it is necessary to vaccinate mice with a higher dose (~1 log) of PR8/Len than PR8/AA to induce the same levels of protective immunity against a heterologous challenge.

Discussion and Conclusions

One mutation in PB2 (N265S), three substitutions in PB1 (K391E, E581G and A661T) and one amino acid change in NP (D34G) are the major contributors to the *ts, ca* and *att* phenotype of US AA MDV. Mutations located in the PB2 (V478L), PB1 (K265N and V591I) and in the NEP (M100I) are responsible for the *ts, ca* and *att* phenotype of the Russian Len MDV (**Figure 9**). Using a bat influenza A virus polymerase structure solved by X-ray crystallography as a reference model (PDB ID 5M3H), which is homologous to H1N1 virus polymerase complex with greater than 80% sequence similarity (PB2: 83%, PB1: 89% and PA: 83%), the location of these mutations are identified as distal from the endonuclease catalytic site of the PA subunit and appear rather random. However, upon closer inspection, we realize many of these mutations are at or near the interface between subunits, in particular, A661T mutation present in the PB1 from US AA MDV, and V591I and K265N mutations found in the PB1 from Russian Len MDV (**Figure 9B,D**, respectively). Therefore, we speculate that the mutations responsible for the ts, ca and att phenotype may relate to their effect on polymerase complex formation, possibly affecting the stability of the complex, rather than affecting the stability of each subunit itself. Of particular note, it is interesting to see the presence of a mutation within the cap-binding domain of PB2 subunit (V478L, **Figure 9C**), possibly affecting its cap-snatching activity to generate a 5′-capped primer for transcription initiation. This mutation is only found in the Russian Len MDV, and perhaps explains the difference seen in its attenuation when compared to that of US AA MDV. However, further experiments are necessary to elucidate the roles of the LAIV mutations and to gain a better mechanistic understanding of these attenuated LAIVs.

Figure 9. Location of the *ts, ca* and *att* mutations of AA and Len MDV in the viral polymerase complex



LEGEND. (A) PB1 (green spheres) and PB2 (purple sphere) mutations responsible for the *ts, ca* and *att* phenotype of AA are shown on the reference model of the RNA dependent RNA polymerase, RdRp, complex (PDB ID 5M3H). The RdRp complex is shown as a surface-rendering model with its subunits PA (blue), PB1 (yellow) and PB2 (purple), and bound vRNA (red). Dotted square (red) indicates the PB2 cap-binding domain. Red asterisk shows the approximate location of the endonuclease catalytic site of PA. **(B)** Close-up images of the locations of the AA PB1 mutations E581G and A661T (left) and K391E (right). **(C)** Same as in (A) but for Len. **(D)** Close up locations of LenV591I (PB1, left), K265N (PB1, right) and V478L (PB2, right) mutations. All images were generated and rendered in the program Pymol.

3A2. Temperature sensitivity of live attenuated Influenza A virus mutants is associated with a temperature-dependent reduction in functional activity and physical stability of the purified tripartite RNA-dependent RNA-polymerase complex

Summary

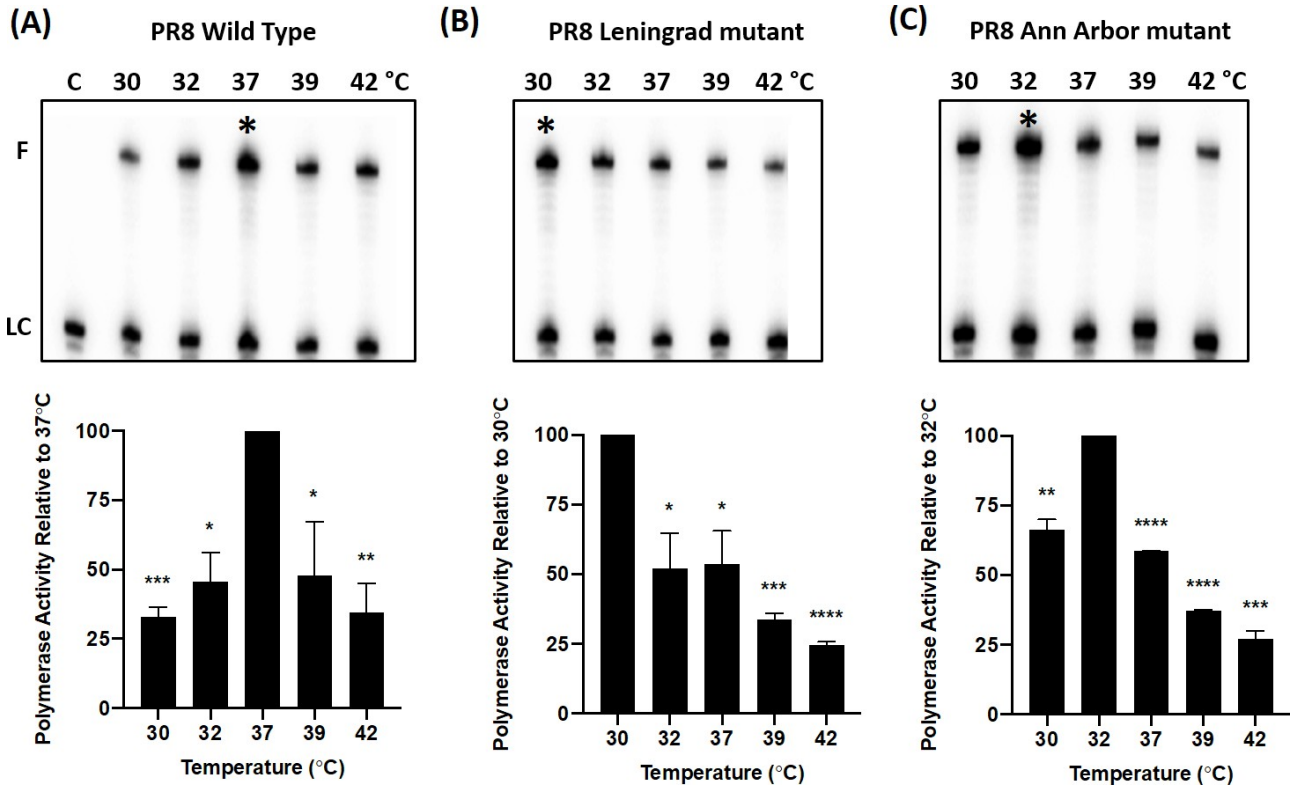
Live Attenuated Influenza Vaccines (LAIVs) are one of the currently FDA approved vaccines to prevent seasonal Influenza infection. Mutations in the Influenza RNA dependent RNA polymerase (RdRp) have been previously identified as being responsible for the temperature sensitive (ts) and attenuated (att) phenotypes of LAIV, but the effects of these mutations on the enzymatic function and physical stability of the tripartite RdRp complex are unclear. To address this question, we performed biochemical assays of the RNA-dependent RNA-polymerase activity of purified RdRp complexes corresponding to the wild type A/PR/8/34 virus (PR8) and two derivatives of this complex, containing the mutations present in the clinically used Ann Arbor (AA) and Leningrad (Len) LAIVs. Polymerase activity was compared across a range of physiologically relevant temperatures (30,32, 37, 39, 42^{o}C), and the wild-type PR8 RdRp complex was found to have maximal activity at 37^{o}C. In contrast, the two "LAIV" RdRp complexes had maximal activity at 32^{o}C (AA) or 30^{o}C (Len), and markedly lower activity at 37^{o}C – consistent with the ts phenotype of these two LAIVs. We also examined the physical stability of the RdRp complex across the same range of temperatures, by performing immunoprecipitation experiments using a PA-specific antibody. These experiments revealed that the quantity of co-immunoprecipated PB2 protein was temperature-dependent, being maximal at 37^{o}C for the wild-type PR8 complex, but maximal at 32^{o}C or 30^{o}C for the AA and Len "LAIV" RdRps, respectively - and markedly lower at 37^{o}C (again, consistent with the ts phenotype of these LAIVs). Collectively, these data suggest the temperature sensitive replicative phenotype of LAIVs may be due to a temperature-dependent reduction in the functional activity and physical stability of the viral RNA-dependent RNA-polymerase complex. These findings suggest a novel mechanism for LAIV attenuation and may present new strategies for LAIV design.

The Ann Arbor and Leningrad LAIV mutations confer a temperature sensitive phenotype on the polymerase activity of the purified influenza A virus RdRp complex

We purified recombinant RdRp complexes from insect cells infected with baculovirus vectors expressing PA, PB1 and PB2 proteins from the wild type A/Puerto Rico/8/34 H1N1 (PR8) virus, and from the "LAIV" mutants of PR8 (AA: PB1 K391E, E581G, A661T; PB2 N265S and Len: PB1 K265N, V591I; PB2 V478L) (12,13). We then used these RdRp complexes in ApG-primed RNA synthesis reactions at a range of physiologic relevant temperatures (30°C, 32°C, 37°C, 39°C, 42°C), in the presence of 500 μM of non-radioactive NTPs and 0.5 μM of the radioactive [α-32P] GTP. At the end of each reaction, a 30-nt RNA product was generated from the template, corresponding to the first 30 nucleotides from the 3' end of the PA gene (**Figure 10**).

As shown in **Fig. 10A**, the wild type (WT) PR8 polymerase complex generated maximal levels of the 30-nt full-length product (F) at 37°C. Densitometric analysis, with normalization to a 5'-end labelled 20-nt loading control RNA (LC), revealed that the activity of the WT polymerase was reduced at both lower and higher temperatures (it was 32% and 34% of maximal, at 30°C and 42°C, respectively). In contrast to the WT RdRp complex, the activity of the AA and Len "LAIV" RdRp complexes was maximal at 32°C and 30°C, respectively – and declined substantially at higher temperatures (**Fig. 10B, C**). These findings suggest that the functional activity of the purified AA and Len LAIV RdRp complexes is temperature-sensitive, independent of any human host cell factors (since the complexes were purified from insect cells).

Figure 10. Temperature-dependent dinucleotide ApG-primed RNA transcription profiles of PR8 polymerase complexes purified via the baculovirus expression system.



LEGEND: Using a 30-nt template which codes for the 3' end of the PA gene, RNA synthesis reactions were performed using the purified polymerase complexes for 30 mins at varying temperatures (30°C, 32°C, 37°C, 39°C , 42°C). The resulting 30-nt fully extended RNA products, F generated by (A) PR8 wild type, (B) PR8 Leningrad mutant and (C) PR8 Ann Arbor mutant, were visualized using a phosphorimager. Band intensities were measured and normalized with a 32P- labelled 20-mer primer which was used as a loading control, LC. Readings obtained from each temperature were analyzed and normalized with the temperature at which the highest polymerase activity was recorded for respective mutant. The data represent mean values of triplicates, whereas the error bars denote standard error means. Unpaired t tests analyses were performed to determine the significance of each reading, whereas $p < 0.05$ was represented as *; $p < 0.01$ was represented as **; $p < 0.001$ was represented as ***; and $p < 0.0001$ was represented as ****.

The Ann Arbor and Leningrad LAIV mutations confer a temperature sensitive phenotype on the physical stability of the purified influenza A virus RdRp complex

One possible explanation for the temperature sensitive phenotype of polymerase function observed in Figure 1 is that the physical stability of RdRp complex is itself temperature sensitive. To test this hypothesis, we incubated the three RdRp complexes (WT, AA, Len) for one hour at a range of physiologic relevant temperatures (30°C, 32°C, 37°C, 39°C, 42°C), and then immunoprecipitated the complexes with an immobilized PA-specific antibody. The immunoprecipitates were then separated by SDS/PAGE, and subjected to immunoblot analysis using a PB2-specific antibody. Levels of PB2 in the immunoprecipitates were expected to provide an indication of the physical stability of the three RdRp complexes.

As shown in **Figure 11A**, levels of PB2 in the immunoprecipitated WT RdRp complex were maximal at 37°C, whereas levels of PB2 in the immunoprecipitated AA and Len RdRp complexes were maximal at 32°C and 30°C, respectively (**Fig. 11C, Fig. 11B**). It is notable that the temperatures at which each RdRp complex exhibited the greatest physical stability (**Fig. 11**) were identical to the temperatures at which RdRp complex demonstrated the greatest functional activity (**Fig. 10**). The simplest explanation of these data is that that the mutations present in the AA and Len LAIVs confer a temperature-sensitive phenotype on the functional activity of the corresponding RdRp complexes because they confer a temperature-sensitive phenotype on the physicalstability of the complexes.

Discussion and Conclusions

Cold passage of the A/Ann Arbor/6/60 (H2N2) and A/Leningrad/134/17/57 (H2N2) influenza A virus strains by independent laboratories in the U.S. and in Russia led to the emergence of temperature sensitive (*ts*) and attenuated (*att*) influenza viruses that have served as the progenitors for the two different lineages of live-attenuated influenza vaccines (LAIVs) currently licensed for human use. Interestingly, these LAIVs contain only a small number of mutations relative to the wild-type parental viruses from which they were derived – none of which are shared between the two LAIV lineages. It is striking, however, that almost all of the mutations present in the two LAIV lineages map to the tripartite viral RNA-dependent RNA polymerase. This suggests that the properties of these mutant RdRps are central to the phenotype(s) of the corresponding LAIVs. However, the underlying biochemical mechanism(s) that account for the temperature sensitive phenotype of the AA and Len LAIVs has not previously been examined. We therefore set out to address this knowledge gap.

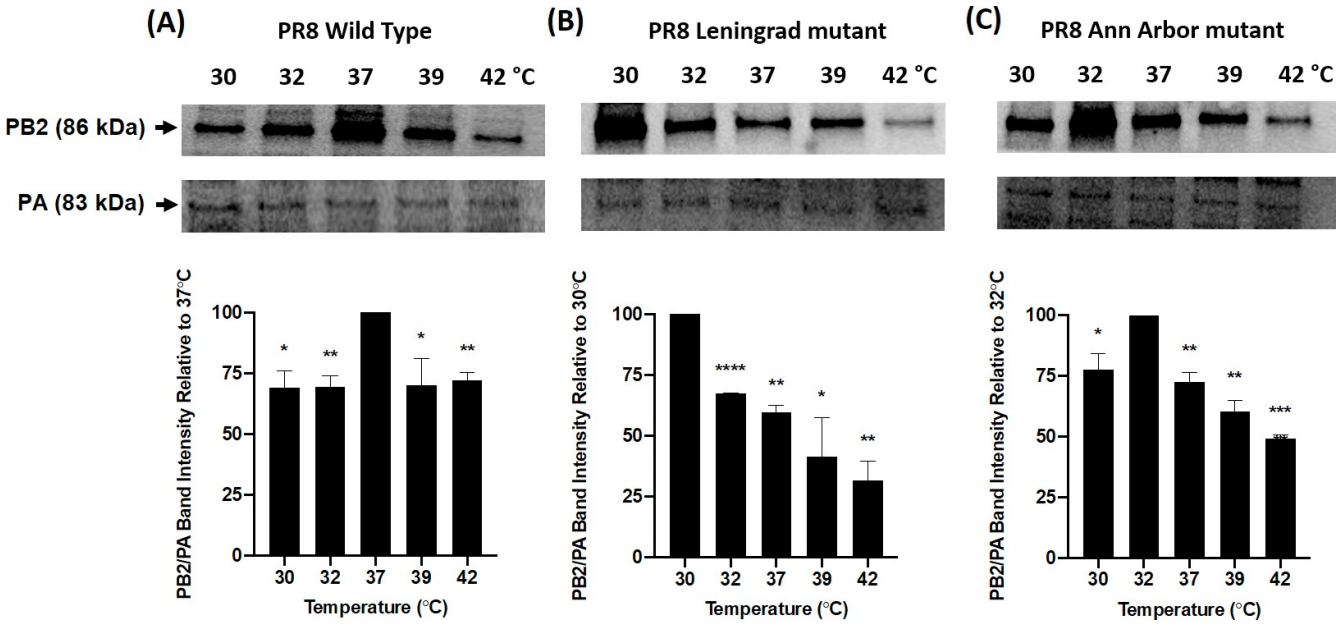
In this study, we have examined the effects of LAIV mutations on the biochemical and structural properties of the purified RdRp complexes from the well-characterized wild type A/Puerto Rico/8/34 H1N1 (PR8) virus, and from AA and Len "LAIV" mutants of PR8. Our data show that the AA and Len "LAIV" mutant RdRp complexes demonstrated maximal polymerase activity and physical stability at lower temperatures (32^{o}C and 30^{o}C, respectively) than the WT PR8 RdRp complex (which had optimal activity and stability at 37^{o}C) (**Figs. 10 and 11**). This suggests that the temperature sensitive phenotype conferred on the viral RdRp complex by the AA and Len LAIV mutations likely accounts for the ts phenotype (and in vivo attenuation) of live-attenuated influenza vaccine viruses.

Prior studies have shown that the Len LAIV mutations confer more pronounced *ts* and *att* phenotypes on wild-type influenza A viruses, than do the AA LAIV mutations (1). The present work is consistent with these findings, in that the purified Len "LAIV" RdRp complex demonstrated maximal polymerase activity and physical stability at 30^{o}C, while the purified AA "LAIV" RdRp complex was most active and most stable at 32^{o}C.

In a previous review, LAIV mutations were mapped to a bat influenza polymerase crystal structure and interestingly, many of the mutations were found to occur at the interfaces between individual RdRp subunits (2). Thus, our data suggest that the temperature sensitive phenotype of the LAIV RdRp complexes can be attributed at least in part to thermal instability of intersubunit interactions – although we cannot rule out the possibility that individual subunit proteins may undergo temperature-dependent internal conformational changes that lead to instability of the overall complex.

Finally, it has been shown that the AA and Len LAIV mutations confer more robust *ts* and *att* phenotypes on some strains of influenza A viruses than others – e.g., the AA LAIV mutations attenuate the A/Cal/04/09 strain by only about 10-fold (3), whereas they attenuate PR8 by over 1,000 fold (4). Although beyond the scope of the present study, it will be of interest to explore whether the AA LAIV mutations confer only a modest (or undetectable) *ts* phenotype on the functional activity and physical stability of the purified RdRp complex from A/Cal/04/09.

Figure 11. Temperature-dependent RNA polymerase complex stability



LEGEND: Using anti-Influenza A virus PA antibody crosslinked with A/G magnetic beads, intact trimeric polymerase complexes were co-immunoprecipitated following 1 h incubation at varying temperatures (30°C, 32°C, 37°C, 39°C, 42°C). **(A)** The resulting eluates were analyzed by western blot using anti-Influenza A virus PA and PB2 antibodies. **(B)** Band intensities were measured and the amount of PB2 of each sample was normalized with its respective PA protein. Densitometry readings obtained were analyzed and normalized with the temperature at which the highest relative levels of PB2 were recorded for respective mutant. The data represent mean values of triplicates, whereas the error bars denote standard error means. Unpaired t tests analyses were performed to determine the significance of each reading, whereas $p < 0.05$ was represented as *; $p < 0.01$ was represented as **; $p < 0.001$ was represented as ***; and $p < 0.0001$ was represented as ****.

References

1. Ilyushina, N. A., Ikizler, M. R., Kawaoka, Y., Rudenko, L. G., Treanor, J. J., Subbarao, K., and Wright, P. F. (2012) Comparative study of influenza virus replication in MDCK cells and in primary cells derived from adenoids and airway epithelium. J. Virol. 86, 11725-11734
2. Rodriguez, L., Blanco-Lobo, P., Reilly, E. C., Maehigashi, T., Nogales, A., Smith, A., Topham, D. J., Dewhurst, S., Kim, B., and Martínez-Sobrido, L. (2019) Comparative Study of the Temperature Sensitive, Cold Adapted and Attenuated Mutations Present in the Master Donor Viruses of the Two Commercial Human Live Attenuated Influenza Vaccines. Viruses 11(10):928. doi: 10.3390/v11100928.
3. Martínez-Sobrido, L., Peersen, O., and Nogales, A. (2018) Temperature Sensitive Mutations in Influenza A Viral Ribonucleoprotein Complex Responsible for the Attenuation of the Live Attenuated Influenza Vaccine. Viruses 10(10):560. doi: 10.3390/v10100560.
4. Nogales, A., Rodriguez, L., DeDiego, M. L., Topham, D. J., and Martínez-Sobrido, L. (2017) Interplay of PA-X and NS1 Proteins in Replication and Pathogenesis of a Temperature-Sensitive 2009 Pandemic H1N1 Influenza A Virus. J Virol. 91(17):e00720-17. doi: 10.1128/JVI.00720-17.
5. Cox, A., Baker, S. F., Nogales, A., Martínez-Sobrido, L., and Dewhurst, S. (2015) Development of a mouse-adapted live attenuated influenza virus that permits in vivo analysis of enhancements to the safety of live attenuated influenza virus vaccine. J. Virol. 89, 3421-3426

3B. What opportunities for training and professional development has the project provided?
The project has provided training and professional development opportunities to the following individuals:

1. **Justin Leach.** PhD trainee in Dr. Dewhurst's lab. Training activities: Mr. Leach is being mentored by Dr. Dewhurst. Professional development: Mr. Leach in his 4th year of graduate training, and plans to complete his thesis with Dr. Dewhurst. He passed his Qualifying Examination, for formal admission into candidacy for the Ph.D. degree in 2020.
2. **Sebastian Bosch.** PhD trainee in Dr. Dewhurst's lab. Training activities: Mr. Bosch is being mentored by Mr. Leach and Dr. Dewhurst. Professional development: Mr. Bosch in his 2nd year of graduate training, and plans to complete his thesis with Dr. Dewhurst. Mr. Bosch is from a racial/ethnic group historically excluded from biomedical research (he is Latinx).
3. **Sarah Belanger.** Undergraduate student who conducted independent research in Dr. Dewhurst's lab during the earlier phases of the project. Training activities: Ms. Belanger was mentored in her research by Mr. Leach. Professional development: Ms. Belanger developwes new technical skills; her research experiences helped her graduate from the UR with a BS in Microbiology (May 2020) and a Certificate in Biotechnology. She is presently enrolled in a M.Ed. program at the Warner School of Education (UR), where she is pursing a Masters in teaching, specializing in high school science education.
4. **Jael Ernest Fleurant.** Undergraduate student who conducted independent research in Dr. Dewhurst's lab pr. Training activities: Ms. Fleurant was mentored in her research by Mr. Leach. Professional development: Ms. Fleurant has developed new technical skills and a greater understanding of what a research career might be like. Ms. Fleurant is from a racial/ethnic group historically excluded from biomedical research (she is Black).

3C. Dissemination of results to communities of interest.
See under Products.

3D. Plans for next reporting period.
All studies have been completed. This is our Final Report.

4. IMPACT

4A. What was the impact on the development of the principal discipline(s) of the project?
We compared the In vitro and in vivo phenotype of recombinant influenza A/Puerto Rico/8/34 H1N1 (PR8) viruses containing the *ts, ca* and *att* mutations of the US (PR8/AA) and the Russian (PR8/Len) Master Donor Viruses (MDVs). Our results show that PR8/Len is more attenuated in vivo than PR8/AA, although both viruses induced similar levels of humoral and cellular responses, and protection against homologous and heterologous viral challenges. **Our findings support the feasibility of using a different virus backbone as MDV for the development of improved LAIVs for the prevention of IAV infections.**

4B. What was the impact on other disciplines?
Nothing to Report.

4C. What was the impact on technology transfer?
Nothing to Report

4D. What was the impact on society beyond science and technology?
This project provided research opportunities for two students from racial/ethnic backgrounds that have historically been excluded from biomedical research (one Black, one Latinx).

5. CHANGES/PROBLEMS

5A. Changes in approach and reasons for change
No changes in approach

5B. Actual or anticipated problems or delays and actions or plans to resolve them
Biochemical studies on the purified viral polymerase (Major Task 1) were slightly delayed due to delays in the production of the relevant baculovirus expression vectors and the generation of purified recombinant proteins. The Emory team, under Dr. Kim, generously continued to work on the project at Emory's expense, after their support from this grant ended. As a result, we were able to make additional progress on this Task.

5C. Changes that had a significant impact on expenditures
None

5D. Significant changes in use or care of human subjects, vertebrate animals, biohazards, and/or select agents
None

6. PRODUCTS

6A. Publications, conference papers, and presentations

3. Rodriguez, L., Blanco-Lobo, P., Reilly, E.C., Maehigashi, T., Nogales, A., Smith, A., Topham, D.J., **Dewhurst, S**., Kim, B., Martínez-Sobrido, L. Comparative Study of the Temperature Sensitive, Cold Adapted and Attenuated Mutations Present in the Master Donor Viruses of the Two Commercial Human Live Attenuated Influenza Vaccines. **Viruses** 11(10). pii: E928, 2019. PMC6832241

4. Smith, A., Rodriguez, L., Ghouayel, M.E., Nogales, A., Chamberlain, J.M., Sortino, K., Reilly, E., Feng, C., Topham, D.J., Martínez-Sobrido, L., **Dewhurst, S**. A live-attenuated influenza vaccine (LAIV) elicits enhanced heterologous protection when the internal genes of the vaccine are matched to the challenge virus. **J Virol.** 94(4):e01065-19, 2020. PMC6997774

6B. Website(s) or other Internet site(s)
Nothing to report

6C. Technologies or techniques
Nothing to report

6D. Inventions, patent applications, and/or licenses
Nothing to report

6E. Other Products
Nothing to report

7. PARTICIPANTS & OTHER COLLABORATING ORGANIZATIONS

7A. What individuals have worked on the project?

Name:	Stephen Dewhurst
Project Role:	PI
Research Identifier (e.g. ORCID ID):	https://orcid.org/0000-0001--7729-7920
Nearest person month worked:	2
Contribution to Project:	Dr. Dewhurst directly oversaw or supervised all project studies
Funding Support:	This award

Name:	Baek Kim
Project Role:	PI (Emory Subcontract)
Research Identifier (e.g. ORCID ID):	https://orcid.org/0000-0001-7986-4335
Nearest person month worked:	1
Contribution to Project:	Dr. Kim continued to direct studies at the Emory site (biochemical studies on the viral polymerase)
Funding Support:	Emory University funds

Name:	Randy Albrecht

Project Role:	PI (Icahn School of Medicine at Mt. Sinai Subcontract)
Research Identifier (e.g. ORCID ID):	https://orcid.org/0000-0003-4008-503X
Nearest person month worked:	3
Contribution to Project:	Dr. Albrecht directed all studies at the Mt. Sinai site.
Funding Support:	This award

Name:	Luis Martínez-Sobrido
Project Role:	Coinvestigator (UR and now at Texas Biomedical Research Institute)
Research Identifier (e.g. ORCID ID):	https://orcid.org/0000-0001-7084-0804
Nearest person month worked:	1
Contribution to Project:	Dr. Martínez-Sobrido assisted Dr. Dewhurst with all minigenome, virus replication and viral immunogenicity/challenge studies at the Rochester site; he has since moved to the Texas Biomedical Research Institute in San Antonio, while continuing to work on this project
Funding Support:	This award

Name:	Kayla Bell
Project Role:	Technician (UR)
Research Identifier (e.g. ORCID ID):	N/A (No ORCID ID or equivalent)
Nearest person month worked:	3
Contribution to Project:	Ms. Bell assisted with plasmid production, minigenome assays and assays of virus replication.
Funding Support:	This award

Name:	Justin Leach
Project Role:	Graduate Student (UR)
Research Identifier (e.g. ORCID ID):	N/A (No ORCID ID or equivalent)
Nearest person month worked:	12
Contribution to Project:	Mr. Leach assisted with plasmid production, viral mutagenesis, and assays of virus replication.
Funding Support:	This award; and NIH T32 GM068411

Name:	Sebastian Bosch
Project Role:	Graduate Student (UR)
Research Identifier (e.g. ORCID ID):	N/A (No ORCID ID or equivalent)

Nearest person month worked:	2
Contribution to Project:	Mr. Bosch assisted with plasmid production, viral mutagenesis, and assays of virus replication.
Funding Support:	This award

Name:	Jael Ernest Fleurant
Project Role:	Undergraduate Student (UR)
Research Identifier (e.g. ORCID ID):	N/A (No ORCID ID or equivalent)
Nearest person month worked:	4
Contribution to Project:	Ms. Fleurant assisted Mr. Leach with plasmid production and mutagenesis studies.
Funding Support:	This award

7B. Has there been a change in the active other support of the PD/PI(s) or senior/key personnel since the last reporting period?

Changes in the support for the PD/PI and senior/key personnel have occurred, and are included in this report.

7C. What other organizations were involved as partners?

As stated in the original grant application, and in the corresponding Notice of Grant Award, the University of Rochester (Rochester, NY; primary institution), as well as Emory University (Atlanta, GA; subcontracting institution) and the Icahn School of Medicine at Mt. Sinai (New York, NY; subcontracting institution) were involved in this project. We also extended a subcontract to the Texas Biomedical Research Institute (San Antonio, TX), after the UR coinvestigator, Dr, Martínez-Sobrido, moved there.

7B: UPDATED OTHER SUPPORT INFORMATION
Other Support information is provided only for the investigators who continued to work on this project during the no-cost extension period: Drs. Dewhurst and Martínez-Sobrido

DEWHURST, Stephen

ACTIVE AWARDS

UM1 AI069511 (Dewhurst/Keefer, MPI) 12/01/20-11/30/27 4.20 calendar
NIH
Title: *University of Rochester HIV/AIDS Clinical Trials Unit*
Major goal: To support and conduct clinical research on HIV/AIDS that contributes to the discovery of a preventive vaccine for HIV, as well as to the discovery of a cure for HIV, and of treatments that reduce the burden of disease due to HIV infection and its complications.
Role: MPI
Program Official: Courtney Southard, courtney.southard@nih.gov

OT2 HD107533 (Foxe/Zand/Dewhurst, MPI) 04/15/21-03/31/23 1.0 calendar NIH
Title: *COV-IDD: Testing for COVID-19 in high risk children with intellectual and developmental disabilities*
Major goal: To develop and implement a COVID-19 strategy for use in community-based organizations that serve children and families affected by intellectual and developmental disabilities.
Role: MPI
Program Official: Christopher Lindsey, chris.lindsey@nih.gov

R01 DA054534 (Goldman, PI) 07/01/21-06/30/26 1.20 calendar
NIH
Title: *A Dual Chimeric Human Astroglial-Microglial Model of HIV and HAND*
Major goal: To develop a novel mouse model for HIV-1 infection of the central nervous system.
Role: Co-Investigator
Program Official: Shang-Yi Tsai, stsai@nih.gov

R61 AI167035 (Miller, B., PI) 01/24/22-12/30/24 0.24 calendar
NIH
Title: *Paper-based HIV self test*
Major goal: Develop a disposable self-test for HIV viral load determination.
Role: Co-Investigator
Program Official: Diane Lawrence, diane.lawrence2@nih.gov

R01 AI150463 (Wedekind, PI) 09/30/17-07/31/22 (NCE) 0.12 calendar NIH
Title: *Cyclic Peptide Inhibitors of HIV-1 Proliferation*
Major goal: To develop novel inhibitors of HIV-1 replication, by targeting the HIV-1 TAR RNA structure, using cyclic peptides.
Role: Co-Investigator
Program Official: Gerard Lacourciere, gerard.lacourciere@nih.gov

1014095 BWF (Dewhurst, Bennett, MPI) 02/02/15-01/31/23 (NCE) 0.60 calendar
Burroughs Wellcome Fund Institutional Program
Unifying Population and Laboratory Based Sciences
Title: *Infection and Immunity: From Molecules to Populations*
Major goal: To train predoctoral students at the intersection of basic/translational research in infectious diseases and immunity, and population health
Role: Co-PI

Program Official: Victoria McGovern, PhD, 919-991-5112, bmcgovern@bwfund.org

K12 GM106997 (Dewhurst/Buckley, MPI) 07/01/21-06/30/26 0.60 calendar
NIH/NIGMS
Title: *Rochester Partnership to Advance Research and Academic Careers in Deaf Scholars*
Major goal: To develop and implement a unique biomedical research training program for deaf scholars.
Role: MPI
Program Official: Edgardo Falcon-Morales, edgardo.falcon@nih.gov

MARTINEZ-SOBRIDO, Luis

ACTIVE AWARDS

R01 AI141607 (de Figueiredo, PI) 02/01/20 – 05/31/24 0.60 calendar
NIH
Title: *Development of a High-Throughput Microfluidics-Enabled Functional Assay for Rapidly Identifying Neutralizing Antibodies*
Major Goal: To test the hypothesis that PRESCIENT can identify in a mixed population of individual human hybridoma cells neutralizing antibodies against pH1N1 virus.
Role: Co-Investigator
Program Official: Mary Chelsea Lane, NIH/NIAID, BG 5601FL RM 8A19, 5601 Fishers Lane, Rockville, MD 20852

R01 AI142985 (de la Torre, PI) 02/01/20 – 03/31/23 0.90 calendar
NIH
Title: *Roles of the Nucleoprotein 3'-5' Exonuclease Domain in Arenavirus Biology*
Goal: To provide a better understanding of arenavirus-host innate defense interactions, which can facilitate the development of novel strategies to combat human pathogenic gamma-arenaviruses.
Role: Co-Investigator
Program Official: Lesley Conrad Dupuy, NIH/NIAID, BG 5601FL RM 8E66, 5601 Fishers Lane, Rockville, MD 20852

R01 AI145332 (Kobie, PI) 02/01/20 – 08/31/23 0.96 calendar
NIH
Title: *Dynamics of the protective vaccine-induced human influenza neuraminidase B cell response*
Major Goal: To define how various influenza vaccine types impact the characteristics of neuraminidase specific antibodies in humans and what properties of neuraminidase specific antibodies are most effective at preventing influenza infection against diverse strains.
Role: Co-Investigator
Program Official: Sonnie Kim, NIH/NIAID, BG 5601FL RM 8E12, 5601 Fishers Lane, Rockville, MD 20852

R01 HL091968 (O'Reilly, PI) 02/01/20 – 08/31/22 0.42 calendar
NIH
Title: *Effects of Neonatal Hyperoxia on Alveolar Development and Infection*
Goal: To test the hypothesis that neonatal hyperoxia enhances sensitivity to IAV infection by inducing epigenetic changes in proliferating AEC2s that are maintained even when they become AEC1s and these changes are mediated by the persistent expression of Ki67.
Role: Co-Investigator
Program Official: Aruna R Natarajan, NHLBI, BG RKL1 RM 403-A1, 6705 Rockledge Drive, Bethesda, MD 20817

N/A (Ivanov, PI) 07/01/20 – 06/30/2022 (NCE) 0.24 calendar
San Antonio Partnership for Precision Therapeutics
Title: *Blocking SARS-CoV-2 evasion from innate antiviral defenses*
Major Goal: To determine the effectivity of AT-100 post-infection in blocking SARS-CoV-2 infectivity.
Role: Co-Investigator
Grants Officer: Liz Tullis, San Antonio Partnership for Precision Therapeutics; LTullis@sappt.org

N/A (Gupta, PI) 07/01/20 – 06/30/22 (NCE) 0.24 calendar
San Antonio Partnership for Precision Therapeutics
Title: *Mechanism-based Targeting of an RNA Processing Pathway of SARS-CoV-2*
Mahor Goal: To determine the structural basis of RNA processing in host immune and inflammatory response critical for viral survival and growth, using HTS screening, medicinal chemistry, and in vitro and in vivo studies towards rapid clinical translation.
Role: Co-Investigator
Program Official: Liz Tullis, San Antonio Partnership for Precision Therapeutics LTullis@sappt.org

W81XWH1910496 (Martínez-Sobrido, PI) 05/01/20 – 10/31/23 0.90 calendar
DoD
Title: *Development of Live-Attenuated Vaccine Platform Against Hemorrhagic fever causing Arenaviruses*
Major Goal: To test whether recombinant forms of the prototypic gammarenavirus lymphocytic choriomeningitis virus (LCMV) containing a codon deoptimized (CD) nucleoprotein (NP) expressing glycoproteins (GP) of hemorrhagic fever (HF)-causing LASV and JUNV (rLCMV/NPCD/GPHF) can be used for the development of a safe and protective individual or blended live-attenuated vaccine (LAV) to combat HF disease caused by LASV and JUNV infections.
Role: PI
Program Official: Stephanie Davis, 820 Chandler Street, Fort Detrick, MD 21705-5104

INV-019155 (PI: Torrelles) 09/16/20 – 12/31/22 1.80 calendar
Bill & Melinda Gates Foundation
Title: *COVID-19 CTA: Preclinical models for SARS-CoV-2 infection*
Goal: To determine if human monoclonal antibodies (hmAbs) shown in vitro to block SARS-CoV-2 infection are also effective, alone or in combination, in vivo using two rodent animal models of SARS-CoV-2 infection and associated COVID-19 disease.
Role: Co-Investigator
Program Official: Jacqueline Kirchner, P.O. Box 23350, Seattle, WA 98102

W81XWH2110095 (Shetty, PI) 02/01/2021 – 01/31/2023 0.6 calendar
Department of Defense
Title: *Development of a Novel Drug Candidate, CSP7, for the Treatment of COVID-19*
Major Goal: To determine the efficacy of the novel drug candidate, CSP7, for the treatment of COVID-19, using hACE2 mice infected with CoV2.
Role: Co-Investigator
Program Official: Abigail Strock, Fort Detrick CDMRP 1120 Fort Detrick, Federick, MD 21702
No overlap

W81XWH2110103 (Pertsemlidis, PI) 02/01/21 – 01/31/22 0.60 calendar
DOD
Title: *SARS-CoV-2 Viral RNAs as Unique Biomarkers and Therapeutic Targets*
Major Goal: To identify and characterize novel small RNAs produced by SARS-CoV-2 and exploit them as biomarkers and therapeutic targets. We propose a combination of computational biology, synthetic biology, genome editing, and chemistry approaches. The successful delivery of a v-miRNA inhibitor in cell culture will establish a foundation for preclinical and clinical characterization.
Role: Co-Investigator
Program Official: Abigail Strock, Fort Detrick CDMRP 1120 Fort Detrick, Federick, MD 21702

Subcontract # ID07200010-501-1 (Mallory, PI) 07/01/2021 – 9/30/2022 0.38 calendar
DOD
Title: *Viral and Microbial Decontamination Strategies for Medical Treatment Facilities, Close Quarters, and Austere Settings (Zeolites task order)*

Major Goal: To test the hypothesis that surfaces treated with Zeolite will become inhospitable to bacteria and destroy the virulence of viruses coming in contact with treated surfaces for extended periods of time without reapplications.
Role: Co-Investigator
Program Official: David J. Kilbourne, GSA (David.kilbourne@gsa.gov)

Subcontract # ID07200010-501-2 (Mallory, PI) 07/01/2021 – 9/30/2022 0.25 calendar
DOD
Title: *Viral and Microbial Decontamination Strategies for Medical Treatment Facilities, Close Quarters, and Austere Settings (CIMR Efficacy task order)*
Major Goal: To test the efficiency of a H2O2 generating Continuous Infection Microbial Reduction device (CIMR) against SARS-CoV-2 and other respiratory pathogens, such as viruses: Influenza (seasonal H1N1/H3N2, and influenza B) and adenovirus; bacteria [Streptococcus pneumonia (Gram positive), and Legionella pneumophila (gram negative)]; and mold (Aspergillus fumigatus).
Role: Co-Investigator
Program Official: David J. Kilbourne, GSA (David.kilbourne@gsa.gov)

R43 AI165089 (Huang, PI) 07/09/21 – 6/30/22 0.6 calendar
NIH
Title: *Developing a Thermostable SARS-CoV-2 RBD-particle Vaccine*
Major Goal: To demonstrate that RBD-particles can elicit robust and protective antibody responses against SARS-CoV-2 with thermostability after lyophilization.
Role: Co-Investigator
Program Official: Ashley Colette Ranellone, ranelloneac@niaid.nih.gov, 301-594-8541

R01 AI161363 (Gupta, PI) 08/01/21 – 07/31/26 0.6 calendar
NIH
Title: *Mechanism-based Targeting of the RNA Processing Machinery of SARS-CoV-2*
Major Goal: To determine the prophylactic and therapeutic activities of the identified compounds in vitro in cultured cells and in vivo in K18 human angiotensin converting enzyme 2 (hACE2) transgenic (wild-type SARS-CoV-2) or wild-type (mouse adapted SARS-CoV-2) mice and/or golden Syrian hamsters to determine their antiviral activity against SARS-CoV-2.
Role: Co-Investigator
Program Official: Nicole A. Guidetti, Nicole.guidetti@nih.gov, 301-761-6934

Subaward from UTHSCSA (Gupta, PI) 09/01/21 – 08/31/22 0.01 calendar
San Antonio Medical Foundation
Title: *Repurposing Drugs for COVID-19 Therapy*
Major Goal: To evaluate the toxicity and anti-SARS-CoV-2 activity of the selected compounds both in vitro using cell cultures and in vivo using mice/hamsters.
Role: Co-Investigator
Program Official: Pam Leissner, San Antonio Medical Foundation, PO Box 29736, SATX 78229

75N93021C00014 (Garcia-Sastre, PI) 09/01/21 – 9/01/23 0.6 calendar
NIH, Centers of Excellence for Influenza Research and Response
Title: *A multi-fluorescent microneutralization assay to rapidly evaluate SARS-CoV-2 neutralizing antibody (NAb) responses (NIAID Centers of Excellence for Influenza Research and Response)*
Major Goal: To develop a novel multi-fluorescent microneutralization assay (MFMA) using different fluorescent-expressing recombinant (r)SARS-CoV-2 for the rapid, sensitive, and simultaneous identification of neutralizing antibody (NAb) responses against SARS-CoV-2, including those with broadly neutralizing activity against variants of concern (VoC), within the same well.
Role: PI

R01 AI161175 (Kobie, PI) 09/01/21 – 08/31/24 1.2 calendar
NIH
Title: *The origin and future protective activity of SARS-CoV-2 RBD specific neutralizing antibodies*
Major Goal: To perform the experiments related to the protective activity of SARS-CoV-2 RBD specific neutralizing antibodies *in vitro* and *in vivo* in the mouse model.
Role: Co-Investigator

75N95C21P00127 (Martínez-Sobrido, PI) 09/03/21 – 08/25/22 0.01 calendar
NIH
Title: Evaluating the efficacy of ROC-35 in a SARS-CoV-2 humanized ACE2-transgenic mouse model
Major Goal: To evaluate the efficacy of ROC-35 in a SARS-CoV-2 humanized ACE2-transgenic mouse model.
Role: PI

Proposal 20-243 (Torrelles, PI)) 09/01/20 – 03/31/22 0.20 calendar
Heat Biologics Inc.
Title: *Test gp96-based SARS-CoV-2 vaccine in hACE2 Tg mice – COVID-19 Efficacy Challenge Study*
Major Goal: To understand if our proprietary product (N. Oleander) is effective as a prophylactic and/or for treatment and follow-up therapy for COVID-19 infected animals.
Role: Co-Investigator

8. SPECIAL REPORTING REQUIREMENTS

None

9. APPENDICES

PDFs of Publications:

1. Rodriguez, L., Blanco-Lobo, P., Reilly, E.C., Maehigashi, T., Nogales, A., Smith, A., Topham, D.J., **Dewhurst, S**., Kim, B., Martínez-Sobrido, L. Comparative Study of the Temperature Sensitive, Cold Adapted and Attenuated Mutations Present in the Master Donor Viruses of the Two Commercial Human Live Attenuated Influenza Vaccines. **Viruses** 11(10). pii: E928, 2019. PMC6832241
2. Smith, A., Rodriguez, L., Ghouayel, M.E., Nogales, A., Chamberlain, J.M., Sortino, K., Reilly, E., Feng, C., Topham, D.J., Martínez-Sobrido, L., **Dewhurst, S**. A live-attenuated influenza vaccine (LAIV) elicits enhanced heterologous protection when the internal genes of the vaccine are matched to the challenge virus. **J Virol.** 94(4):e01065-19, 2020. PMC6997774

viruses

MDPI

Article

Comparative Study of the Temperature Sensitive, Cold Adapted and Attenuated Mutations Present in the Master Donor Viruses of the Two Commercial Human Live Attenuated Influenza Vaccines

Laura Rodriguez [1,†], Pilar Blanco-Lobo [1], Emma C. Reilly [1,2], Tatsuya Maehigashi [3], Aitor Nogales [1], Andrew Smith [1,4], David J. Topham [1,2], Stephen Dewhurst [1], Baek Kim [3,5] and Luis Martínez-Sobrido [1,*]

1 Department of Microbiology and Immunology, University of Rochester, Rochester, New York, NY 14642, USA; laurita85oviedo@hotmail.com (L.R.); piblanlo@gmail.com (P.B.-L.); emma_reilly@urmc.rochester.edu (E.C.R.); nogales.aitor@inia.es (A.N.); Andrew_Smith72@URMC.Rochester.edu (A.S.); David_topham@urmc.rochester.edu (D.J.T.); stephen_dewhurst@me.com (S.D.)
2 David H. Smith Center for Vaccine Biology and Immunology, University of Rochester, Rochester, New York, NY 14642, USA
3 Center for Drug Discovery, Department of Pediatrics, School of Medicine, Emory University, Atlanta, Georgia, GA 30322, USA; t.maehigashi@emory.edu (T.M.); baek.kim@emory.edu (B.K.)
4 Medical Scientist Training Program (MSTP), University of Rochester, Rochester, New York, NY 14642, USA
5 College of Pharmacy, Kyung-Hee University, Seoul 02447, Korea
* Correspondence: luis_martinez@urmc.rochester.edu
† Current address: Agencia Española de Medicamentos y Productos Sanitarios, E-28022 Madrid, Spain.

Received: 10 September 2019; Accepted: 8 October 2019; Published: 10 October 2019



Abstract: Influenza viruses cause annual, seasonal infection across the globe. Vaccination represents the most effective strategy to prevent such infections and/or to reduce viral disease. Two major types of influenza vaccines are approved for human use: inactivated influenza vaccines (IIVs) and live attenuated influenza vaccines (LAIVs). Two Master Donor Virus (MDV) backbones have been used to create LAIVs against influenza A virus (IAV): the United States (US) A/Ann Arbor/6/60 (AA) and the Russian A/Leningrad/134/17/57 (Len) H2N2 viruses. The mutations responsible for the temperature sensitive (*ts*), cold-adapted (*ca*) and attenuated (*att*) phenotypes of the two MDVs have been previously identified and genetically mapped. However, a direct comparison of the contribution of these residues to viral attenuation, immunogenicity and protection efficacy has not been conducted. Here, we compared the In vitro and in vivo phenotype of recombinant influenza A/Puerto Rico/8/34 H1N1 (PR8) viruses containing the *ts*, *ca* and *att* mutations of the US (PR8/AA) and the Russian (PR8/Len) MDVs. Our results show that PR8/Len is more attenuated in vivo than PR8/AA, although both viruses induced similar levels of humoral and cellular responses, and protection against homologous and heterologous viral challenges. Our findings support the feasibility of using a different virus backbone as MDV for the development of improved LAIVs for the prevention of IAV infections.

Keywords: influenza; vaccine; live-attenuated vaccine

1. Introduction

In the United States (US), the Centers for Disease Control and Prevention (CDC) has estimated that influenza has caused between 9.3 and 49.0 million illnesses each year, since 2010- along with between

12,000 and 79,000 deaths annually [1]. Two types of influenza cause seasonal, global epidemics in human populations each year: influenza A virus (IAV) and influenza B virus (IBV) [2,3]. IAVs can also cause sporadic pandemics of great consequences when new viruses are introduced into humans [4].

Vaccination is the most cost-effective approach to prevent influenza infections [5]. Currently, three major influenza vaccines are approved for human use in the US: recombinant (r) hemagglutinin (HA) protein, inactivated influenza vaccines (IIVs) and live attenuated influenza vaccines (LAIVs) [1]. IIVs are delivered by the intramuscular route and principally induce humoral responses against the viral HA protein [6–8], one of the major antigenic determinants of influenza viruses which is responsible for viral entry [9]. On the other hand, LAIVs are administrated intranasally (mimicking the natural route of infection) and induce both humoral and cellular immune responses in the mucosa [10–13]. In the US and the European Union, the age indication for both vaccines is different: in general, IIVs are used in children 6 months of age and in all adults; and LAIVs are used in individuals between 2 to 49 years old, with the exception of pregnant woman and/or immunocompromised people [1]. However, since the introduction of the quadrivalent vaccine formulation during the 2013–2014 influenza season, different studies revealed less than expected effectiveness of the LAIV and, therefore, a recommendation of the IIVs over LAIV over IIVs.

LAIVs have been generated by passaging influenza viruses at gradually reduced temperatures in eggs or cultured cells to generate temperature sensitive (*ts*) viruses that replicate efficiently at low temperatures (cold adapted, *ca*) but not at elevated temperatures (temperature sensitive; *ts*); such viruses also possess an attenuated phenotype (*att*) in vivo [14–18]. The generation of these viral variants was based on the ability of influenza viruses to replicate in the upper (25–33 °C) and lower (37 °C) respiratory tract (URT and LRT, respectively). LAIVs have restricted replication at non-permissive temperatures encountered in the LRT (37 °C–39 °C) but are able to replicate efficiently at permissive temperatures encountered in the URT and nose (33 °C). As a consequence, they induce mucosal immunity at the site of infection (URT) [11–13,19–21], as well as robust humoral [11–13,21–24] and cellular [22] immunity -leading to the recruitment of influenza-specific CD8 T cells into the lungs and protection against subsequent infections [11–13,25–28].

The traditional methods for generating seasonal LAIVs is based on the co-infection of embryonated chicken eggs with a Master Donor Virus (MDV) and the seasonal virus recommended by the CDC and international health agencies to be part of the vaccine [29]. The viral passages are carried out at low temperatures (25–26 °C) [29] and the reassortant virus (6 + 2) containing the six internal genes of the MDV (PB2, PB1, PA, NP, M and NS) and the HA and NA from the seasonal viral strain is cloned by limited dilution in the presence of antibodies against the surface glycoproteins (HA and NA) of the MDV strain. Thus, all LAIVs share the same internal genes (derived from the MDV) and differ only in their HA and NA components. More recently, reverse genetics techniques have been used to generate seasonal LAIVs (e.g., Flumist® Quadrivalent Vaccine, AstraZeneca).

Two approaches have been used to develop seasonal IAV LAIVs that differ in the MDV: (1) the US A/Ann Arbor/6/60 H2N2 LAIV (AA) that is commercialized under the names of FluMist in the US and Canada, and Fluenz in the European Union; and (2) the Russian A/Leningrad/134/17/57 H2N2 LAIV (Len) that is commercialized under the names Ultravac (Russia) and Nasovac-S (India) [30] and also used in China and Thailand [31]. In the case of the US AA MDV, the mutations responsible for the *ts*, *ca* and *att* phenotype have been mapped to PB2 (N265S), PB1 (K391E, E581G and A661T) and NP (D34G) [32,33]. In the case of the Russian Len MDV, the mutations responsible for the *ts*, *ca* and *att* phenotype have been mapped to PB2 (V478L), PB1 (K265N and V591I) and NEP (M100I) [34]. Introduction of the US AA MDV mutations into the genomes of IAVs such as A/Puerto Rico/8/34 H1N1 (PR8) [35,36], A/canine/NY/dog23/09 H3N8 [11,12,21] or A/equine/Ohio/1/03H3N8 [13] resulted in similar *ts*, *ca* and *att* phenotypes as that of the original US AA MDV. However, introduction of the mutations of the US AA MDV into the pandemic A/California/04/09 H1N1 virus (Cal/09) resulted in reduced *ts* and *ca* in vitro and limited attenuation in vivo [37–39]. These results suggest that the *ts*, *ca* and *att* phenotypes induced by the mutations of the US AA MDV are influenced by the virus backbone

into which they are introduced. Although some groups have generated recombinant viruses by using the internal genes of AA or the Len (with the LAIV mutations) as MDVs with different HA and NA combinations [40–42], a direct comparison of the contribution of the US and Russian MDVs residues to viral attenuation, immunogenicity and protection efficacy in the same viral genetic background has not been conducted.

Here, we compared the contribution of the mutations present in the US AA and the Russian Len MDVs using the backbone of influenza PR8 In vitro and in vivo. Our results show that PR8 containing the mutations of the Russian Len MDV (PR8/Len) is more attenuated in vivo than the PR8 containing the mutations of the US AA MVD (PR8/AA). However, both PR8/AA and PR8/Len induced similar levels of humoral and cellular responses and both induce protection against homologous (PR8, H1N1) and partially heterologous (X31, H3N2) viral challenges. Collectively, these findings support the feasibility of using the mutations of the US AA or the Russian Len MDVs in the PR8 virus backbone for the development of novel and improved LAIVs for the prevention of IAV infections. The use of circulating IAVs as MDVs in new LAIVs could grant a higher level of protection by the induction of more robust cellular immune responses against internal viral proteins (current H2N2 AA and Len LAIV backbones were isolated in 1960 and 1957, respectively). In addition, our findings have an important impact on the development and implementation of LAIVs with high levels of attenuation.

2. Materials and Methods

2.1. Cells and Viruses

Human embryonic kidney 293T (HEK293T; ATCC CRL-11268) and Madin-Darby canine kidney (MDCK; ATCC CCL-34) cells were maintained in Dulbecco's modified Eagle's medium (DMEM; Mediatech, Inc.) supplemented with 10% fetal bovine serum (FBS), and 1% PSG (penicillin, 100 units/mL; streptomycin 100 µg/mL; L-glutamine, 2 mM) at 37 °C with 5% CO_2 as described [12].

The recombinant A/Puerto Rico/8/34 H1N1 (PR8) virus containing the *ts*, *ca* and *att* mutations of the Russian MDV A/Leningrad/134/17/57 LAIV (PR8/Len) was generated using previously described plasmid-based reverse techniques [43]. The recombinant PR8 wild-type (PR8/WT) and the mutant virus containing the *ts*, *ca*, and *att* mutations of the USA/Ann Arbor/6/60 H2N2 (PR8/AA) are described elsewhere [35,44]. All viruses were propagated in MDCK cells at 33 °C. A recombinant virus containing the HA and NA viral segments of influenza A/Hong Kong/1/1968 H3N2 in the background of PR8 virus (X31) was also used in our studies [45,46].

For viral infections, viral stocks were diluted in phosphate buffered saline (PBS) containing 0.3% bovine albumin (BA) and 1% penicillin and streptomycin (PS) (PBS/BA/PS). After 1 h viral adsorption at room temperature (RT), MDCK cells were maintained in post-infection (p.i.) DMEM media supplemented with 0.3% BA, 1% PSG, and 1 µg/mL of *N*-tosyl-L-phenylalanine chloromethyl ketone (TPCK)-treated trypsin (Sigma). Viral titers were determined by immunofocus assay (fluorescent forming units, FFU/mL) in MDCK cells at 33 °C using a monoclonal antibody (mAb) against influenza virus nucleoprotein, NP (ATCC HB-65, HL16-L10-4R5); as described [46].

2.2. Plasmids

To generate PR8/Len, the PR8/WT PB2, PB1 and NS viral segments were subcloned into a pUC19 plasmid (New England BioLabs) to introduce, using site-directed mutagenesis, the mutations responsible for the *ts*, *ca* and *att* phenotypes of the MDV A/Leningrad/134/17/57 H2N2 LAIV: PB2 V478L; PB1 K265N and V591I; and NEP M100I. Mutations were confirmed by sequencing (ACGT). Mutated PB2, PB1 and NS PR8/Len viral segments were subcloned from the shuttle pUC19 vector into the ambisense pDZ plasmid for virus rescue with the rest of the PR8 viral genes [35,47]. The PR8 PB2 and PB1 pDZ plasmids containing the *ts*, *ca* and *att* mutations of the MDV A/Ann Arbor/6/60 H2N2 LAIV: PB2 N265S; PB1 K391E, E581G and A661T were previously described [35].

2.3. Minigenome Assays

The ability of PR8/WT, PR8/AA and PR8/Len viral polymerase complexes to replicate and transcribe at different temperatures (33 °C, 37 °C and 39 °C) were evaluated in HEK293T cells (12-well plate format, 5×10^5 cells/well, triplicates). Cells were co-transfected in suspension, using Lipofectamine 2000 (Invitrogen, Carlsbad, CA, US), with 250 ng of the indicated combinations of ambisense pDZ-PB2 (WT, AA or Len), pDZ-PB1 (WT, AA or Len), pDZ-PA and pDZ-NP plasmids, together with 500 ng of two reporter viral (v)RNA-like expression plasmids encoding the GFP and Gluc driven by a human RNA polymerase I promoter (hPol-I-GFP and hPol-I-Gluc, respectively), and 100 ng of a reporter plasmid expressing Cypridina luciferase (Cluc) under the control of the constitutively active simian virus 40 (SV40) promoter (pSV40-Cluc) to normalize transfection efficiencies. Cells transfected in the absence of pDZ-NP were included as a negative control. Empty pDZ plasmid was used to keep the amount of transfected plasmid DNA constant in the negative control. At 24 h post-transfection (p.t.), cells were analyzed for GFP expression and photographed using a fluorescent microscope (Olympus IX81) and camera (QIMAGING, Retiga 2000R); Gluc and Cluc expression levels were determined in tissue culture supernatants (TCS) using the BioluxGaussia and Cypridina Luciferase Assay kits (New England BioLabs) and quantified with a Lumicount luminometer (Packard). Reporter Gluc gene activation was normalized to that of Cluc and shown as fold induction over the level of induction of the negative control (no pDZ-NP). Mean values and standard deviations (SDs) were calculated and statistical analysis was performed using a two-tailed Student *t*-test with Microsoft Excel software. Data are represented as relative activity considering the activity of each polymerase complex combination at 33 °C as 100%.

2.4. Virus Rescue

PR8/Len virus rescue was performed as described for PR8/WT and PR8/AA viruses [11,12,43,46]. Briefly, co-cultures (1:1) of HEK293T and MDCK cells (6-well plate format, 1×10^6 cells/well, triplicates) were co-transfected in suspension, using Lipofectamine 2000, with 1 µg of the eight-ambisense PR8 pDZ-PB2-Len, -PB1-Len, -PA, -HA, -NP, -NA, -M, and -NS-Len plasmids. At 12 h p.t., medium was replaced with p.i. medium and TCS were collected at three days p.t., clarified, and used to infect fresh monolayers of MDCK cells. After three days p.i., PR8-Len virus was plaque purified and scaled up using MDCK cells at 33 °C, as described [43].

2.5. Virus Growth Kinetics

Multicycle growth kinetics were carried out by infecting MDCK cells (12-well plate format, 5×10^5 cells/well, triplicates) with PR8/WT, PR8/AA and PR8/Len at a multiplicity of infection (MOI) of 0.001. After 1 h of viral adsorption at RT, infection medium was replaced by p.i. medium and plates were incubated at different temperatures (33 °C, 37 °C and 39 °C). TCS were collected at the indicated times p.i. and viral titers were determined by immunofocus assay (FFU/mL) in MDCK cells as indicated before [46]. Mean values and SDs were calculated using Microsoft Excel software.

2.6. Plaque Assays

Monolayers of MDCK cells (6-well plate format, 1×10^6 cells/well) were infected with PR8/WT, PR8/AA and PR8/Len for 1 h at RT, overlaid with agar, and incubated at 33 °C, 37 °C, or 39 °C [13]. At three days p.i., cells were fixed for 1 h at RT with 4% paraformaldehyde (PFA) and the overlays were removed. Cells were then permeabilized (0.5% Triton X-100 in PBS) for 15 min at RT and immunostained using the anti-NP mAb HB-65 and Vector kits (Vectastain ABC Vector kits and DAB HRP substrate kit; Vector) according to the manufacturer's specifications.

2.7. Animal Experiments

Six-to-eight-week-old female C57BL/6 mice were purchased from the National Cancer Institute (NCI) and maintained in the animal care facility at the University of Rochester under specific pathogen-free conditions. All animal protocols were approved by the University Committee of Animal Resources (UCAR-2014-019E, approval date 08/29/2919) and complied with the recommendations in the Guide for the Care and Use of Laboratory Animals of the National Research Council [48]. To evaluate the in vivo attenuation of PR8/AA and PR8/Len viruses, mice (N = 5) were anesthetized intraperitoneally (i.p.) with 2,2,2-tribromoethanol (Avertin; 240 mg/kg of body weight) and inoculated intranasally (i.n.) with 30 µL of a virus preparation containing the indicated doses of virus diluted in PBS [49]. Mice were monitored daily for 14 days for morbidity (body weight loss) and mortality (survival). Mice showing 25% loss of their initial body weight were considered to have reached the experimental endpoint and were humanely euthanized [49]. The 50% mouse lethal dose (MLD_{50}) was determined using the Reed and Muench method [50]. To evaluate virus replication, mice (N = 6) were anesthetized and infected as described and viral titers in homogenized lungs at 2 (N = 3) and 4 (N = 3) days p.i. were determined by immunofocus assay (FFU/mL) as previously described in MDCK cells at 33 °C [11–13,21,49]. The mean values and SDs were calculated using Microsoft Excel software.

For the vaccination and challenge experiments, 6–8-week-old female C57BL/6 mice (N = 5) were anesthetized and vaccinated i.n. with the indicated doses and viruses. A group of mice (N = 5) was also mock vaccinated with PBS as negative control. At fourteen days post-vaccination, mouse sera were collected by submandibular bleeding to evaluate the presence of total influenza antibodies (Abs) by enzyme-linked immunosorbent assay (ELISA) and hemagglutination inhibiting antibodies by hemagglutination inhibition (HAI) assay [49]. Twenty-four hours after bleeding, animals were challenged i.n. with the indicated dose of homologous (PR8) or heterologous (X31) WT viruses. After challenge, mice were monitored daily for 14 days for morbidity (body weight loss) and mortality (survival) as described above. Viral titers in the lungs of challenged mice were also calculated (see above). In the homologous (PR8) challenge, and to compare the differences in the protection efficacy provided by PR8/AA and PR8/Len viruses, we used a high dose (1000 MLD_{50}) of WT PR8. For the heterologous challenge, since the majority of the neutralizing antibodies induced after LAIV vaccination are directed against the viral surface HA and NA glycoproteins that are different between our vaccine PR8 viruses and the challenge X31 virus, a low viral dose (50 MLD_{50}) was used in these experiments.

2.8. Enzyme-Linked Immunosorbent Assays (ELISAs)

We evaluated the levels of total virus-specific Abs in the sera of vaccinated mice by ELISA as described [11,21,38,46,49,51]. Briefly, 96-well plates were coated with cell lysates from mock-, PR8/WT- and X31-infected MDCK cells or with 250 ng/well of recombinant PR8 HA protein (NR-19240; BEI Resources) and incubated ON at 4 °C. Mouse sera were tested as two-fold dilutions (starting dilution of 1:50) and titers determined as described [46,49].

2.9. Hemagglutination Inhibition (HAI) Assays

To evaluate the presence of hemagglutination inhibiting antibodies, mouse sera were treated with receptor-destroying enzyme (RDE; Denka Seiken) for 16 h at 37 °C and heat inactivated for 30 min at 56 °C. Then, sera were serially 2-fold diluted (starting dilution of 1:50) in 96-well V-bottom plates and mixed 1:1 with 4 hemagglutinating units (HAU) of the indicated viruses during 30 min at RT. HAI titers were determined by adding 0.5% turkey red blood cells to the virus-Ab mixtures followed by a 30 min incubation on ice [11]. The geometric mean titers and SDs from individual mice (N = 5) were calculated from the last well where hemagglutination was inhibited [49].

2.10. Evaluation of T Cell Responses

Six-to-eight-week-old female C57BL/6 mice (N = 5) were anesthetized and immunized with 10^3 FFU of PR8/AA or with 10^3 and 10^4 FFU of PR8/Len, or mock- vaccinated with PBS. At 10 days p.i., lungs and spleens were collected and processed to obtain cellular preparations. Lungs were perfused with PBS before being surgically removed and dissociated in Gentle MACS (MiltenyiBiotek) C tubes using the Lung01 program. Samples were incubated in 5 mL (2 µg/mL) of Collagenase II in RPMI-1640 medium containing 8% FBS for 30 min at 37 °C with gentle agitation every 10 min. After digestion, samples were further dissociated using the Heart01 program. Cell suspensions were filtered through 70 µm filters prior to 75:40 Percoll (GE Healthcare) discontinuous gradient separation. The top layer (containing fat and other debris) was eliminated by aspiration. The cell layer was then harvested and washed, prior to counting and staining. Single-cell suspensions were prepared from collected spleens by disruption in RPMI +8% FBS; yields were quantitated by viable cell counts using Trypan blue exclusion on a hemocytometer.

Single cell suspensions were prepared for Flow cytometry analysis by staining in PBS containing 1% FBS, purified CD16/32 (clone 2.4G2), NP and PA tetramers, and the following antibodies: TCRβ-PerCPCy5.5, CD8α-FITC, CD4-BV421, CD44-APCCy7, and CD62L-PECy7. Cells were subsequently stained for viability using Live Dead Aqua (Invitrogen). All antibodies were obtained from eBioscience, BD Biosciences, or Biolegend. PA and NP tetramers [11,12,25,52] were obtained from the NIH tetramer core facility (Atlanta, GA). Cells were analyzed by an LSRII (BD Biosciences) in the University of Rochester Flow Cytometry core facility and analyzed using FlowJo software (Tree Star).

3. Results

3.1. Mutations of the US AA MDV and Russian Len MDV Confer Different Levels of Temperature Sensitivity to the Polymerase of PR8

In a previous work [35], we introduced four of the five mutations (NP already contains a G at position 34) responsible for the *ts*, *ca* and *att* phenotypes of the US AA MDV [32,33] into the PB2 (N265S) and PB1 (K391E, E581G and A661T) genes of PR8 to create a PR8 LAIV (named henceforth PR8/AA) (Figure 1A). In vitro, these mutations affected viral replication at non-permissive temperatures (37 °C–39 °C), and the virus was attenuated in a mouse model of infection as compared to wild-type PR8 (PR8/WT) [35].

To evaluate if the *ts*, *ca* and *att* mutations of the Russian Len MDV [34] resulted in a similar phenotype in the backbone of PR8 (named henceforth PR8/Len), we introduced the amino acid substitutions into PR8's PB2 (V478L), PB1 (K265N and V591I) and NEP (M100I) (Figure 1A) and tested them in a minigenome assay (Figure 1B,C). Green Fluorescence Protein (GFP) and Gaussia luciferase (Gluc) expression levels induced by PR8/WT polymerase were similar at the three temperatures assayed (33 °C, 37 °C and 39 °C). In the case of cells transfected with the PR8/AA polymerase complex, GFP and Gluc expression were reduced at 37 °C and, more notably, at 39 °C in comparison with the expression levels at 33 °C (~ 50% and ~ 70% reduction, respectively). Likewise, GFP and Gluc expression levels in cells transfected with the PR8/Len polymerase were highly reduced at 37 °C and almost undetectable at 39 °C as compared to the levels observed at 33 °C. These results demonstrate that the mutations of the Russian Len MDV induce a more robust temperature sensitive phenotype than the mutations of the US AA MDV in the context of the viral polymerase complex of PR8.

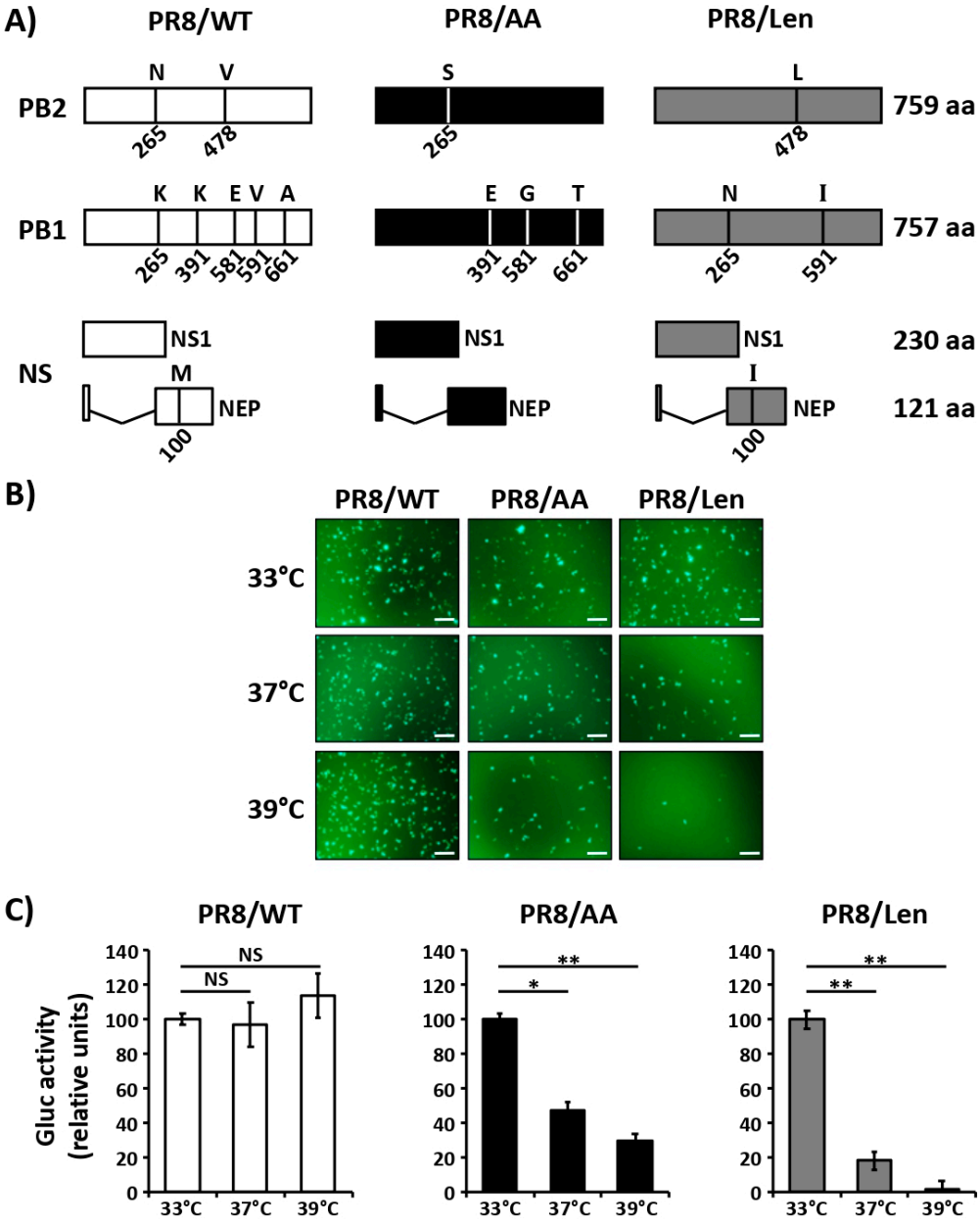


Figure 1. Effect of temperature on the polymerase activity of PR8/AA and PR8/Len. (**A**) Schematic representation of segments 1 (PB2), 2 (PB1) and 8 (NS) of PR8/WT (white, left), PR8/AA (black, middle) and PR8/Len (grey, right). Amino acid substitutions to generate PR8/AA and PR8/Len are indicated. B-C) Minigenome activity: HEK293T cells (12-well plate format, 4×10^5 cells/well, triplicates) were transiently co-transfected with 250 ng of ambisense pDZ expression plasmids encoding the minimal requirements for viral genome replication and gene transcription (PB2, PB1, PA, and NP) together with 500 ng of a vRNA-like expression plasmid encoding GFP (**B**) or Gluc (**C**) under the control of the human polymerase I promoter (hPol-I-GFP and -Gluc, respectively), and 100 ng of an SV40 Cluc expressing plasmid to normalize transfection efficiencies. After transfection, cells were placed at 33 °C, 37 °C, or 39 °C, and viral replication and transcription was evaluated 24 h later by GFP (**B**) and luciferase (**C**) expression. Gluc activity was normalized to that of Cluc. Data represent means and SDs of the triplicates. Normalized reporter expression is relative to that obtained in the absence of pDZ NP. Data were represented as relative activity considering the activity of each polymerase complex at 33 °C as 100%. *, $P < 0.05$; **, $P < 0.01$; NS, no statistical differences (Student *t* test). Scale bars, 200 μm.

Both of the commercial/licensed lineages of LAIV (AA and Len) have mutations in the PB2 and PB1 viral segments. Thus, we next evaluated which of the viral segments has a more significant impact on the temperature sensitive phenotype in PR8. Using the same minigenome approach and different combinations of PB2 and PB1 viral segments of PR8/WT, PR8/AA or PR8/Len, GFP (Figure 2A) and Gluc (Figure 2B) expression levels were evaluated. PR8/WT polymerase activity was similar at the three tested temperatures (33 °C, 37 °C and 39 °C), while reporter gene expression by PR8/AA and PR8/Len polymerase complexes was reduced at 37 °C and, more markedly, at 39 °C, similar to our initial minigenome studies (Figure 1). When PR8/AA PB2 or PB1 were combined with PR8/WT PB1 and PB2, respectively, we observed reduced GFP and Gluc expression levels at 37 °C and 39 °C as compared to those at 33 °C (Figure 2A,B). However, the AA PB1 mutations conferred a stronger *ts* phenotype effect than the AA PB2 mutations. In the case of PR8/Len, both the PB1 and PB2 segments induced a similar decrease in GFP and Gluc expression at 37 °C and 39 °C (Figure 2A,B). Remarkably, the combinations that contain only one of the viral segments (PB2 or PB1) with the LAIV mutations (AA or Len) had an accentuated *ts* phenotype in our minigenome assays. These results demonstrate that mutations in both PB2 and PB1 segments are responsible for the *ts* phenotype of AA and Len MDV and an additive effect in the polymerase activity at high temperatures is observed when both viral proteins (PB2 and PB1) have the aforementioned mutations.

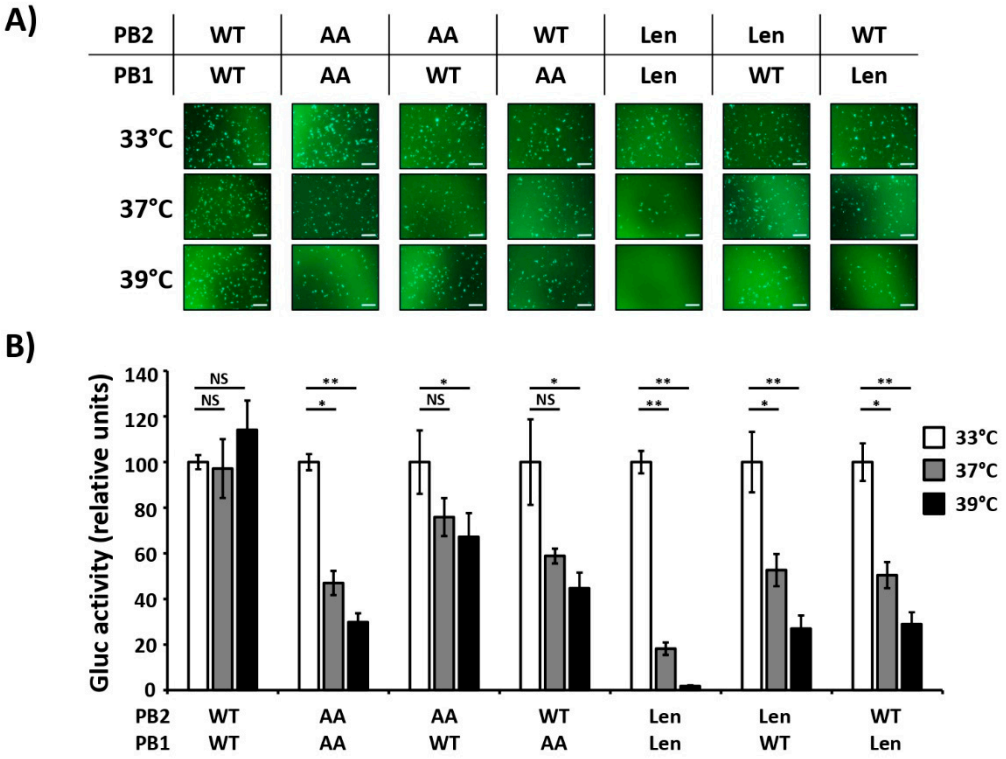


Figure 2. Contribution of PB2 and PB1 mutations of PR8/AA and PR8/Len in the viral polymerase activity at different temperatures. HEK293T cells (12-well plate format, 4×10^5 cells/well, triplicates) were transiently co-transfected with 250 ng of the indicated combinations of ambisense pDZ expression plasmids encoding the PB2 and PB1 from PR8/WT, PR8/AA and PR8/Len together with the pDZ encoding PA and NP PR8/WT proteins; together with 500 ng of the hPol-I-GFP (**A**) and -Gluc (**B**), and 100 ng of SV40 Cluc to normalize transfection efficiencies. After transfection, cells were placed at 33 °C, 37 °C, or 39 °C, and reporter gene expression was evaluated 24 h later by GFP imaging (**A**) and Gluc expression (**B**). Gluc activity was normalized to that of Cluc. Data represent means and SDs of the triplicates. Normalized reporter expression is relative to that in the absence of pDZ NP plasmid. Data were represented as relative activity considering the activity of each polymerase complex at 33 °C as 100%. *, $P < 0.05$; **, $P < 0.01$; NS, no statistical differences (Student *t* test). Scale bars, 200 μm.

Viruses **2019**, *11*, x FOR PEER REVIEW 9 of 19

3.2. Recombinant PR8/Len is More Temperature Sensitive than PR8/AA

Based on the minigenome results using transfected cells in which Len MDV mutations induced a stronger reduction in the PR8 polymerase activity at high temperatures (37 °C and 39 °C) than those induced by the AA MDV mutations (Figures. 1 and 2), we next evaluated the impact of the AA and Len MDV mutations in the context of PR8 viral infections. To that end, we used reverse genetics [43] to rescue a PR8/Len virus and then evaluated and compared the viral replication kinetics (Figure 3A) and plaque phenotype (Figure 3B) of PR8/Len with those of PR8/WT and our previously described PR8/AA [35] at different temperatures (33 °C, 37 °C and 39 °C). At 33 °C, PR8/WT reached higher viral titers than PR8/AA and PR8/Len viruses at early times (12 h and 24 h) post-infection (p.i.), but at 72 h p.i. the three viruses reached similar viral titers (Figure 3A). Replication of PR8/WT at 37 °C and 39 °C was similar to that observed at 33 °C. However, as previously described [35], PR8/AA replication was reduced at 37 °C and abolished at 39 °C. In the case of PR8/Len, replication was only reduced at the earliest time point (12 h) at 37 °C, and was similar to PR8/WT at later times p.i. At 39 °C, PR8/Len was also reduced at early times p.i. but reached similar viral titers than PR8/WT at 72 h p.i. Likewise, the plaque phenotype of PR8/WT was similar at 33 °C and 37 °C and slightly reduced at 39 °C (Figure 3B), in agreement with the results of the growth kinetic studies (Figure 3A). In the case of PR8/AA, both the number and the size of the plaques were reduced (37 °C), or not detected (39 °C), when compared to 33 °C. PR8/Len could only generate plaques at 33 °C, corroborating the growth kinetics results (Figure 3A). Taken together, these results demonstrate that the mutations of the Russian Len MDV induce a more clear temperature sensitive phenotype in the backbone of PR8 than the mutations of the US AA MDV.

Based on the minigenome results using transfected cells in which Len MDV mutations induced a stronger reduction in the PR8 polymerase activity at high temperatures (37 °C and 39 °C) than those induced by the AA MDV mutations (Figures. 1 and 2), we next evaluated the impact of the AA and Len MDV mutations in the context of PR8 viral infections. To that end, we used reverse genetics [43] to rescue a PR8/Len virus and then evaluated and compared the viral replication kinetics (Figure 3A) and plaque phenotype (Figure 3B) of PR8/Len with those of PR8/WT and our previously described PR8/AA [35] at different temperatures (33 °C, 37 °C and 39 °C). At 33 °C, PR8/WT reached higher viral titers than PR8/AA and PR8/Len viruses at early times (12 h and 24 h) post-infection (p.i.), but at 72 h p.i. the three viruses reached similar viral titers (Figure 3A). Replication of PR8/WT at 37 °C and 39 °C was similar to that observed at 33 °C. However, as previously described [35], PR8/AA replication was reduced at 37 °C and abolished at 39 °C. In the case of PR8/Len, replication was only reduced at the earliest time point (12 h) at 37 °C, and was similar to PR8/WT at later times p.i. At 39 °C, PR8/Len was also reduced at early times p.i. but reached similar viral titers than PR8/WT at 72 h p.i. Likewise, the plaque phenotype of PR8/WT was similar at 33 °C and 37 °C and slightly reduced at 39 °C (Figure 3B), in agreement with the results of the growth kinetic studies (Figure 3A). In the case of PR8/AA, both the number and the size of the plaques were reduced (37 °C), or not detected (39 °C), when compared to 33 °C. PR8/Len could only generate plaques at 33 °C, corroborating the growth kinetics results (Figure 3A). Taken together, these results demonstrate that the mutations of the Russian Len MDV induce a more clear temperature sensitive phenotype in the backbone of PR8 than the mutations of the US AA MDV.

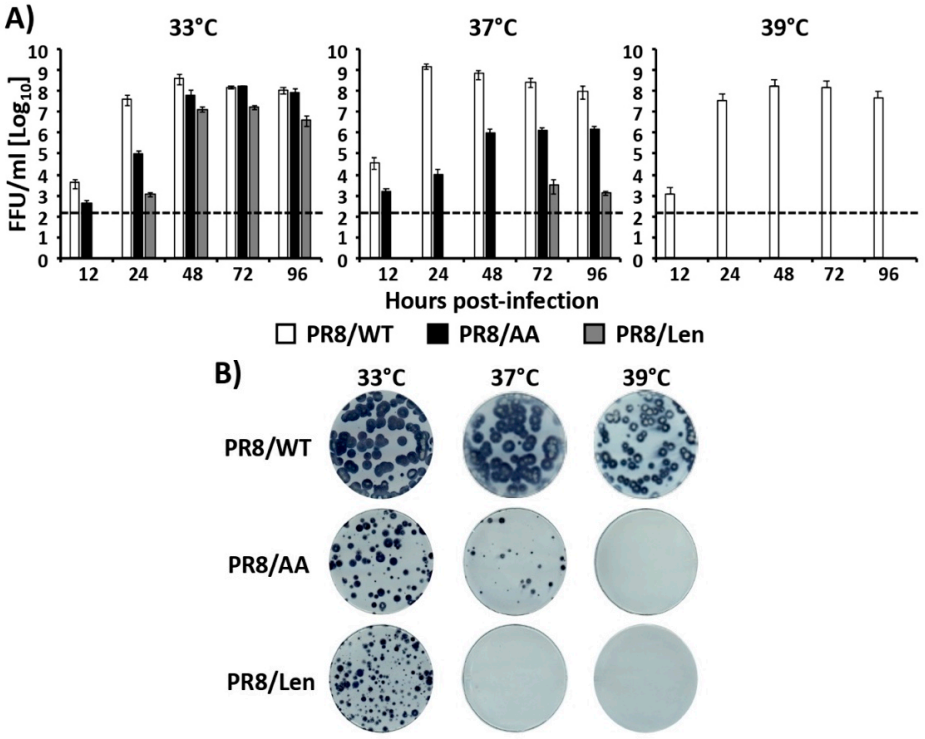


Figure 3. In vitro characterization of PR8/AA and PR8/Len viruses. (**A**) Multicycle growth kinetics: MDCK cells (12-well plate format, 4 × 10^5 cells/well, triplicates) were infected at low MOI (0.001) with PR8/WT (white bars), PR8/AA (black bars) and PR8/Len (grey bars) viruses and placed at 33 °C, 37 °C, or 39 °C. Tissue culture supernatants were recovered at the indicated times post-infection (p.i.) and viral titers were determined by immunofoetis assay (FFU/mL) using an anti-NP mAb (HB-65). Data represent the means and SDs of the results determined from triplicate wells. Dotted black lines indicate the limit of detection (200 FFU/mL). (**B**) Plaque assays: MDCK cells (6-well plate format, 1 × 10^6 cells/well) were infected with PR8/WT, PR8/AA or PR8/Len viruses and incubated at 33 °C, 37 °C, or 39 °C for 3 days. Plaque phenotype was assessed by immunostaining with the HB-65 anti-NP mAb.

Figure 3. In vitro characterization of PR8/AA and PR8/Len viruses. (**A**) Multicycle growth kinetics: MDCK cells (12-well plate format, 4 × 10^5 cells/well, triplicates) were infected at low MOI (0.001) with PR8/WT (white bars), PR8/AA (black bars) and PR8/Len (grey bars) viruses and placed at 33 °C, 37 °C, or 39 °C. Tissue culture supernatants were recovered at the indicated times post-infection (p.i.) and viral titers were determined by immunofoetis assay (FFU/mL) using an anti-NP mAb (HB-65). Data represent the means and SDs of the results determined from triplicate wells. Dotted black lines indicate the limit of detection (200 FFU/mL). (**B**) Plaque assays: MDCK cells (6-well plate format, 1 × 10^6 cells/well) were infected with PR8/WT, PR8/AA or PR8/Len viruses and incubated at 33 °C, 37 °C, or 39 °C for 3 days. Plaque phenotype was assessed by immunostaining with the HB-65 anti-NP mAb.

3.3. Attenuation of PR8/Len and PR8/AA in a Mouse Model of Influenza Infection

In our next set of experiments, we compared the virulence of both PR8 LAIVs in vivo (Figure 4). To that end, groups of C57BL/6 mice (N = 5) were infected with 10^3, 10^4, 10^5 and 10^6 fluorescent forming units (FFU) of PR8/AA (Figure 4A,B) or PR8/Len (Figure 4C,D) and monitored over 14 days p.i. for body weight loss (Figure 4A,C) and survival (Figure 4,D). As previously described [35], mice infected with 10^5 and 10^6 FFU of PR8/AA showed a dramatic weight loss at early times p.i. (Figure 4A), resulting in a rate of mortality of 100% at days 5 and 8 p.i., respectively (Figure 4B). Two mice (40%) infected with 10^4 FFU of PR8/AA lost weight and died at day 8 p.i., while mice infected with 10^3 FFU of PR8/AA virus did not show noticeable weight loss and all of them survived infection, resulting in a theoretical 50% mouse lethal dose (MLD_{50}) of ~1.5×10^4 FFU, as previously described [50]. In the case of PR8/Len (Figure 4C,D), all mice infected with 10^6 FFU died at day 6p.i., 40% of mice survived infection with 10^5 FFU and those infected with 10^4 and 10^3 FFU did not show body weight loss and all survived viral infection, resulting in a calculated MLD_{50} of ~6.8×10^4 FFU (i.e., ~5 fold greater attenuation than PR8/AA) [50].

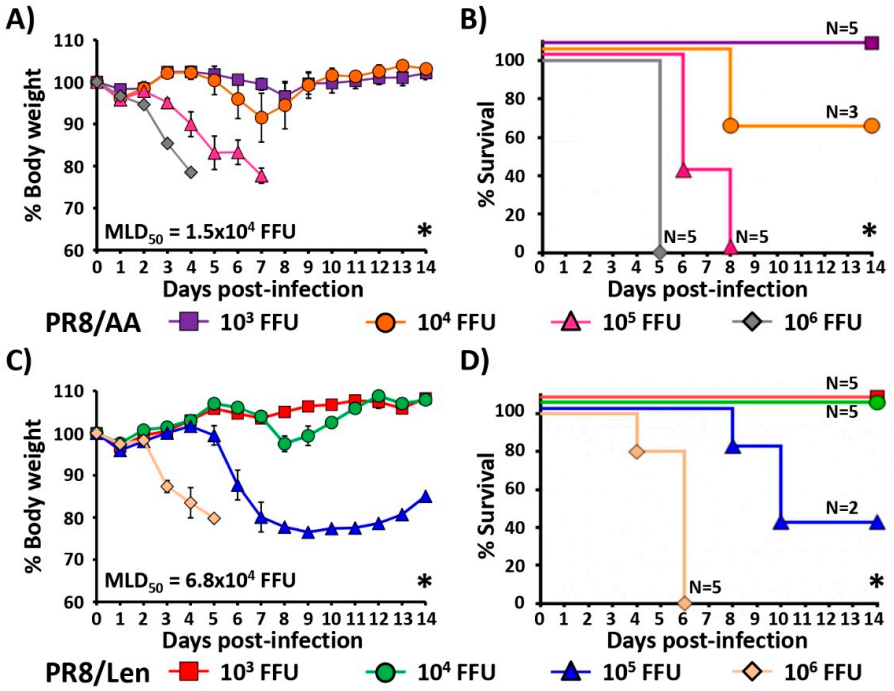


Figure 4. Attenuation of PR8/AA and PR8/Len viruses in vivo. Six-to-8-week-old female C57BL/6 mice (n = 5) were infected intranasally (i.n.) with the indicated FFU of PR8/AA (**A**,**B**) or PR8/Len (**C**,**D**) viruses and then monitored daily for 2 weeks for body weight loss (**A**,**C**) and survival (**B**,**D**). Mice that lost 25% of their initial body weight were sacrificed. Data represent the means and SDs of the results determined for individual mice (n = 5). The viral 50% mouse lethal dose (MLD_{50}) for PR8/AA and PR8/Len were calculated based on survival data using the method of Reed and Muench [50]. (**A**,**C**) Statistical analysis was performed using one-way ANOVA test comparing % body weight loss between groups (* $P < 0.0001$). (**B**,**D**) Statistical analysis was performed using log-rank (Mantel-Cox) test (* $P < 0.0001$).

We also evaluated viral replication in the lungs of mice infected with PR8/Len and PR8/AA. To that end, groups of C57BL/6 mice (N = 6) were infected with 10^3 and 10^4 FFU of PR8/Len or 10^3 FFU of PR8/AA (doses that resulted in 100% survival, Figure 4) and viral replication was evaluated at days 2 (N = 3) and 4 (N = 3) p.i. (Figure 5A). No statistically significant differences were observed in lung viral titers in animals infected with PR8/Len or PR8/AA, although higher viral titers were detected in the lungs of mice infected with 10^4 FFU of PR8/Len.

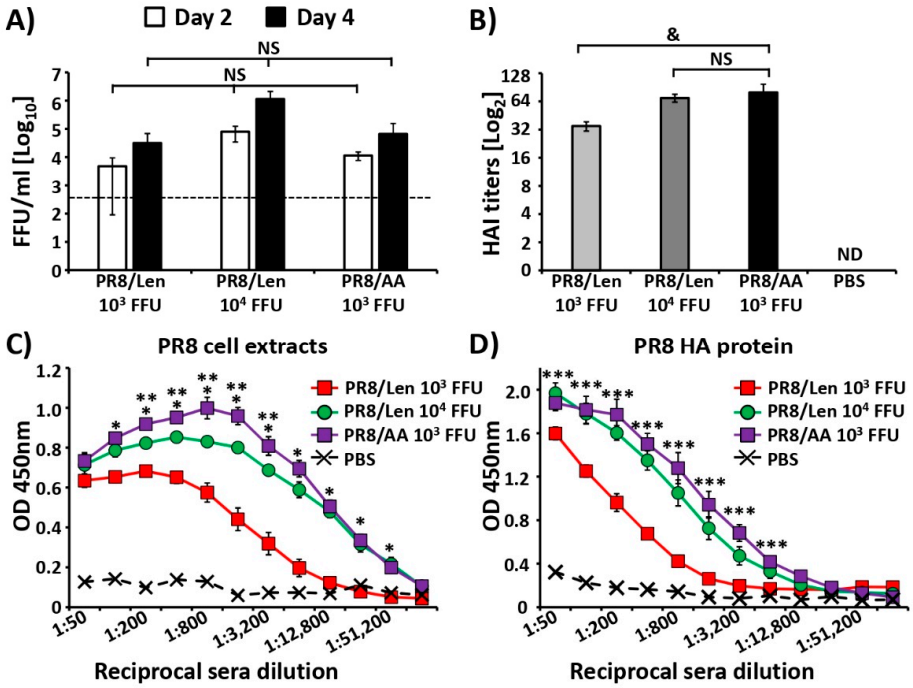


Figure 5. Replication of PR8/AA and PR8/Len viruses in mice and induction of humoral immune responses. (**A**) Lung viral titers: Six-to-eight-week-old female C57BL/6 mice (n = 6) were infected i.n. with 10^3 and 10^4 FFU of PR8/Len and 10^3 FFU of PR8/AA viruses. Viral titer in lungs of infected mice was evaluated at days 2 and 4 p.i. (n = 3) by immunofocus assay (FFU/mL) in MDCK at 33 °C using an anti-NP mAb (HB-65). Data represent the means and SDs of the results determined from each group of mice (n = 3). Dotted black line represents the limit of detection of the assay (200 FFU/mL). NS, no statistical differences (Student t test). (**B**–**D**) Humoral immune responses: Six-to-eight-week-old female C57BL/6 mice (n = 5) were infected i.n. with 10^3 and 10^4 FFU of PR8/Len and 10^3 FFU of PR8/AA viruses, or mock-infected (PBS). At 14 days p.i., mice were bled and sera were collected and evaluated individually by HAI assay for hemagglutination inhibiting antibodies (**B**) and by ELISA for IgG Abs against total influenza viral proteins using cell extracts of MDCK cells infected with PR8/WT (**C**) or against recombinant purified PR8 HA protein (**D**). (**B**) HAI titers: ND, not detected. &, $p < 0.05$ (PR8/Len 10^3 FFU vs PR8/AA 10^4 FFU) (Student t test); NS, no statistical differences (Student t test). (**C**,**D**) ELISAs: OD, optical density. Data represent the means and SDs of the results for five individual mice. *, $p < 0.001$ (PR8/Len 10^3 FFU vs.PR8/AA 10^3 FFU); **, $p < 0.05$ (PR8/Len 10^4 FFU vs.PR8/AA 10^3 FFU); ***, $p < 0.01$ (PR8/Len 10^3 FFU vs.PR8/AA 10^3 FFU) (Student t test).

3.4. Immune Responses and Protection Efficacy of PR8/Len and PR8/AA in Mice against a Homologous Viral Challenge

We next evaluated and compared immune responses induced by PR8/Len and PR8/AA viruses (Figure 5B,D). Groups of C57BL/6 mice (N = 5) were immunized with the same non-lethal doses of PR8/Len (10^3/10^4 FFU) and PR8/AA (10^3 FFU) (Figure 4), or mock infected with PBS. Hemagglutination inhibition (HAI) assay results revealed a higher titer of hemagglutination inhibiting antibodies in mice vaccinated with 10^3 FFU of PR8/AA than those vaccinated with 10^3 FFU of PR8/Len, while no statistical differences were observed between the sera of mice immunized with 10^3 FFU of PR8/AA and 10^4 FFU of PR8/Len (Figure 5B). Humoral immune responses were also evaluated by ELISA using cell extracts from MDCK cells infected with PR8/WT virus (Figure 5C) or purified PR8 HA protein (Figure 5D). Sera from all virus-vaccinated mice showed antibodies against total PR8 viral proteins and against the viral HA (Figure 5C,D, respectively). Interestingly, sera from mice vaccinated with 10^3 FFU of PR8/AA showed a significantly higher titer of antibodies than sera from mice immunized

with 10^3 FFU of PR8/Len, while comparable antibody responses were detected in the sera from mice immunized with 10^3 FFU of PR8/AA and 10^4 FFU of PR8/Len.

To have a more complete analysis of immune responses, we also evaluated and compared the induction of CD8 T cell responses by PR8/AA and PR8/Len (Figure 6). To that end, groups of C57BL/6 mice (N = 5) were immunized with 10^3 or 10^4 FFU of PR8/Len, 10^3 FFU PR8/AA, or mock-vaccinated (PBS). At 10 days p.i., lungs and spleens were recovered and processed to collect CD8 T cells. The results showed that vaccination with both PR8 LAIVs induced NP- and PA-specific CD8 T cells in the lungs (Figure 6A,C) and the spleen (Figure 6D,F). Although no statistical differences were observed when comparing the responses induced by PR8/Len versus PR8/AA (with the exception of the levels of PA-specific CD8 T cells in the lungs of mice vaccinated with 10^3 and 10^4 FFU of PR8/Len, Figure 6C), the number of CD8 T cells in the lungs and spleen tended to be greater after vaccination with 10^4 FFU of PR8/Len and 10^3 FFU of PR8/AA than with 10^3 FFU PR8/Len. These results suggest that vaccination with both LAIVs elicits a robust virus-specific CD8 T cell response in the spleen and lung.

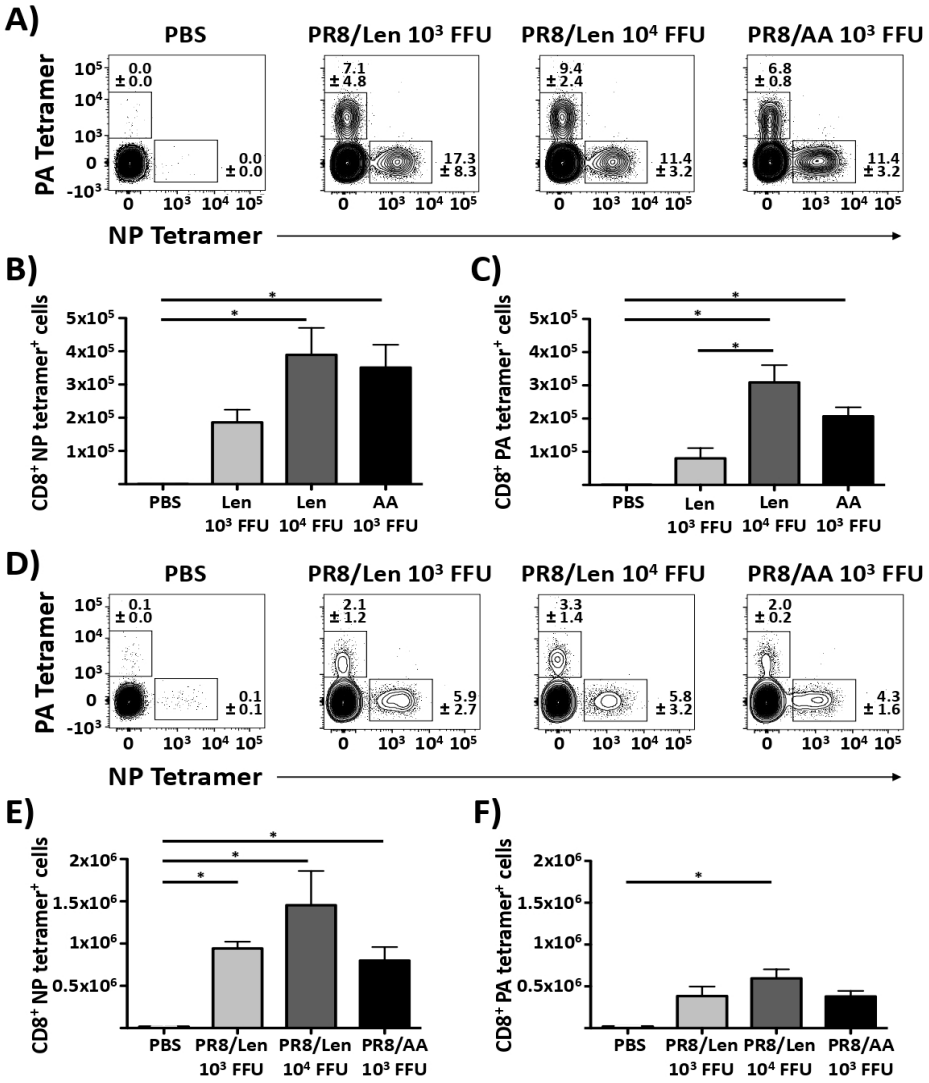


Figure 6. Induction of CD8 T cell responses by PR8/AA and PR8/Len viruses: Female six-to-eight-week-old C57BL/6 mice (n = 5) were infected (i.n.) with 10^3 and 10^4 FFU of PR8/Len and 10^3 FFU of PR8/AA viruses. Mice were also mock (PBS) infected as an internal control. Ten days p.i., lungs (**A**–**C**) and spleens (**D**–**F**) were collected and resident cells were prepared for flow cytometry. Live CD8 T cells specific for NP (**B**,**E**) or PA (**C**,**F**) tetramers were counted. Data represent the means +/− SDs of the results for 5 individual mice. *, $p < 0.001$ for the indicated pair wise comparisons (Student t test).

Figure 6. Induction of CD8 T cell responses by PR8/AA and PR8/Len viruses: Female six-to-eight-week-old C57BL/6 mice (n = 5) were infected (i.n.) with 10^3 and 10^4 FFU of PR8/Len and 10^3 FFU of PR8/AA viruses. Mice were also mock (PBS) infected as an internal control. Ten days p.i., lungs (**A**–**C**) and spleens (**D**–**F**) were collected and resident cells were prepared for flow cytometry. Live CD8 T cells specific for NP (**B** and **E**) or PA (**C** and **F**) tetramers were counted. Data represent the means +/− SDs of the results for 5 individual mice. *, $p < 0.001$ for the indicated pair wise comparisons (Student t test).

Having confirmed the immunogenicity of both LAIVs, we proceeded with challenge experiments, initially focusing on a homologous viral challenge (Figure 7). Groups of C57BL/6 mice ($N = 5$) were vaccinated with the same PR8/LAIVs doses used in the immunogenicity studies, or mock (PBS) vaccinated (Figure 6). At day 15 post-vaccination, mice were challenged with 1000× MLD$_{50}$ of PR8/WT and monitored over 10 days for body weight loss (Figure 7A) and survival (Figure 7B). All mice mock vaccinated lost weight quickly and died at days post-challenge. All mice vaccinated with PR8/Len (independently of the dose) and PR8/AA survived without body weight loss. These results indicate that although PR8/Len is more attenuated than PR8/AA (Figure 4), it is able to confer protection against a homologous PR8 viral challenge with the same viral dose (10^3 FFU, Figure 4). Since all mice survived the challenge with PR8/WT, we cannot conclude which one of the two LAIVs (PR8/AA or PR8/Len) is more protective.

Having confirmed the immunogenicity of both LAIVs, we proceeded with challenge experiments, initially focusing on a homologous viral challenge (Figure 7). Groups of C57BL/6 mice ($N = 5$) were vaccinated with the same PR8/LAIVs doses used in the immunogenicity studies, or mock (PBS) vaccinated (Figure 6). At day 15 post-vaccination, mice were challenged with 1000× MLD$_{50}$ of PR8/WT and monitored over 10 days for body weight loss (Figure 7A) and survival (Figure 7B). All mice mock vaccinated lost weight quickly and died at days post-challenge. All mice vaccinated with PR8/Len (independently of the dose) and PR8/AA survived without body weight loss. These results indicate that although PR8/Len is more attenuated than PR8/AA (Figure 4), it is able to confer protection against a homologous PR8 viral challenge with the same viral dose (10^3 FFU, Figure 4). Since all mice survived the challenge with PR8/WT, we cannot conclude which one of the two LAIVs (PR8/AA or PR8/Len) is more protective.

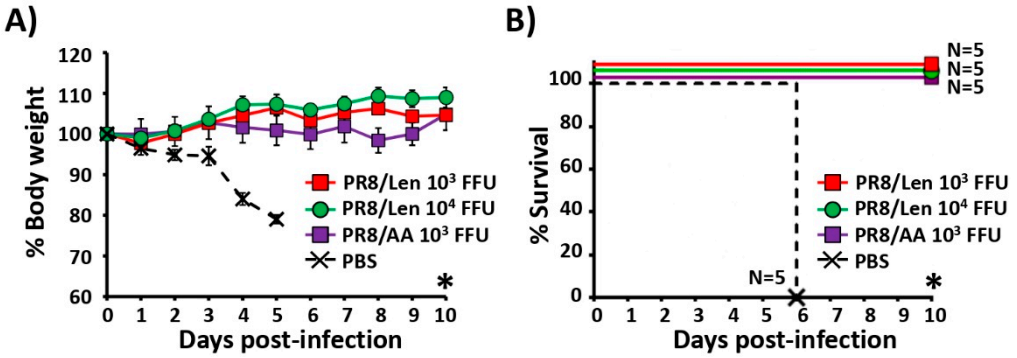


Figure 7. Protection efficacy of PR8/AA and PR8/Len against homologous viral challenge: Six-to-eight-week-old female C57BL/6 mice (n = 5) were infected i.n. with 10^3 and 10^4 FFU of PR8/Len and 10^3 FFU of PR8/AA viruses, or mock vaccinated (PBS). At 15 days p.i., mice were challenged i.n. with 1,000 MLD$_{50}$ of PR8/WT and monitored daily over 10 days for body weight loss (**A**) and survival (**B**). Mice that lost 25% of their initial body weight were sacrificed. Data represent the means and SDs of the results determined for individual mice (n = 5). Statistical analysis was performed using one-way ANOVA (**A**) and Dunnett's (**B**) tests comparing the PBS group to the other groups (* $P < 0.0001$).

3.5. Immune Responses and Protection Efficacy of PR8/Len and PR8/AA Against a Heterologous Viral Challenge

We next examined the humoral immune responses and the protection efficacy of PR8/Len and PR8/AA against a heterologous challenge with X31 (H3N2) (Figure 8). Groups of C57BL/6 mice ($N = 5$) were vaccinated with the same PR8/Len and PR8/AA viral doses used in the homologous challenge studies (Figure 7). Fourteen days post-vaccination, mice were bled and the presence of total antibodies against X31 were analyzed by ELISA. Sera from mice immunized with 10^3 FFU of PR8/AA showed significantly higher antibody titers than sera from mice vaccinated with 10^3 FFU of PR8/Len and, to a lower extent, than mice vaccinated with 10^4 FFU of PR8/Len. It is worth mentioning that X31 is a PR8 virus containing the HA and NA of A/Hong Kong/68 H3N2. Contrarily, the PR8 LAIVs (both AA and Len) contain their respective H1N1 glycoproteins and, therefore, the antibodies detected in the ELISA are mainly directed against internal PR8 viral proteins, which are the same in all viruses.

We next examined the humoral immune responses and the protection efficacy of PR8/Len and PR8/AA against a heterologous challenge with X31 (H3N2) (Figure 8). Groups of C57BL/6 mice ($N = 5$) were vaccinated with the same PR8/Len and PR8/AA viral doses used in the homologous challenge studies (Figure 7). Fourteen days post-vaccination, mice were bled and the presence of total antibodies against X31 were analyzed by ELISA. Sera from mice immunized with 10^3 FFU of PR8/AA showed significantly higher antibody titers than sera from mice vaccinated with 10^3 FFU of PR8/Len and, to a lower extent, than mice vaccinated with 10^4 FFU of PR8/Len. It is worth mentioning that X31 is a PR8 virus containing the HA and NA of A/Hong Kong/68 H3N2. Contrarily, the PR8 LAIVs (both AA and Len) contain their respective H1N1 glycoproteins and, therefore, the antibodies detected in the ELISA are mainly directed against internal PR8 viral proteins, which are the same in all viruses.

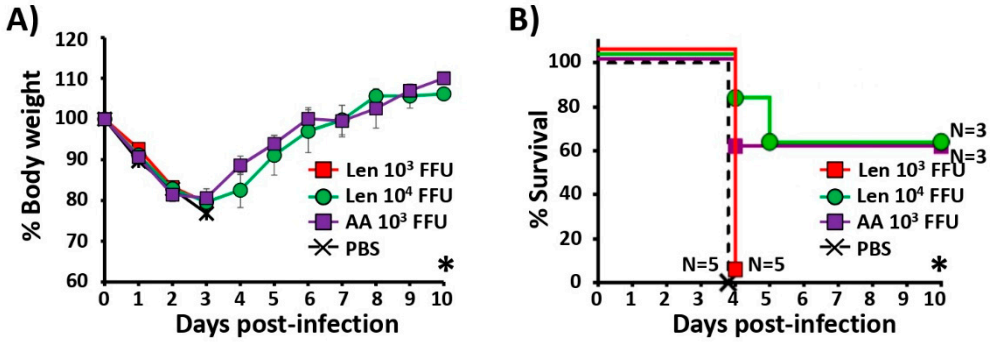


Figure 8. Protection efficacy induced by PR8/AA and PR8/Len against heterologous virus challenge. Six-to-eight-week-old female C57BL/6 mice (n = 5) were infected i.n. with 10^3 and 10^4 FFU of PR8/Len or 10^3 FFU of PR8/AA viruses, or mock-infected (PBS). At 15 days p.i., mice were challenged i.n. with 50 MLD_{50} of X-31 and then monitored daily over 10 days for body weight loss (**A**) and survival (**B**). Mice that lost 25% of their initial body weight were sacrificed. Data represent the means and SDs of the results determined for individual mice (n = 5). Statistical analysis was performed using one-way ANOVA (**A**) and Dunnett's (**B**) tests comparing the PBS group to the other groups (* $P < 0.0001$).

Then, fifteen days post-vaccination, mice were challenged with 50× MLD_{50} of X31 H3N2 and monitored daily over 10 days for body weight loss (Figure 8A) and survival (Figure 8B). Mock-vaccinated mice and mice vaccinated with 10^3 FFU of PR8/Len lost weight and all succumbed to viral challenge with X31 at day 4 post-challenge (Figure 8A,B). Mice vaccinated with 10^3 FFU of PR8/AA and 10^4 FFU of PR8/Len also lost weight (Figure 8A) but 60% of them (in both groups) recovered and survived the X31 lethal challenge (Figure 8B). These results indicate that, at the same dose, PR8/AA induces stronger immune responses and protection against a heterologous viral challenge than PR8/Len. However, induction of immune responses and protection efficacy with 10^4 FFU of PR8/Len is equivalent to that induced with 10^3 FFU of PR8/AA. Altogether, these results indicate that it is necessary to vaccinate mice with a higher dose (~1 log) of PR8/Len than PR8/AA to induce the same levels of protective immunity against a heterologous challenge.

4. Discussion

The mutations responsible for the *ts*, *ca* and *att* phenotypes of the two commercially available MDVs (US (AA) and Russian (Len)) have been previously described [22,24,30,53–57]. One mutation in PB2 (N265S), three substitutions in PB1 (K391E, E581G and A661T) and one amino acid change in NP (D34G) are the major contributors to the *ts*, *ca* and *att* phenotype of US AA MDV. Mutations located in the PB2 (V478L), PB1 (K265N and V591I) and in the NEP (M100I) are responsible for the *ts*, *ca* and *att* phenotype of the Russian Len MDV (Figure 9). Using a bat influenza A virus polymerase structure solved by X-ray crystallography as a reference model (PDB ID 5M3H, [58]), which is homologous to H1N1 virus polymerase complex with greater than 80% sequence similarity (PB2: 83%, PB1: 89% and PA: 83%), the location of these mutations are identified as distal from the endonuclease catalytic site of the PA subunit and appear rather random. However, upon closer inspection, we realize many of these mutations are at or near the interface between subunits, in particular, A661T mutation present in the PB1 from US AA MDV, and V591I and K265N mutations found in the PB1 from Russian Len MDV (Figure 9B,D, respectively). Therefore, we speculate that the mutations responsible for the *ts*, *ca* and *att* phenotype may relate to their effect on polymerase complex formation, possibly affecting the stability of the complex, rather than affecting the stability of each subunit itself. Of particular note, it is interesting to see the presence of a mutation within the cap-binding domain of PB2 subunit (V478L, Figure 9C), possibly affecting its cap-snatching activity to generate a 5′-capped primer for transcription initiation. This mutation is only found in the Russian Len MDV, and perhaps explains the difference seen in its attenuation when compared to that of US AA MDV. However, further experiments are

necessary to elucidate the roles of the LAIV mutations and to gain a better mechanistic understanding of these attenuated LAIVs.

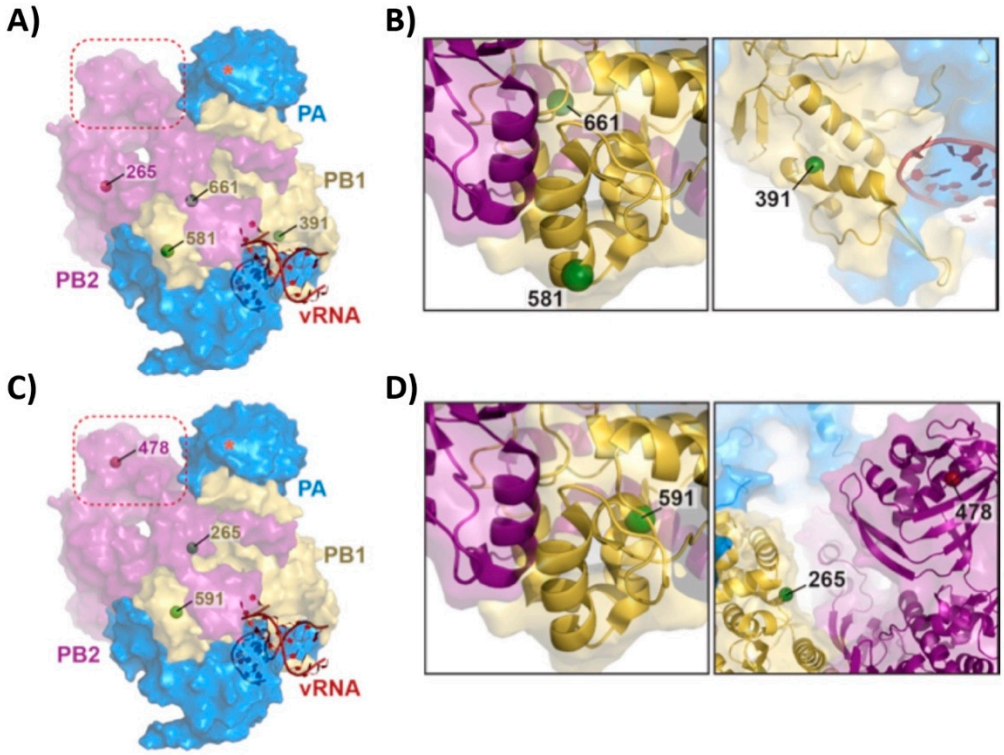


Figure 9. Location of the *ts*, *ca* and *att* mutations of AA and Len MDV in the viral polymerase complex. (**A**) PB1 (green spheres) and PB2 (purple sphere) mutations responsible for the ts, ca and att phenotype of AA are shown on the reference model of the RNA dependent RNA polymerase, RdRp, complex (PDB ID 5M3H) [58]. The RdRp complex is shown as a surface-rendering model with its subunits PA (blue), PB1 (yellow) and PB2 (purple), and bound vRNA (red). Dotted square (red) indicates the PB2 cap-binding domain. Red asterisk shows the approximate location of the endonuclease catalytic site of PA. (**B**) Close-up images of the locations of the AA PB1 mutations E581G and A661T (left) and K391E (right). (**C**) Same as in (**A**) but for Len. (**D**) Close up locations of LenV591I (PB1, left), K265N (PB1, right) and V478L (PB2, right) mutations. All images were generated and rendered in the program Pymol [59].

Since a direct comparison of the mutations responsible for the *ts*, *ca* and *att* phenotype of the US AA and the Russian Len MDVs in the same virus backbone had not been conducted, we introduced the mutations of the Russian Len MDV into PR8, and compared them to our previously described PR8 containing the US AA MDV mutations [35]. Using a minigenome assay, we observed that the mutations of the Russian Len MDV resulted in a greater reduction in polymerase activity at non-permissive (37ºC and 39ºC) temperatures compared to those of the US AA MDV (Figure 1). Similar results were obtained when the replicative phenotype of a recombinant PR8 containing the mutations in the PB2, PB1 and NEP of the Russian Len MDV (PR8/Len) was examined, and compared to our previously described PR8/AA [35]. In vitro results (multicycle growth kinetics and plaque phenotype) demonstrated that PR8/Len was more attenuated at high temperatures (37 °C and 39 °C) than PR8/AA (Figure 3), similar to our minigenome results (Figures 1 and 2). Analogous results were obtained in vivo since PR8/Len was more attenuated than PR8/AA, with the PR8/Len MLD_{50} being ~5× greater than the MLD_{50} of PR8/AA (Figure 4).

When we compared the ability of PR8/AA and PR8/Len to induce protective immune responses against homologous (Figure 5) and heterologous (Figure 8) viral challenges, as well as CD8T cell responses (Figure 6), we found that it was necessary to immunize mice with a ~ 1 log higher dose of PR8/Len (10^4 FFU) than PR8/AA (10^3 FFU) to reach similar levels of humoral (Figures 5 and 8)

and cellular (Figure 6) responses. Notably, vaccination with 10^3 FFU of PR8/Len induced complete protection against a homologous challenge with PR8 (Figure 7), while similar levels of protection against heterologous challenge with X-31 were observed using 10x more PR8/Len than PR8/AA (Figure 8). Although no statistically significant differences were observed in the levels of influenza-specific CD8 T cells induced with 10^3 or 10^4 FFU of PR8/Len, or 10^3 of PR8/AA (Figure 6A–C), levels of positive CD8 T cells in the lungs from mice vaccinated with 10^4 FFU PR8/Len and 10^3 FFU PR8/AA were similar - and greater than those observed in mice infected with 10^3 FFU of PR8/Len, correlating with the level of protection against X31 challenge (Figure 8).

Collectively, these results demonstrate that the mutations responsible for the *ts*, *ca* and *att* phenotypes of the US AA MDV can attenuate a broad range of other influenza viral strains, including human [35], canine [11,12,21] and equine [13] IAVs. Likewise, the mutations of the Russian Len MDV conferred robust *ts*, *ca* and *att* phenotypes in the genetic background of PR8. It remains to be determined whether this also applies to different influenza virus strains and/or subtypes. Nevertheless, our results have important implications for the development of new and improved LAIVs for the treatment of human and/or animal influenza infections. Specifically, our findings with PR8 suggest that it may be possible to update the MDV backbone of the currently available US or Russian H2N2 LAIVs by simply introducing the mutations of the Russian Len or US AA MDVs into the backbone of a more recent H1N1 (and maybe H3N2) seasonal circulating strain. However, it will be important to demonstrate that introduction of these *ts*, *ca* and *att* mutations results in the desired attenuated phenotype since we have previously shown that introduction of the US AA MDV mutations into the backbone of a recent pandemic Cal/09 did not resulted in an attenuated phenotype in vivo [37–39].

Author Contributions: Project was conceptualized by L.R., P.B.-L., E.C.R., T.M., A.N., A.S., D.J.T., S.D., B.K. and L.M.-S. Experiments were performed by L.R., P.B.-L., E.C.R. and A.N. Figure 9 was provided by T.M. and B.K. Manuscript was written by L.R. Manuscript was edited by P.B.-L., E.C.R., T.M., A.N., A.S., D.J.T., S.D., B.K. and L.M.-S.

Funding: This research was partially funded by the New York Influenza Center of Excellence (NYICE) (NIH 272201400005C), a member of the National Institute of Allergy and Infectious Diseases (NIAID), National Institutes of Health (NIH), Department of Health and Human Services, Centers of Excellence for Influenza Research and Surveillance (CEIRS) contract No. HHSN272201400005C (NYICE); the Department of Defense (DoD) Peer Reviewed Medical Research Program (PRMRP) grant W81XWH-18-1-0460 to LMS; and NIH T32GM068411 and T32GM007356 (to AS).

Acknowledgments: We thank the Biodefense and Emerging Infectious Research Resources Repository (BEI Resources) for providing reagents.

Conflicts of Interest: The authors declare no conflict of interest.

References

1. CDC. Disease Burden of Influenza. 2018. Available online: https://www.cdc.gov/flu/about/disease/burden.htm#economic (accessed on 9 October 2019).
2. Lynch, J.P., III; Walsh, E.E. Influenza: Evolving strategies in treatment and prevention. *Semin. Respir. Crit. Care Med.* **2007**, *28*, 144–158. [CrossRef] [PubMed]
3. Barr, I.G.; McCauley, J.; Cox, N.; Daniels, R.; Engelhardt, O.G.; Fukuda, K.; Grohmann, G.; Hay, A.; Kelso, A.; Klimov, A.; et al. Epidemiological, antigenic and genetic characteristics of seasonal influenza A(H1N1), A(H3N2) and B influenza viruses: Basis for the WHO recommendation on the composition of influenza vaccines for use in the 2009–2010 Northern Hemisphere season. *Vaccine* **2010**, *28*, 1156–1167. [CrossRef] [PubMed]
4. Smith, G.J.; Vijaykrishna, D.; Bahl, J.; Lycett, S.J.; Worobey, M.; Pybus, O.G.; Ma, S.K.; Cheung, C.L.; Raghwani, J.; Bhatt, S.; et al. Origins and evolutionary genomics of the 2009 swine-origin H1N1 influenza A epidemic. *Nature* **2009**, *459*, 1122–1125. [CrossRef] [PubMed]
5. Pica, N.; Palese, P. Toward a universal influenza virus vaccine: Prospects and challenges. *Annu. Rev. Med.* **2013**, *64*, 189–202. [CrossRef] [PubMed]

6. Belongia, E.A.; Kieke, B.A.; Donahue, J.G.; Greenlee, R.T.; Balish, A.; Foust, A.; Lindstrom, S.; Shay, D.K. Effectiveness of inactivated influenza vaccines varied substantially with antigenic match from the 2004–2005 season to the 2006–2007 season. *J. Infect. Dis.* **2009**, *199*, 159–167. [CrossRef] [PubMed]
7. Osterholm, M.T.; Kelley, N.S.; Sommer, A.; Belongia, E.A. Efficacy and effectiveness of influenza vaccines: A systematic review and meta-analysis. *Lancet Infect. Dis.* **2012**, *12*, 36–44. [CrossRef]
8. Cox, M.M.; Patriarca, P.A.; Treanor, J. FluBlok, a recombinant hemagglutinin influenza vaccine. *Influenza Other Respir Viruses* **2008**, *2*, 211–219. [CrossRef]
9. Palese, P.S.; Megan, L. *Fields Virology*, 5th ed.; Lippincott Williams & Wilkins: Philadelphia, PA, USA, 2007; Volume 2.
10. Hoft, D.F.; Babusis, E.; Worku, S.; Spencer, C.T.; Lottenbach, K.; Truscott, S.M.; Abate, G.; Sakala, I.G.; Edwards, K.M.; Creech, C.B.; et al. Live and inactivated influenza vaccines induce similar humoral responses, but only live vaccines induce diverse T-cell responses in young children. *J. Infect. Dis.* **2011**, *204*, 845–853. [CrossRef]
11. Nogales, A.; Rodriguez, L.; Chauche, C.; Huang, K.; Reilly, E.C.; Topham, D.J.; Murcia, P.R.; Parrish, C.R.; Martinez-Sobrido, L. A temperature sensitive live-attenuated canine influenza virus H3N8 vaccine. *J. Virol.* **2016**, *91*. [CrossRef]
12. Rodriguez, L.; Nogales, A.; Reilly, E.C.; Topham, D.J.; Murcia, P.R.; Parrish, C.R.; Martinez Sobrido, L. A live-attenuated influenza vaccine for H3N2 canine influenza virus. *Virology* **2017**, *504*, 96–106. [CrossRef]
13. Rodriguez, L.; Reedy, S.; Nogales, A.; Murcia, P.R.; Chambers, T.M.; Martinez-Sobrido, L. Development of a novel equine influenza virus live-attenuated vaccine. *Virology* **2018**, *516*, 76–85. [CrossRef] [PubMed]
14. Maassab, H.F. Adaptation and growth characteristics of influenza virus at 25 degrees c. *Nature* **1967**, *213*, 612–614. [CrossRef] [PubMed]
15. Aleksandrova, G.I.; Mikutskaia, B.A.; Pleshanova, R.A.; Panova, N.G.; Smorodintsev, A.A. The reactive and immunogenic properties and epidemiological effectiveness of further attenuated influenza virus vaccinal strains (observed in preschool children). *Vopr. Virusol.* **1965**, *10*, 67–73. [PubMed]
16. Wilson, W.D.; Robinson, D. Field safety of a modified-live, cold-adapted intranasal equine influenza vaccine (HESKAFlu Avert IN vaccine) in horses. *J. Equine Vet. Sci.* **2000**, *20*, 8–10. [CrossRef]
17. Youngner, J.S.; Whitaker-Dowling, P.; Chambers, T.M.; Rushlow, K.E.; Sebring, R. Derivation and characterization of a live attenuated equine influenza vaccine virus. *Am. J. Vet. Res.* **2001**, *62*, 1290–1294. [CrossRef] [PubMed]
18. Chan, W.; Zhou, H.; Kemble, G.; Jin, H. The cold adapted and temperature sensitive influenza A/Ann Arbor/6/60 virus, the master donor virus for live attenuated influenza vaccines, has multiple defects in replication at the restrictive temperature. *Virology* **2008**, *380*, 304–311. [CrossRef]
19. Murphy, B.R.; Coelingh, K. Principles underlying the development and use of live attenuated cold-adapted influenza A and B virus vaccines. *Viral Immunol.* **2002**, *15*, 295–323. [CrossRef] [PubMed]
20. Kohlmeier, J.E.; Woodland, D.L. Immunity to respiratory viruses. *Annu. Rev. Immunol.* **2009**, *27*, 61–82. [CrossRef]
21. Rodriguez, L.; Nogales, A.; Murcia, P.R.; Parrish, C.R.; Martinez-Sobrido, L. A bivalent live-attenuated influenza vaccine for the control and prevention of H3N8 and H3N2 canine influenza viruses. *Vaccine* **2017**, *35*, 4374–4381. [CrossRef]
22. Cheng, X.; Zengel, J.R.; Suguitan, A.L., Jr.; Xu, Q.; Wang, W.; Lin, J.; Jin, H. Evaluation of the humoral and cellular immune responses elicited by the live attenuated and inactivated influenza vaccines and their roles in heterologous protection in ferrets. *J. Infect. Dis.* **2013**, *208*, 594–602. [CrossRef] [PubMed]
23. Victor, S.T.; Watanabe, S.; Katsura, H.; Ozawa, M.; Kawaoka, Y. A replication-incompetent PB2-knockout influenza A virus vaccine vector. *J. Virol.* **2012**. [CrossRef]
24. De Villiers, P.J.; Steele, A.D.; Hiemstra, L.A.; Rappaport, R.; Dunning, A.J.; Gruber, W.C.; Forrest, B.D. Efficacy and safety of a live attenuated influenza vaccine in adults 60 years of age and older. *Vaccine* **2009**, *28*, 228–234. [CrossRef] [PubMed]
25. Baker, S.F.; Guo, H.; Albrecht, R.A.; Garcia-Sastre, A.; Topham, D.J.; Martinez-Sobrido, L. Protection against Lethal Influenza with a Viral Mimic. *J. Virol.* **2013**, *87*, 8591–8605. [CrossRef] [PubMed]
26. Powell, T.J.; Silk, J.D.; Sharps, J.; Fodor, E.; Townsend, A.R. Pseudotyped influenza A virus as a vaccine for the induction of heterotypic immunity. *J. Virol.* **2012**, *86*, 13397–13406. [CrossRef] [PubMed]

27. Uraki, R.; Kiso, M.; Iwatsuki-Horimoto, K.; Fukuyama, S.; Takashita, E.; Ozawa, M.; Kawaoka, Y. A novel bivalent vaccine based on a PB2-knockout influenza virus protects mice from pandemic H1N1 and highly pathogenic H5N1 virus challenges. *J. Virol.* **2013**, *87*, 7874–7881. [CrossRef]
28. Katsura, H.; Iwatsuki-Horimoto, K.; Fukuyama, S.; Watanabe, S.; Sakabe, S.; Hatta, Y.; Murakami, S.; Shimojima, M.; Horimoto, T.; Kawaoka, Y. A replication-incompetent virus possessing an uncleavable hemagglutinin as an influenza vaccine. *Vaccine* **2012**, *30*, 6027–6033. [CrossRef] [PubMed]
29. World Health Organization (WHO). Recommendations to assure the quality, safety and efficacy of influenza vaccines (human, live attenuated) for intranasal administration. *WHO Tech. Rep. Ser.* **2013**, *977*, 153–227.
30. World Health Organization (WHO). *WHO Meeting on Live Attenuated Influenza Vaccine Effectiveness*; WHO: Geneva, Switzerland, 2016.
31. Rudenko, L.; Yeolekar, L.; Kiseleva, I.; Isakova-Sivak, I. Development and approval of live attenuated influenza vaccines based on Russian master donor viruses: Process challenges and success stories. *Vaccine* **2016**, *34*, 5436–5441. [CrossRef]
32. Cox, N.J.; Kitame, F.; Kendal, A.P.; Maassab, H.F.; Naeve, C. Identification of sequence changes in the cold-adapted, live attenuated influenza vaccine strain, A/Ann Arbor/6/60 (H2N2). *Virology* **1988**, *167*, 554–567. [CrossRef]
33. Snyder, M.H.; Betts, R.F.; DeBorde, D.; Tierney, E.L.; Clements, M.L.; Herrington, D.; Sears, S.D.; Dolin, R.; Maassab, H.F.; Murphy, B.R. Four viral genes independently contribute to attenuation of live influenza A/Ann Arbor/6/60 (H2N2) cold-adapted reassortant virus vaccines. *J. Virol.* **1988**, *62*, 488–495.
34. Isakova-Sivak, I.; Chen, L.M.; Matsuoka, Y.; Voeten, J.T.; Kiseleva, I.; Heldens, J.G.; den Bosch, H.; Klimov, A.; Rudenko, L.; Cox, N.J.; et al. Genetic bases of the temperature-sensitive phenotype of a master donor virus used in live attenuated influenza vaccines: A/Leningrad/134/17/57 (H2N2). *Virology* **2011**, *412*, 297–305. [CrossRef] [PubMed]
35. Cox, A.; Baker, S.F.; Nogales, A.; Martinez-Sobrido, L.; Dewhurst, S. Development of a mouse-adapted live attenuated influenza virus that permits in vivo analysis of enhancements to the safety of live attenuated influenza virus vaccine. *J. Virol.* **2015**, *89*, 3421–3426. [CrossRef] [PubMed]
36. Jin, H.; Zhou, H.; Lu, B.; Kemble, G. Imparting temperature sensitivity and attenuation in ferrets to A/Puerto Rico/8/34 influenza virus by transferring the genetic signature for temperature sensitivity from cold-adapted A/Ann Arbor/6/60. *J. Virol.* **2004**, *78*, 995–998. [CrossRef] [PubMed]
37. Zhou, B.; Li, Y.; Speer, S.D.; Subba, A.; Lin, X.; Wentworth, D.E. Engineering temperature sensitive live attenuated influenza vaccines from emerging viruses. *Vaccine* **2012**, *30*, 3691–3702. [CrossRef] [PubMed]
38. Nogales, A.; Rodriguez, L.; DeDiego, M.L.; Topham, D.J.; Martinez-Sobrido, L. Interplay of PA-X and NS1 Proteins in Replication and Pathogenesis of a Temperature-Sensitive 2009 Pandemic H1N1 Influenza A Virus. *J. Virol.* **2017**, *91*. [CrossRef] [PubMed]
39. Broadbent, A.J.; Santos, C.P.; Godbout, R.A.; Subbarao, K. The temperature-sensitive and attenuation phenotypes conferred by mutations in the influenza virus PB2, PB1, and NP genes are influenced by the species of origin of the PB2 gene in reassortant viruses derived from influenza A/California/07/2009 and A/WSN/33 viruses. *J. Virol.* **2014**, *88*, 12339–12347. [CrossRef] [PubMed]
40. Czako, R.; Vogel, L.; Sutton, T.; Matsuoka, Y.; Krammer, F.; Chen, Z.; Jin, H.; Subbarao, K. H5N2 vaccine viruses on Russian and US live attenuated influenza virus backbones demonstrate similar infectivity, immunogenicity and protection in ferrets. *Vaccine* **2018**, *36*, 1871–1879. [CrossRef]
41. Chen, Z.; Baz, M.; Lu, J.; Paskel, M.; Santos, C.; Subbarao, K.; Jin, H.; Matsuoka, Y. Development of a high-yield live attenuated H7N9 influenza virus vaccine that provides protection against homologous and heterologous H7 wild-type viruses in ferrets. *J. Virol.* **2014**, *88*, 7016–7023. [CrossRef]
42. Peng, Y.; Wang, B.; Talaat, K.; Karron, R.; Powell, T.J.; Zeng, H.; Dong, D.; Luke, C.J.; McMichael, A.; Subbarao, K.; et al. Boosted Influenza-Specific T Cell Responses after H5N1 Pandemic Live Attenuated Influenza Virus Vaccination. *Front. Immunol.* **2015**, *6*, 287. [CrossRef]
43. Martinez-Sobrido, L.; Garcia-Sastre, A. Generation of recombinant influenza virus from plasmid DNA. *J. Vis. Exp.* **2010**. [CrossRef]
44. Grimm, D.; Staeheli, P.; Hufbauer, M.; Koerner, I.; Martinez-Sobrido, L.; Solorzano, A.; Garcia-Sastre, A.; Haller, O.; Kochs, G. Replication fitness determines high virulence of influenza A virus in mice carrying functional Mx1 resistance gene. *Proc. Natl. Acad. Sci. USA* **2007**, *104*, 6806–6811. [CrossRef] [PubMed]

45. Kilbourne, E.D. Future influenza vaccines and the use of genetic recombinants. *Bull. World Health Organ.* **1969**, *41*, 643–645. [PubMed]
46. Nogales, A.; Baker, S.F.; Ortiz-Riano, E.; Dewhurst, S.; Topham, D.J.; Martinez-Sobrido, L. Influenza A Virus Attenuation by Codon Deoptimization of the NS Gene for Vaccine Development. *J. Virol.* **2014**, *88*, 10525–10540. [CrossRef] [PubMed]
47. Schickli, J.H.; Flandorfer, A.; Nakaya, T.; Martinez-Sobrido, L.; Garcia-Sastre, A.; Palese, P. Plasmid-only rescue of influenza A virus vaccine candidates. *Philos. Trans. R. Soc. Lond. B Biol. Sci.* **2001**, *356*, 1965–1973. [CrossRef] [PubMed]
48. National Research Council (U.S.); Committee for the Update of the Guide for the Care and Use of Laboratory Animals; Institute for Laboratory Animal Research (U.S.); National Academies Press (U.S.). *Guide for the Care and Use of Laboratory Animals*, 8th ed.; National Academies Press: Washington, DC, USA, 2011; p. 220.
49. Rodriguez, L.; Nogales, A.; Martinez-Sobrido, L. Influenza A Virus Studies in a Mouse Model of Infection. *J. Vis. Exp.* **2017**. [CrossRef] [PubMed]
50. Reed, L.J.; Muench, H. A simple method of estimating fifty percent endpoints. *Am. J. Hyg.* **1938**, *27*, 493–497.
51. Nogales, A.; DeDiego, M.L.; Topham, D.J.; Martinez-Sobrido, L. Rearrangement of Influenza Virus Spliced Segments for the Development of Live-Attenuated Vaccines. *J. Virol.* **2016**, *90*, 6291–6302. [CrossRef]
52. Reilly, E.C.; Lambert-Emo, K.; Topham, D.J. The Effects of Acute Neutrophil Depletion on Resolution of Acute Influenza Infection, Establishment of Tissue Resident Memory (TRM), and Heterosubtypic Immunity. *PLoS ONE* **2016**, *11*, e0164274. [CrossRef]
53. Belshe, R.; Lee, M.S.; Walker, R.E.; Stoddard, J.; Mendelman, P.M. Safety, immunogenicity and efficacy of intranasal, live attenuated influenza vaccine. *Expert Rev. Vaccines* **2004**, *3*, 643–654. [CrossRef]
54. Belshe, R.B.; Edwards, K.M.; Vesikari, T.; Black, S.V.; Walker, R.E.; Hultquist, M.; Kemble, G.; Connor, E.M.; Group, C.T.C.E.S. Live attenuated versus inactivated influenza vaccine in infants and young children. *N. Engl. J. Med.* **2007**, *356*, 685–696. [CrossRef]
55. Gorse, G.J.; Belshe, R.B.; Munn, N.J. Superiority of live attenuated compared with inactivated influenza A virus vaccines in older, chronically ill adults. *Chest* **1991**, *100*, 977–984. [CrossRef] [PubMed]
56. Rudenko, L.G.; Slepushkin, A.N.; Monto, A.S.; Kendal, A.P.; Grigorieva, E.P.; Burtseva, E.P.; Rekstin, A.R.; Beljaev, A.L.; Bragina, V.E.; Cox, N.; et al. Efficacy of live attenuated and inactivated influenza vaccines in schoolchildren and their unvaccinated contacts in Novgorod, Russia. *J. Infect. Dis.* **1993**, *168*, 881–887. [CrossRef] [PubMed]
57. Slepushkin, A.N.; Obrosova-Serova, N.P.; Burtseva, E.I.; Rudenko, L.G.; Govorkova, E.A.; Vartanyan, R.V.; Verestsinsky, A.I.; Lonskaya, N.I.; Harmon, M.W.; Torok, T.; et al. Comparison of live attenuated and inactivated influenza vaccines in schoolchildren in Russia: I. Safety and efficacy in two Moscow schools, 1987/88. *Vaccine* **1993**, *11*, 323–328. [CrossRef]
58. Lukarska, M.; Fournier, G.; Pflug, A.; Resa-Infante, P.; Reich, S.; Naffakh, N.; Cusack, S. Structural basis of an essential interaction between influenza polymerase and Pol II CTD. *Nature* **2017**, *541*, 117–121. [CrossRef] [PubMed]
59. DeLano, W.L. *The PyMOL Molecular Graphics System*; Schrodinger LLC: New York, NY, USA, 2002.



© 2019 by the authors. Licensee MDPI, Basel, Switzerland. This article is an open access article distributed under the terms and conditions of the Creative Commons Attribution (CC BY) license (http://creativecommons.org/licenses/by/4.0/).

AMERICAN SOCIETY FOR MICROBIOLOGY | Journal of Virology®

VACCINES AND ANTIVIRAL AGENTS

A Live Attenuated Influenza Vaccine Elicits Enhanced Heterologous Protection When the Internal Genes of the Vaccine Are Matched to Those of the Challenge Virus

Andrew Smith,[a,b] Laura Rodriguez,[a]* Maya El Ghouayel,[a] Aitor Nogales,[a] Jeffrey M. Chamberlain,[a] Katherine Sortino,[a] Emma Reilly,[a,c] Changyong Feng,[d] David J. Topham,[a,c] Luis Martínez-Sobrido,[a] Stephen Dewhurst[a]

[a]Department of Microbiology and Immunology, University of Rochester, Rochester, New York, USA
[b]Medical Scientist Training Program, University of Rochester, Rochester, New York, USA
[c]David H. Smith Center for Vaccine Biology and Immunology, University of Rochester, Rochester, New York, USA
[d]Department of Biostatistics and Computational Biology, University of Rochester, Rochester, New York, USA

ABSTRACT Influenza A virus (IAV) causes significant morbidity and mortality, despite the availability of viral vaccines. The efficacy of live attenuated influenza vaccines (LAIVs) has been especially poor in recent years. One potential reason is that the master donor virus (MDV), on which all LAIVs are based, contains either the internal genes of the 1960 A/Ann Arbor/6/60 or the 1957 A/Leningrad/17/57 H2N2 viruses (i.e., they diverge considerably from currently circulating strains). We previously showed that introduction of the temperature-sensitive (*ts*) residue signature of the AA/60 MDV into a 2009 pandemic A/California/04/09 H1N1 virus (Cal/09) results in only 10-fold *in vivo* attenuation in mice. We have previously shown that the *ts* residue signature of the Russian A/Leningrad/17/57 H2N2 LAIV (Len LAIV) more robustly attenuates the prototypical A/Puerto Rico/8/1934 (PR8) H1N1 virus. In this work, we therefore introduced the *ts* signature from Len LAIV into Cal/09. This new Cal/09 LAIV is *ts in vitro*, highly attenuated (*att*) in mice, and protects from a lethal homologous challenge. In addition, when our Cal/09 LAIV with PR8 hemagglutinin and neuraminidase was used to vaccinate mice, it provided enhanced protection against a wild-type Cal/09 challenge relative to a PR8 LAIV with the same attenuating mutations. These findings suggest it may be possible to improve the efficacy of LAIVs by better matching the sequence of the MDV to currently circulating strains.

IMPORTANCE Seasonal influenza infection remains a major cause of disease and death, underscoring the need for improved vaccines. Among current influenza vaccines, the live attenuated influenza vaccine (LAIV) is unique in its ability to elicit T-cell immunity to the conserved internal proteins of the virus. Despite this, LAIV has shown limited efficacy in recent years. One possible reason is that the conserved, internal genes of all current LAIVs derive from virus strains that were isolated between 1957 and 1960 and that, as a result, do not resemble currently circulating influenza viruses. We have therefore developed and tested a new LAIV, based on a currently circulating pandemic strain of influenza. Our results show that this new LAIV elicits improved protective immunity compared to a more conventional LAIV.

KEYWORDS influenza, live attenuated influenza vaccine, LAIV, inactivated influenza vaccine, IIV, master donor virus, MDV, heterologous immunity and protection

Influenza A virus (IAV) infects 50 million people every year in the United States, leading to between 2,000 and 49,000 annual deaths (1, 2). The last influenza season alone saw over 700,000 hospitalizations and more than 80,000 deaths (3, 4). Currently, both an inactivated influenza vaccine (IIV) and a live attenuated influenza vaccine (LAIV)

Citation Smith A, Rodriguez L, El Ghouayel M, Nogales A, Chamberlain JM, Sortino K, Reilly E, Feng C, Topham DJ, Martínez-Sobrido L, Dewhurst S. 2020. A live attenuated influenza vaccine elicits enhanced heterologous protection when the internal genes of the vaccine are matched to those of the challenge virus. J Virol 94:e01065-19. https://doi.org/10.1128/JVI.01065-19.

Editor Mark T. Heise, University of North Carolina at Chapel Hill

Copyright © 2020 Smith et al. This is an open-access article distributed under the terms of the Creative Commons Attribution 4.0 International license.

Address correspondence to Stephen Dewhurst, Stephen_Dewhurst@urmc.rochester.edu.

* Present address: Laura Rodriguez, Agencia Española de Medicamentos y Productos Sanitarios, Madrid, Spain.

Received 25 June 2019
Accepted 8 November 2019
Accepted manuscript posted online 20 November 2019
Published 31 January 2020

Downloaded from http://jvi.asm.org/ on September 28, 2020 by guest

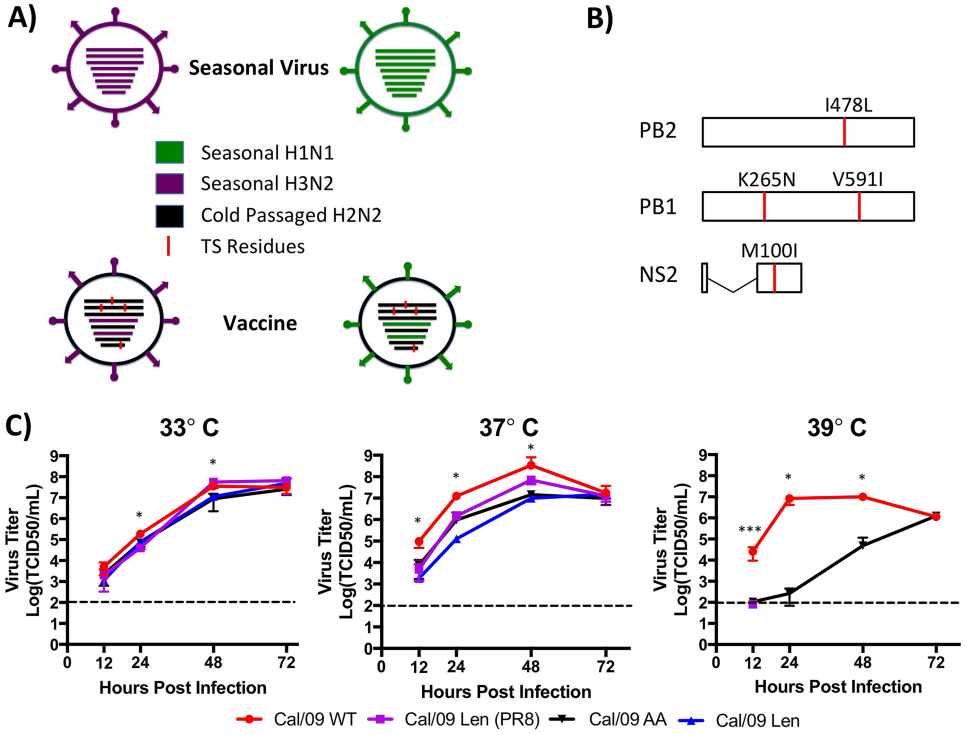


FIG 1 Cal/09 Len has a more robust *ts* phenotype than Cal/09 AA. (A) Schematic representation of currently licensed Russian LAIV. Gene segments from a seasonally circulating strain (green), as well as gene segments from cold-passaged H2N2 virus (black), and *ts* mutations (red) are indicated in the center of virions arranged in order of segment length (PB2, PB1, PA, HA, NP, NA, M, and NS from longest to shortest). Surface antigens from seasonal strains are also denoted on the periphery of virions (green). (B) Schematic representation of viral genes PB2, PB1, and NS. Polymerase subunits PB2 (top) and PB1 (middle), as well as the nuclear export protein NS2 (bottom) of Cal/09 containing the mutations responsible for the temperature-sensitive (*ts*) phenotype of the Leningrad-based LAIV (red), are indicated. (C) Viral growth kinetics. MDCK cells were infected at a low MOI of 0.001 with recombinant Cal/09 WT (red), Cal/09 Len (blue), Cal/09 Len (PR8) (purple), and Cal/09 AA (black) viruses and then incubated at 33°C (left), 37°C (middle), or 39°C (right). Tissue culture supernatants from infected cells were collected at the indicated times postinfection, and viral titers were determined as the $TCID_{50}$/ml. Data represent the means ± the SD of results determined from triplicate wells. Asterisks indicate that the differences in viral titer between experimental groups are statistically significant when data are compared using one-way analysis of variance (ANOVA) with Tukey's multiple-comparison procedure (*, $P < 0.05$; **, $P < 0.01$; ***, $P < 0.001$). Dotted lines indicate the limit of detection (100 $TCID_{50}$/ml). Statistical analyses were performed as follows. (i) For the 33°C panel, the virus titers for Cal/09 WT were statistically significantly different from all other viruses at 24 h ($P < 0.05$). The virus titers for Cal/09 AA and Cal Len (PR8) were statistically significantly different from each other at 48 h ($P < 0.05$). (ii) For the 37°C panel, the virus titers for Cal/09 WT were statistically significantly different from all other viruses at 12 and 24 h ($P < 0.05$). The virus titers for Cal/09 Len and Cal Len (PR8) were statistically significantly from each other at 24 h ($P < 0.05$). The virus titers for Cal/09 WT were statistically significantly different from Cal Len at 48 h ($P < 0.05$). (iii) For the 39°C panel, the virus titers for Cal/09 WT were statistically significantly different from all other viruses at all time points ($P < 0.05$, except for the 12-h time point, where $P < 0.001$).

are licensed and recommended for the prevention of influenza infection in the United States. (5). Seasonal formulations for both IIVs and LAIVs are developed each year to contain the surface antigens, hemagglutinin (HA) and neuraminidase (NA), of the predicted predominantly circulating strains of IAV (6) (Fig. 1A). Nonetheless, vaccine efficacy for seasonal influenza ranges only between 40 and 60%, which is far less than for most other common vaccines (7, 8).

While humoral immunity is the predominant goal of current vaccination strategies, the T-cell response is also important. The presence of influenza subtype-specific CD8 T cells reduces both the severity and duration of IAV infections in humans, and mouse studies have shown an influenza-specific T-cell response is required for viral clearance in the lungs (9, 10). Furthermore, resident memory CD8 T cells (TRM) have been shown to underlie heterosubtypic immunity (i.e., antibody-independent immunity to a novel influenza virus, in mice previously infected with a different strain of influenza [11–13]). CD8 TRM cells generated by a single IAV infection have limited longevity in the lungs

Downloaded from http://jvi.asm.org/ on September 28, 2020 by guest

compared to CD8 TRM cells in other tissues, corresponding to a waning in heterosubtypic immunity (12, 14). However, recent studies have demonstrated that repeated antigen exposure extends the durability of lung CD8 TRM cells and that CD8 TRM cells in the upper respiratory tract not only greatly exceed the longevity of lung CD8 TRM cells but also are independently capable of preventing pulmonary influenza infection (15, 16).

One of the theoretical benefits of LAIVs over IIVs is that LAIVs generate IAV-specific T-cell immunity, owing to the fact that LAIV is a live replicating virus (17–23). However, on average over multiple influenza seasons, there is no superiority of LAIV compared to IIV in adults, even in years when vaccine surface proteins for both LAIV and IIV were poor antigenic matches for the circulating strains, and one might have expected to see at least partial protection by T-cell responses to conserved viral internal proteins (24). One possible reason for this unexpected observation is that the vaccine master donor virus (MDV) that provides the six internal gene segments other than HA and NA has been unchanged since LAIV was developed by cold passaging the H2N2 subtype seasonal strain A/Ann Arbor/6/60 H2N2 (AA/60) in 1960 (25) (Fig. 1A). H2N2 subtype IAV has not circulated as a seasonal strain since it was supplanted by H3N2 subtype IAV in 1968 (26). In addition, the internal, i.e., non-HA and non-NA, gene segments of current seasonal H3N2 and H1N1 strains, which contain the major immunodominant viral T-cell epitopes (27), are significantly different than their H2N2 counterparts at the amino acid level. Thus, generating an LAIV with internal gene segments better matched to currently circulating strains of H1N1 and H3N2 IAV might enhance heterosubtypic immunity and make LAIV a superior vaccine, especially in years with a vaccine/circulating strain antigen mismatch.

Both the AA/60 H2N2 LAIV MDV and the LAIV MDV licensed for use in Russia, A/Leningrad/134/17/57 H2N2 (referred to here as "Len"), possess attenuated (*att*) and temperature sensitive (*ts*) phenotypes (28, 29). They replicate well at permissive upper airway temperatures of 33°C due to their cold-adapted (*ca*) phenotype but not at lower airway temperatures of 37°C (28, 29). The amino acid residues conferring these *ts*, *ca*, and *att* phenotypes have been mapped for both viruses and share no residues in common, although they fall almost exclusively into the genes encoding viral RNA-dependent RNA polymerase (28, 29). Moreover, our group and others have introduced the mutations responsible for the *ts* and *att* phenotype of AA/60 H2N2 into different IAV subtype and strain backgrounds and have shown that they confer a *ts* phenotype in cell culture and an *att* phenotype in animal models (30–37).

The 2009 pandemic isolate, A/California/04/2009 (Cal/09), possesses internal gene segments that are almost identical to currently circulating H1N1 strains. Thus, we hypothesized that creating a LAIV in the genetic background of Cal/09 might be an ideal approach to improving this vaccine and eliciting H1N1 subtype-specific T-cell immunity.

We have shown that the *ts* residue signature of AA/60 attenuates Cal/09 by only 10-fold in mice, which is insufficient to give confidence about the safety of such an LAIV (38). However, we have recently demonstrated that an LAIV in the background of the prototypical A/Puerto Rico/8/1934 (PR8) H1N1 virus with the *ts* residue signature of the Russian Len LAIV is >100-fold more *ts* at 37°C and is >4.5-fold more attenuated in mice than a PR8 LAIV with signature *ts* residues from the American Ann Arbor LAIV (39).

In the present study, we therefore introduced the *ts* residue signature of the Russian Len LAIV into the background of Cal/09 (Cal/09 Len). In contrast to Cal/09 AA, Cal/09 Len is both *ts in vitro* and highly *att* in mice, and these phenotypes are unaffected by differences in viral surface proteins assessed. We also show that this novel Cal/09 Len LAIV generates robust humoral immunity at a safe dose and protects mice from a lethal homologous challenge. Finally, we generated a second control LAIV containing identical surface antigens, but internal gene segments that were mismatched to our challenge virus. The novel Cal/09-based LAIV elicited superior (and protective) T-cell-mediated immunity to a heterologous challenge virus, unlike the control LAIV. These finding suggest the feasibility of improving the efficacy of the currently available U.S.

Downloaded from http://jvi.asm.org/ on September 28, 2020 by guest

(AA) or Russian (Len) LAIVs by better matching the sequence of the MDV to currently circulating viral strains.

RESULTS

Generation and phenotypic characterization of Cal/09 Len LAIV. In order to generate a Cal/09 Len LAIV (Cal/09 Len), we introduced the following four residues previously identified as conferring the *ts* phenotype in the licensed Len MDV into the rescue plasmids of Cal/09: PB2 I478L, PB1 K265N and V591I, and NS2 M100I (Fig. 1B) (29). We next generated two recombinant Cal/09 Len viruses, one with wild-type (WT) Cal/09 HA and NA (Cal/09 Len) and one with the HA and NA of PR8 [Cal/09 Len (PR8)], a much older H1N1 virus strain, containing HA and NA segments that are substantially divergent from the contemporary Cal/09 counterpart. We then performed *in vitro* multicycle viral growth kinetic studies comparing the replication of both Cal/09 Len [Cal/09 Len and Cal/09 Len (PR8)] to WT Cal/09 at 33, 37, and 39°C (Fig. 1C). The previously characterized Cal/09 virus with the mutations responsible for the *ts* phenotype of AA/60 (Cal/09 AA) (38) was also included in the assay.

At 33°C, all LAIV viruses [Cal/09 Len, Cal/09 Len (PR8), and Cal/09 AA) reached viral titers within 1 log (50% tissue culture infective dose [$TCID_{50}$]/ml) of Cal/09 WT at all tested times postinfection (p.i.). At 37°C, Cal/09 WT reached high viral titers similar to those obtained at 33°C, while the three LAIV viruses [Cal/09 Len, Cal/09 Len (PR8), and Cal/09 AA] achieved lower viral titers than at 33°C. Finally, at 39°C, viral replication of Cal/09 WT was similar to that observed at 37°C, while Cal/09 AA viral titers were reduced, as previously described (38). Cal/09 Len (PR8) was only detected at 12 h p.i., and the replication of Cal/09 Len was undetectable at 39°C (Fig. 1C). These results suggest that the amino acid substitutions of the Russian Len MDV LAIV confer a more stringent shutoff temperature to the Cal/09 virus than those of the AA MDV LAIV.

***In vivo* attenuation of Cal/09 Len LAIV.** We next compared the virulence of our Cal/09 LAIV viruses in mice. Groups of mice were inoculated intranasally with increasing $\log_{10}$ doses of the indicated viruses and were monitored for 14 days for weight loss (left panels) and mortality (right panels) (Fig. 2A and B). As expected, based on the difference in *ts* phenotype, Cal/09 Len was more *att* than Cal/09 AA; Cal/09 Len did not induce weight loss below baseline until given at doses of 10^5 and only began causing mortality at doses of 10^6 PFU (Fig. 2A), resulting in a theoretical 50% mouse lethal dose (MLD_{50}) of $>10^6$ PFU. In contrast, Cal/09 AA induced weight loss even at the lowest dose of 10^2, with a calculated MLD_{50} of $\sim10^3$ (Fig. 2B), as we have previously described (38).

To examine *in vivo* viral replication, we determined the virus titers from the lungs and nares of three mice at both day 3 and day 6 p.i. at several doses of Cal/09 Len (10^3, 10^4, and 10^5 PFU) and one comparable dose of Cal/09 AA (10^3 PFU) (Fig. 3A and B). In the lungs, Cal/09 Len titers were undetectable at an inoculation dose of 10^3 PFU, whereas Cal/09 AA at the same dose resulted in high viral lung titers at both day 3 and day 6 p.i. (Fig. 3A). Cal/09 Len titers were detectable at inoculation doses of 10^4 and 10^5 PFU, with the 10^5 dose as high as the Cal/09 AA 10^3 dose titers on both days 3 and 6 p.i. This was notable given that none of the mice given the 10^5 dose of Cal/09 Len died or lost weight below baseline, whereas 50% of the mice given the 10^3 dose of Cal/09 AA died, and the group lost more than 20% of their weight on average (Fig. 2). In the nares, measurable titers of Cal/09 Len were detectable after infection with 10^5 PFU of virus at both days 3 and 6, but Cal/09 AA titers were undetectable at both time points, despite the use of a virus inoculum approaching the MLD_{50} for this virus (10^3 PFU) (Fig. 3B).

Taken together, these findings suggest that Cal/09 Len is more attenuated than Cal/09 AA and that the difference in attenuation cannot entirely be explained by differential viral replication in the lungs. Similar results were also observed, although to a lesser extent, in our previous report using the backbone of PR8 (39).

Cal/09 Len induces robust humoral immunity and is efficacious against homologous challenge a safe dose. To examine humoral immunity elicited by Cal/09 Len, groups of mice were inoculated with increasing $\log_{10}$ doses of virus. Fourteen days later, sera were collected and used to determine hemagglutination inhibition (HAI)

Downloaded from http://jvi.asm.org/ on September 28, 2020 by guest

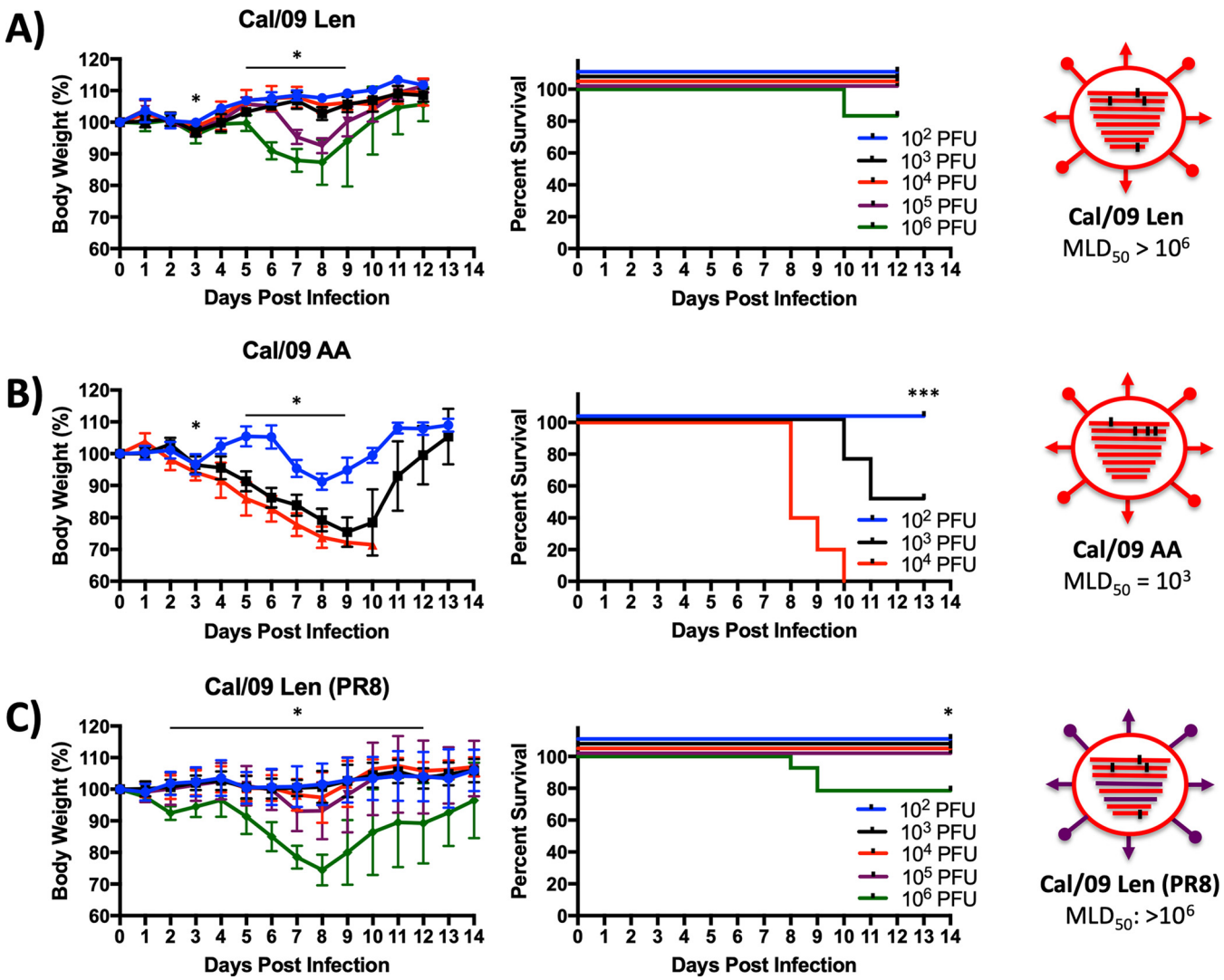


FIG 2 Attenuation of Cal/09Len and Cal/09AA in mice. Mice (see Materials and Methods) were infected i.n. with the indicated PFU of Cal/09 Len ($n = 4$ to 5/group) (A), Cal/09 AA ($n = 4$ to 5/group) (B), and Cal/09 Len (PR8) ($n = 11$/group) (C) recombinant viruses and monitored daily for 2 weeks for body weight (left panels) and survival (right panels). A group size of $n = 10$ to 11 was used for mice infected with Cal/09 Len (PR8) because these same mice were used in the subsequent heterologous challenge experiment (Fig. 5), during which six of the animals were sacrificed before the end of the infection period in order to titer viral replication in lungs and nares. Mice that lost 30% of their initial body weight were sacrificed. Data represent means ± the SD of the results determined for individual mice ($n = 4$ to 11/group). The viral MLD_{50} values were calculated based on the survival data using the method of Reed and Muench. Asterisks indicate that the differences in body weight or survival between experimental groups are statistically significant when data are compared using one-way ANOVA with Tukey's multiple-comparison procedure (body weight) or log-rank test (survival) (*, $P < 0.05$; ***, $P < 0.001$). Schematic representations of the viruses used to inoculate mice (far right) depict Cal/09 Len (A), Cal/09 AA (B), and Cal/09 Len (PR8) (C). Cal/09 gene segments (red) with *ts* amino acid residues (black) and surface antigens from Cal/09 (red) or PR8 (purple) are shown. Statistical analyses were performed. (A, left) Body weights were statistically significantly different from each other at day 3 (a 10^2 PFU inoculum compared to a 10^6 PFU inoculum; $P < 0.05$). Body weights were also statistically significantly from each other at days 5 through 9 (a 10^2 PFU inoculum compared to a 10^6 PFU inoculum; $P < 0.05$). (B, left) Body weights in the experimental groups were statistically significantly different from each other at day 3 (a 10^2 PFU inoculum compared to a 10^6 PFU inoculum; $P < 0.05$). Body weights were also statistically significantly different from each other at day 5 through 9 (a 10^2 PFU inoculum compared to a 10^6 PFU inoculum; $P < 0.05$). (B, right) Survival in the experimental groups was statistically significantly different from each other at day 14 (a 10^2 PFU inoculum compared to all groups; $P < 0.001$). (C, left) Body weights were statistically significantly different from each other at day 2 through 12 (10^2 PFU inoculum compared to 10^6 PFU inoculum; $P < 0.05$). (C, right) Survival in the experimental groups was statistically significantly different from each other at day 14 (10^2 PFU inoculum compared to 10^6 PFU inoculum; $P < 0.05$).

titers against WT Cal/09 virus (Fig. 3C). Most mice vaccinated with doses of 10^3 PFU and all mice inoculated with doses of $\geq 10^4$ PFU of Cal/09 Len had HAI titers of 1:40 or above (Fig. 3C and D), a threshold generally considered to correspond to a 50% protection from IAV infection (40).

We next proceeded with homologous challenge studies using Cal/09 WT. At 21 days after vaccination with Cal/09 Len (and 7 days after bleeding to determine HAI titers), mice were challenged with 100× MLD_{50} of WT Cal/09, and five mice from each group

Downloaded from http://jvi.asm.org/ on September 28, 2020 by guest

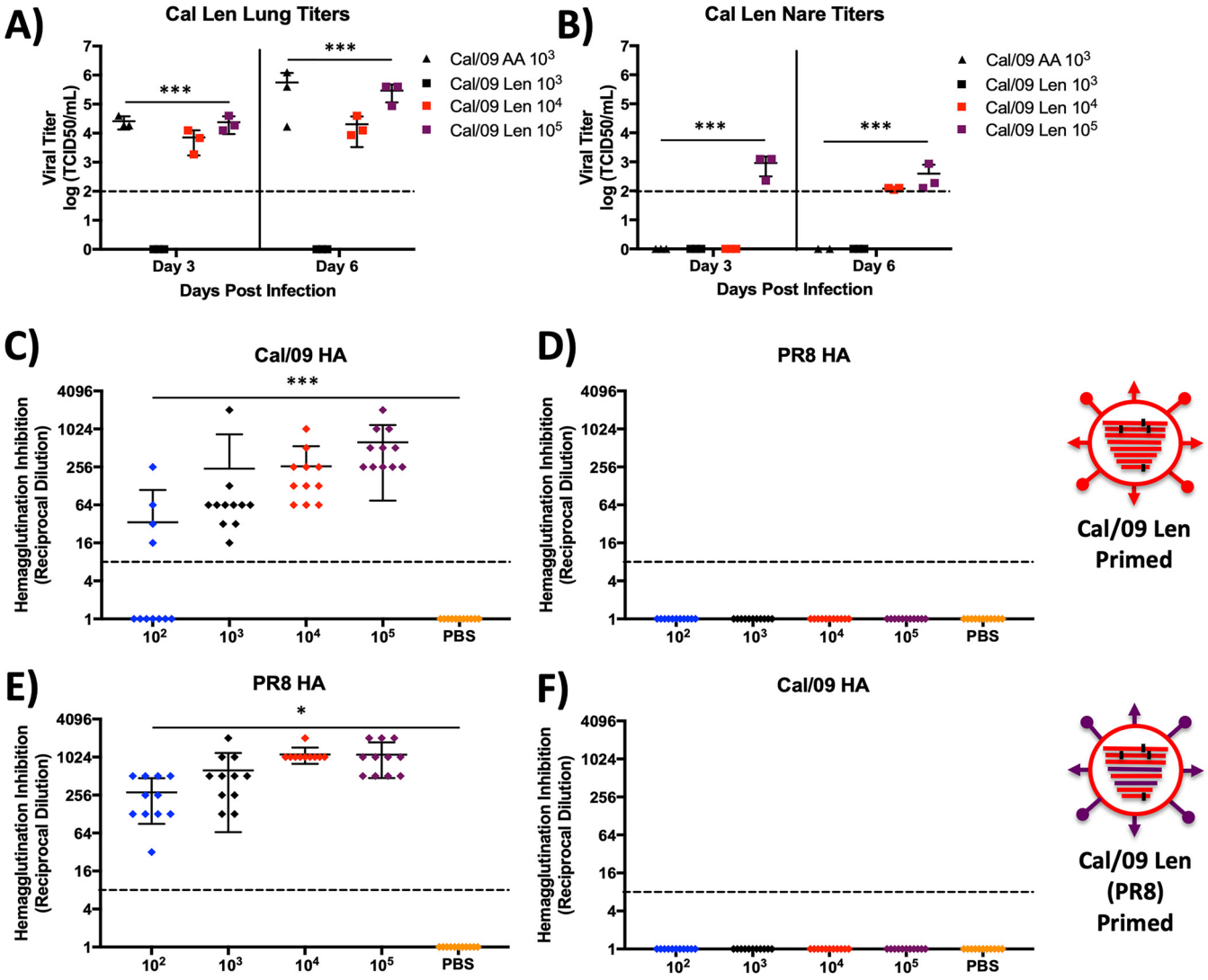


FIG 3 Cal/09 Len replicates at lower levels *in vivo* than Cal/09 AA but still generates a robust antibody response at a safe dose. (A and B) *In vivo* viral replication. Mice ($n = 3$/group) were inoculated i.n. with the indicated doses in PFU of Cal/09 Len or Cal/09 AA. At days 3 and 6 p.i., virus titers ($TCID_{50}$/ml) were determined from total lung (A) and nare (B) homogenates on MDCK cells. The mean virus titers (longest lines) ± the SD (error bars) for each group of mice are indicated. Asterisks indicate that the differences in viral titers between experimental groups are statistically significant when data are compared using one-way ANOVA with Tukey's multiple-comparison procedure (***, $P < 0.001$). Dotted lines indicate the limit of detection (100 $TCID_{50}$/ml). (C to F) Induction of HAI antibodies. Mice ($n = 11$/group) mice were bled at 14 days postpriming with Cal/09 Len (C and D) or Cal/09 Len (PR8) (E and F). Four hemagglutinating units of WT Cal/09 (C and F) or WT PR8 (D and E) were incubated with 2-fold serial dilutions of serum from Cal/09 Len-vaccinated mice (C and D) or CA/09 Len (PR8)-vaccinated mice (E and F) to determine the ability of the sera to prevent virus from binding to RBCs. A 1/8 dilution is the limit of detection in the assay and is indicated by a dotted line. Each symbol represents the value for an individual mouse, and the mean (longest lines) ± the SD for the groups of mice are also shown. Asterisks indicate that the differences in hemagglutination inhibition between experimental groups are statistically significant when data are compared using one-way ANOVA with Tukey's multiple-comparison procedure (***, $P < 0.001$). Statistical analyses were performed. (A) Virus titers in lung tissue were statistically significantly different on day 3 and day 6 for the 10^3 Cal/09 Len inoculum compared to all other groups ($P < 0.001$). (B) Virus titers in the nares were statistically significantly different on day 3 for the 10^5 Cal/09 Len inoculum compared to all other groups ($P < 0.001$). Virus titers in nares were statistically significantly different on day 6 for the 10^4 and 10^5 Cal/09 Len inocula compared to all other groups ($P < 0.001$). (C) HAI titers were statistically significantly different for the 10^3, 10^4, and 10^5 virus inocula compared to the PBS control ($P < 0.001$). (E) HAI titers were statistically significantly different for the 10^2, 10^3, 10^4, and 10^5 virus inocula compared to the PBS control ($P < 0.05$).

were monitored for 14 days for weight loss (left panel) and mortality (right panel) (Fig. 4A). All mice vaccinated with doses of $\geq 10^3$ PFU of Cal/09 Len were completely protected from the lethal challenge, as determined by both weight loss and survival (Fig. 4A). Virus titers in lungs and nares of three mice from each group were also measured at days 3 and 6 postchallenge (Fig. 4B and C); mice immunized with $\geq 10^3$ PFU of Cal/09 Len had undetectable challenge virus titers (Fig. 4B and C). Collectively, these data demonstrate that a well-tolerated safe dose of Cal/09 Len, 10^4 PFU, induces

Downloaded from http://jvi.asm.org/ on September 28, 2020 by guest

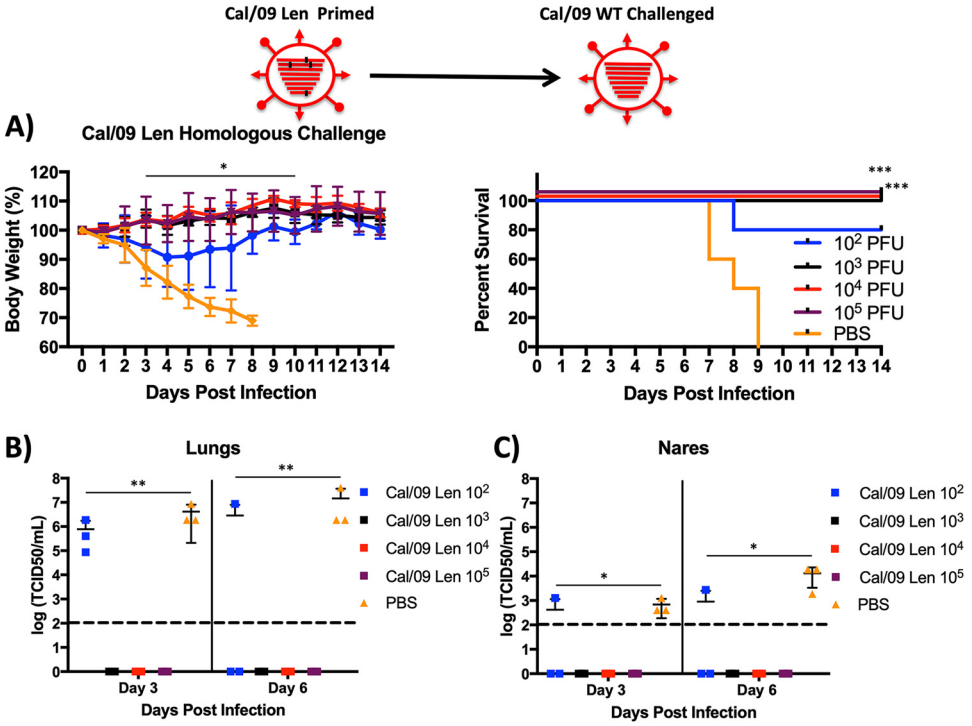


FIG 4 Cal/09 Len protects mice from a lethal homologous challenge at safe doses. Mice ($n = 11$/group) were inoculated i.n. with PBS (orange line) or the indicated doses in PFU of Cal/09 Len (10^2 to 10^5). At 3 weeks postpriming, the mice were challenged i.n. with 100 MLD_{50} of a homologous virus (WT Cal/09). For 2 weeks postchallenge, weight loss (A, left panel) (plotted data represent means ± the SD) and survival (A, right panel) were monitored daily ($n = 5$/group). Mice that lost 30% of their initial body weight were sacrificed. Asterisks indicate that the differences in body weight or survival between experimental groups are statistically significant when data are compared using one-way ANOVA with Tukey's multiple-comparison procedure (body weight) or log-rank test (survival) (*, $P < 0.05$; ***, $P < 0.001$). At days 3 and 6 postchallenge, the challenge virus titer ($TCID_{50}$/ml) was determined from total lung ($n = 3$/group) (B) and nare ($n = 3$) (C) homogenates on MDCK cells. The mean virus titers (longest lines) ± the SD (error bars) for the groups of mice are indicated. Asterisks indicate that the differences in viral titer between experimental groups are statistically significant when data are compared using one-way ANOVA with Tukey's multiple-comparison procedure (**, $P < 0.01$; ***, $P < 0.001$). Dotted lines indicate the limit of detection (100 $TCID_{50}$/ml). Statistical analyses were performed. (A, left) Body weights in the groups were statistically significantly different from each other at day 3 through 10 (10^3, 10^4, and 10^5 PFU inoculum groups compared to the PBS control; $P < 0.05$). (A, right) Survival in the experimental groups was statistically significantly from each other at day 14 (all inoculum groups, compared to the PBS control; $P < 0.001$). (B) Virus titers in lung tissue were significantly different on day 3 and day 6 for the 10^3, 10^4, and 10^5 Cal/09 Len inocula compared to the PBS control group ($P < 0.01$). (C) Virus titers in nares were significantly different on day 3 and day 6 for the 10^3, 10^4, and 10^5 Cal/09 Len inocula compared to the PBS control group ($P < 0.5$).

a robust antibody response capable of completely protecting mice from a lethal homologous viral challenge.

Designing a challenge virus to test the importance of the internal genes of Cal/09 Len in heterologous protection. In order to examine heterologous protection induced by Cal/09 Len, we took advantage of the fact that antibodies elicited against PR8 H1N1 HA and NA fail to inactivate the 2009 pH1N1 Cal/09 virus (41). Thus, we used the Cal/09 Len virus with PR8 HA and NA components [Cal/09 Len (PR8)], immunized mice with this virus, and then challenged them with 100× MLD_{50} of WT Cal/09.

As a prelude to these challenge experiments, we first investigated the *in vivo* attenuation of, and humoral immune response to, Cal/09 Len (PR8) in order to ensure it was similarly attenuated to Cal/09 Len and did not induce antibodies reactive to the Cal/09 HA. To this end, groups of mice were inoculated with increasing $\log_{10}$ doses of Cal/09 Len (PR8) and then tracked for weight loss and death for 14 days (Fig. 2C). Sera were collected from surviving mice at day 14 p.i. and used to determine HAI titers against the WT PR8 and Cal/09 viruses (Fig. 3E and F).

There was little difference in morbidity or mortality caused by infection with Cal/09 Len (PR8) and Cal/09 Len (Fig. 2A and C). Both viruses did not induce significant weight

Downloaded from http://jvi.asm.org/ on September 28, 2020 by guest

loss until given at doses of 10^5 PFU and only began causing mortality at doses of 10^6 PFU, with a theoretical MLD_{50} of $>10^6$ PFU (Fig. 2A and C). Interestingly, at the highest dose level (10^6 PFU) Cal/09 Len (PR8) caused more pronounced weight loss that Cal/09 Len, even though the viruses were indistinguishable in terms of mortality (Fig. 2A and C). Furthermore, mice inoculated with Cal/09 Len (PR8) developed robust HAI titers against WT PR8 but did not develop measurable HAI titers against WT Cal/09 (Fig. 3E and F), suggesting that there would be no PR8-Cal/09 antibody cross-protection, as was expected based on prior findings (41).

Heterologous protection elicited by Cal/09 Len is enhanced when the internal genes of the vaccine match the challenge virus. In order to evaluate the importance of internal genes to heterologous protection elicited by Cal/09 Len, we designed heterologous challenge experiments using Cal/09 WT. As a first step, we compared the protective efficacy of Cal/09 Len (PR8) to a PR8-based LAIV with Len *ts* mutations (PR8/Len) (39). These two H1N1 LAIVs contain identical surface antigens and *ts*-conferring amino acids. However, the internal proteins of PR8 and Cal/09 are significantly divergent, and their differences include immunodominant CD8 T-cell epitopes recognized in C57BL/6 mice (42, 43).

We inoculated groups of mice with increasing nonlethal $\log_{10}$ doses of either Cal/09 Len (PR8) (Fig. 2C) or PR8/Len (a virus that replicates to comparable titers in lungs of C57BL/6 mice [39]). At 21 days postvaccination, mice were challenged with 100× MLD_{50} of WT Cal/09, and then each group was monitored for 13 days for weight loss (left panels) and mortality (right panels) (Fig. 5A and B). All mice vaccinated with10^2 PFU Cal/09 Len (PR8) were completely protected from death following challenge with Cal/09 WT (Fig. 5A), whereas 80% of mice vaccinated with 10^2 PFU of PR8/Len died (Fig. 5B). Furthermore, even at vaccination doses of 10^3 PFU, mice receiving PR8/Len lost approximately 10% more weight on average than did animals immunized with 10^3 PFU of Cal/09 Len (PR8) (Fig. 5A and B).

In order to assess the differential effect of the two LAIVs on replication of challenge virus *in vivo*, the lungs and nares of three mice from each group were harvested on days 3 and 6 postchallenge. Challenge virus was detectable in lungs of mice vaccinated with doses of both 10^2 and 10^3 PFU of PR8/Len, but only in the 10^2 PFU group of Cal/09 Len (PR8)-vaccinated mice (Fig. 5C). Similarly, Cal/09 challenge virus was undetectable in nares of Cal/09 Len (PR8)-vaccinated mice but detectable in the 10^2 PFU group of PR8/Len-vaccinated animals (Fig. 5D) These results demonstrate that a Cal/09-based LAIV (Cal/09 Len) provides enhanced heterosubtypic protection at lower doses against a Cal/09 backbone challenge than did a PR8-based LAIV (PR8 Len) in terms of mortality, weight loss, and *in vivo* replication.

Enhanced heterologous protection conferred by Cal/09 Len is not antibody mediated. As previously discussed, antibodies developed against PR8 H1N1 do not protect against Cal/09 H1N1 (41). To ensure that the enhanced heterologous protection observed with Cal/09 Len was not mediated by antibodies, passive-transfer studies were performed. We inoculated groups of mice with phosphate-buffered saline (PBS) and 21 days later, all mice were challenged with 10× MLD_{50} WT Cal/09 (Fig. 6A). Prior to challenge, mice received sera from animals infected with either Cal/09 Len or Cal/09Len (PR8). As expected, sera transferred from Cal/09 Len-infected mice completely protected mice from an otherwise lethal challenge with Cal/09 WT (Fig. 6A). However, sera from Cal/09 Len (PR8)-infected mice had no such protective effect (Fig. 6A), consistent with the fact that anti-PR8 HA antibodies do not bind Cal/09 HA (Fig. 3E and F) and are not protective against WT Cal/09 infection (41). These results affirmed that the heterologous protection achieved by Cal/09 Len was not mediated by antibodies or serum components.

T-cell responses underlie the enhanced heterologous protection conferred by Cal/09 Len. To determine whether the enhanced heterologous protection observed with Cal/09 Len was mediated by T cells, we performed an additional heterologous challenge experiment in mice depleted of CD4, CD8, or both CD4 and CD8 T cells (Fig. 6B). We inoculated groups of mice with 10^3 PFU of Cal/09 Len (PR8); 21 days later, the

Downloaded from http://jvi.asm.org/ on September 28, 2020 by guest

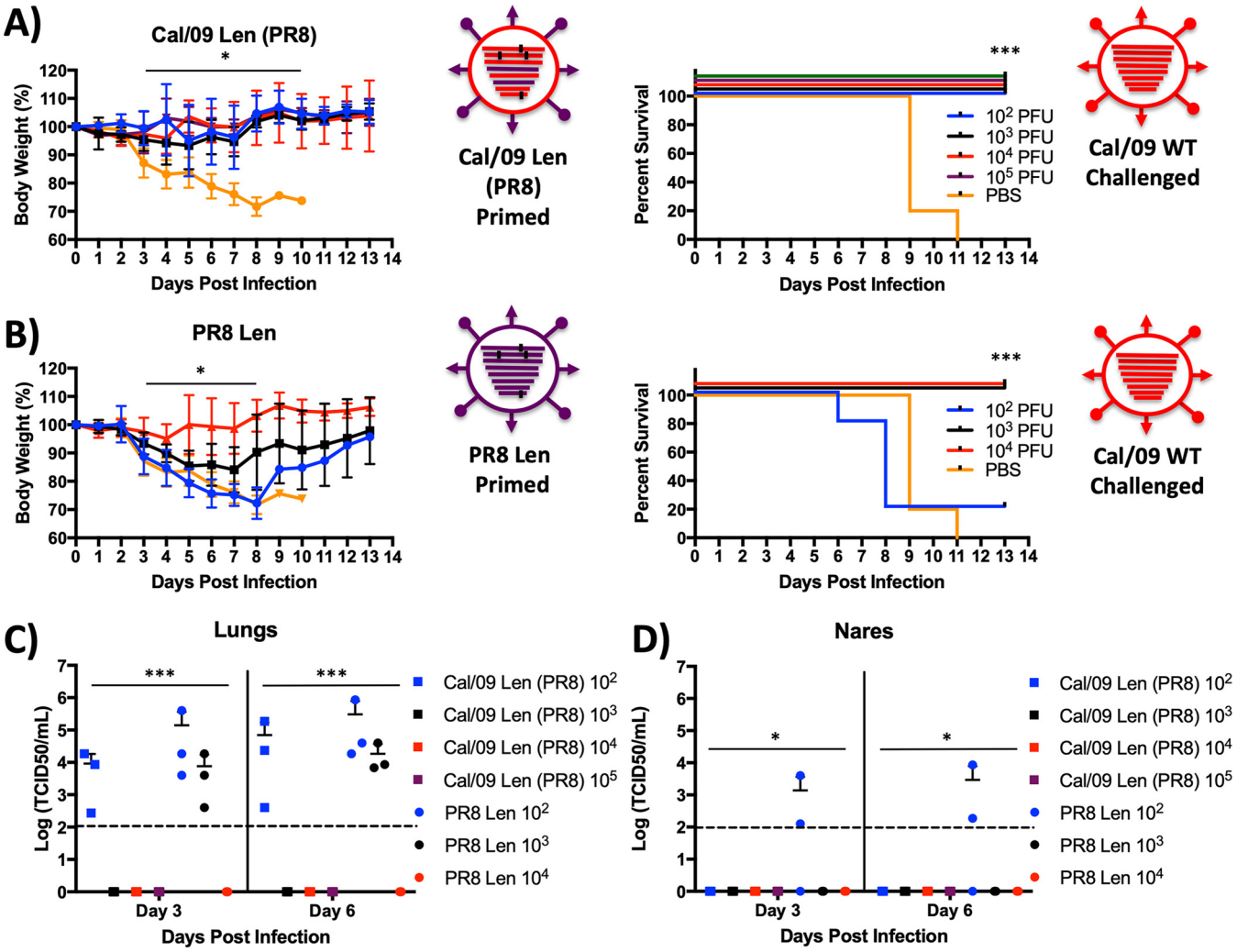


FIG 5 Cal/09 Len confers better protection against a lethal heterologous challenge than PR8/Len. Mice ($n = 11$/group) were inoculated i.n. with PBS (orange line) or with the indicated doses in PFU of Cal/09 Len (PR8) (A) and PR8/Len (B). At 3 weeks postpriming, the mice were challenged i.n. with 100 MLD_{50} of a heterologous virus (WT Cal/09 H1N1). For 2 weeks postchallenge, weight loss (left panels) (plotted data represent means ± the SD) and survival (right panels) were monitored daily ($n = 5$). Mice that lost 30% of their initial body weight were sacrificed. Asterisks indicate that the differences in body weight or survival between experimental groups are statistically significant when data are compared using one-way ANOVA with Tukey's multiple-comparison procedure (body weight) or log-rank test (survival) (*, $P < 0.05$; ***, $P < 0.001$). At days 3 and 6 postchallenge, the challenge virus titer ($TCID_{50}$/ml) was determined from total lung ($n = 3$) (C) and nare ($n = 3$) (D) homogenates on MDCK cells using the method of Reed and Muench. The mean virus titers (longest lines) ± the SD (error bars) for the groups of mice are indicated. Asterisks indicate that the differences in viral titer between experimental groups are statistically significant when data are compared using one-way ANOVA with Tukey's multiple-comparison procedure (*, $P < 0.05$; ***, $P < 0.001$). Dotted lines indicate the limit of detection (100 $TCID_{50}$/ml). Statistical analyses were performed. (A, left) Body weights in the groups were statistically significantly different from each other at days 3 through 10 (10^3, 10^4, and 10^5 PFU inoculum groups compared to the PBS control; $P < 0.05$). (A, right) Survival in the experimental groups was statistically significantly from each other at day 14 (all inoculum groups, compared to the PBS control; $P < 0.001$). (B, left) Body weights in the groups were statistically significantly different from each other at days 3 through 8 (10^4 PFU inoculum group compared to the PBS control; $P < 0.05$). (B, right) Survival in the groups was statistically significantly from each other at day 14 (10^3 and 10^4 inoculum groups, compared to the PBS control; $P < 0.001$). (C, left) Virus titers in lung tissue were statistically significantly different on day 3 and day 6 for the 10^3, 10^4, and 10^5 Cal/09 Len (PR8) and the 10^4 PR8 Len inocula compared to the other groups ($P < 0.001$). (C, right) Virus titers in nares were statistically significantly different on day 3 and day 6 for the 10^2 PR8 Len inoculum compared to other groups ($P < 0.05$).

mice were challenged with 100× MLD_{50} WT Cal/09. Prior to challenge, mice received anti-CD8, anti-CD4, both anti-CD8 and anti-CD4, or control anti-rat IgG monoclonal antibodies. T-cell depletion was verified by flow cytometry (Fig. 7).

Mice depleted of either CD8 or CD4 T cells lost more weight after WT Cal/09 challenge than vaccinated mice treated with the control anti-rat IgG antibody, and one mouse from the CD8- and CD4-depleted group died (Fig. 6B). However, mice depleted of both CD8 and CD4 T cells lost the greatest amount of weight of any vaccinated group and experienced the highest level of mortality (Fig. 6B). Taken together, with the results of our serum transfer experiment, these data suggest that the superior heter-

Downloaded from http://jvi.asm.org/ on September 28, 2020 by guest

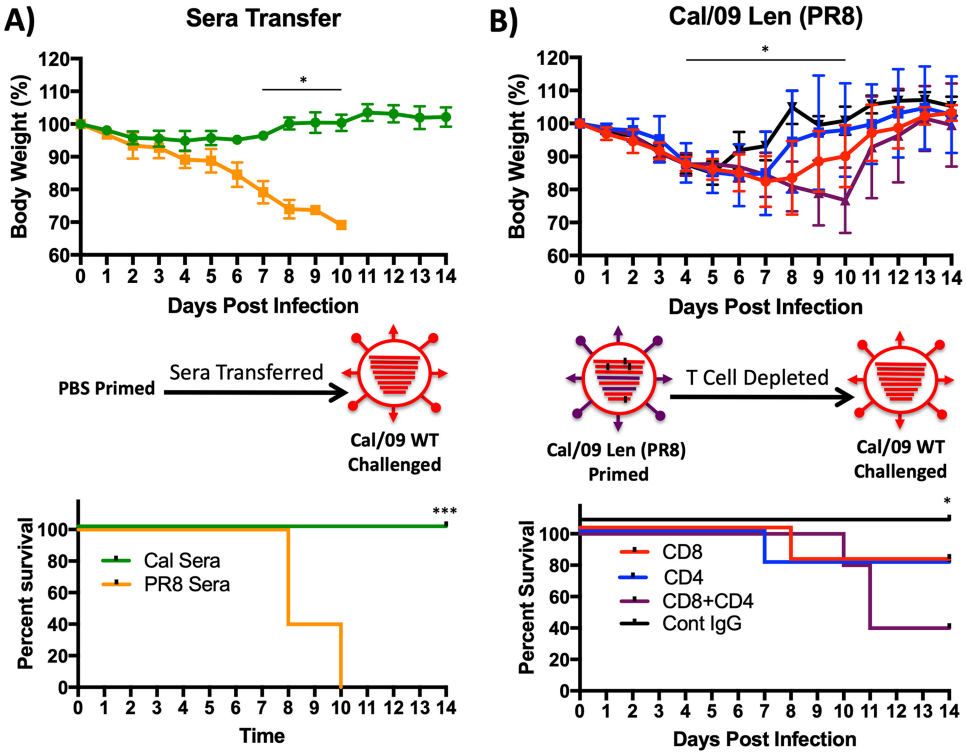


FIG 6 Enhanced heterologous protection conferred by Cal/09 Len is T cell mediated. (A) Cal/09 Len heterologous protection is not antibody mediated. Passive-transfer studies were performed. Mice ($n = 5$/group) were inoculated i.n. with PBS. At 3 weeks postpriming, the mice were challenged i.n. with 10 MLD_{50} of a heterologous virus (WT Cal/09). At 12 h before challenge, PBS mock-vaccinated mice were injected with 400 μl of sera from mice that had been infected with either Cal/09 Len (PR8) (orange) or Cal/09 Len (green). For 2 weeks postchallenge, weight loss (top panel) (plotted data represent means ± the SD) and survival (bottom panel) were monitored daily ($n = 5$/group). Mice that lost 30% of their initial body weight were sacrificed. Asterisks indicate that the differences in body weight or survival between experimental groups are statistically significant when data are compared using one-way ANOVA with Tukey's multiple-comparison procedure (body weight) or log-rank test (survival) (*, $P < 0.05$; ***, $P < 0.001$). (B) Heterologous protection is decreased in T-cell-depleted mice. Mice ($n = 5$/group) were inoculated i.n. with 10^3 PFU of Cal/09 Len (PR8). At 3 weeks postpriming, the mice were challenged i.n. with 100 MLD_{50} of a heterologous virus (WT Cal/09). At 6, 4, and 2 days prechallenge and at day 2 postchallenge, groups of mice ($n = 5$) were injected with 200 μg of αCD8 (red) or αCD4 (blue), a combination of 200 μg of both αCD8 and αCD4 (purple), or a nonmouse control IgG antibody (black). For 2 weeks postchallenge, weight loss (top panel) (plotted data represent means ± the SD) and survival (bottom panel) were monitored daily ($n = 5$/group). Mice that lost 30% of their initial body weight were sacrificed. Asterisks indicate that the differences in body weight or survival between experimental groups are statistically significant when data are compared using one-way ANOVA with Tukey's multiple-comparison procedure (body weight) or log-rank test (survival) (*, $P < 0.05$; ***, $P < 0.001$). Statistical analyses were performed. (A, upper) Body weights in the two groups were statistically significantly different from each other at days 7 through 10 ($P < 0.05$). (A, lower) Survival in the two groups was statistically significantly different from each other at day 14 ($P < 0.001$). (B, upper) Body weights in the groups were statistically significantly different from each other at days 4 through 10 (CD4/CD8-depleted group compared to the control IgG group; $P < 0.05$). (B, lower) Survival in the groups was statistically significantly different at day 14 (CD4/CD8-depleted group compared to the control IgG group; $P < 0.05$).

ologous protection to pH1N1 Cal/09 virus conferred by vaccination with Cal/09 Len (PR8) compared to PR8/Len is due to T-cell immunity.

DISCUSSION

T-cell-mediated immunity is critical for protective immune responses against natural IAV infection (9–16), but current influenza vaccines elicit poor $CD8^+$ T-cell responses (44). Despite this, few studies have attempted to enhance T-cell immunity in an IAV vaccine, and those that have have focused principally on a single protein component of IAV (45–48). Much greater efforts have been directed toward the generation of broadly reactive (and broadly neutralizing) antibody responses (49, 50).

In this work, we addressed the question of whether the effectiveness of LAIV can be enhanced by using an MDV with internal components that better match a potential

Downloaded from http://jvi.asm.org/ on September 28, 2020 by guest

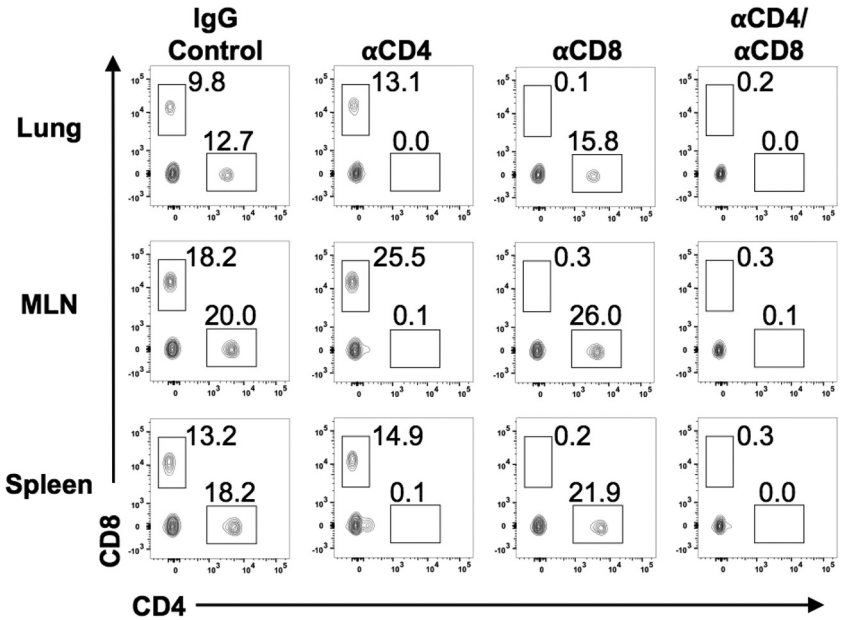


FIG 7 Depleting antibodies effectively diminish T-cell subsets. Cells from lungs (top row), MLNs (middle row), and spleens (bottom row) of mice ($n = 1$ to 2) were examined by flow cytometry for the presence of CD8 and CD4 T cells 1 day after WT Cal/09 challenge (following Cal/09 Len vaccination and the indicated antibody treatment). Representative flow cytometry plots show the percentages of viable lymphoid cells.

challenge virus. In order to do this, it was necessary to select a set of *ts* mutations capable of conferring a live-attenuated phenotype on the desired MDV backbone. Previous studies have shown that the *ts* mutations from AA/60 attenuate PR8 significantly in mice but that they fail to attenuate Cal/09 in mice and also fail to attenuate various strains of avian influenza viruses (AIVs) in birds (30, 38, 51). This lack of attenuation in the genetic background of Cal/09 and AIV can be overcome by the addition of other *ts* or *att* mutations (e.g., PB1 319Q [52]) or by the insertion of an attenuating PB1 HA epitope tag (53, 54). However, it is clear that the AA/60 *ts* mutations alone do not reproducibly confer a *ts* or *att* phenotype across diverse viral genetic backgrounds. In contrast, previous reports suggest that the *ts* mutations from Len LAIV may confer a more robust *ts* or *att* phenotype across a variety of viral backgrounds (29, 39). As a result, we chose to use the Len LAIV mutations to attenuate our MDV in the present study.

The studies described here were intended to address this knowledge gap and to examine the phenotypic characteristics and protective efficacy of an LAIV that was created in the backbone of a contemporary H1N1 IAV, Cal/09.

We show that the *ts* mutations from the Russian Len LAIV confer a much more robust *ts* phenotype and a much greater degree of *in vivo* attenuation in mice (by 3 $\log_{10}$) to Cal/09 than do the mutations from the U.S. AA/60 LAIV (Fig. 1C and 2) (38). Nevertheless, a Cal/09 virus containing the Len *ts* mutations (Cal/09 Len) retains the ability to replicate in the lungs and nares of mice and elicits a robust antibody response, including HAI antibodies (Fig. 3A to C), that results in protection against a lethal homologous challenge (Fig. 4). Most importantly, Cal/09 Len provides superior T-cell-mediated immunity to a heterologous challenge virus, as measured by morbidity, mortality, and a reduction in challenge virus replication, compared to a control LAIV containing internal components mismatched to the challenge virus (Fig. 5); moreover, this protection is T cell mediated (Fig. 6).

It is noteworthy that the currently licensed U.S. LAIV contains the internal gene segments of a H2N2 MDV that circulated almost 60 years ago (AA/60). The use of this H2N2 MDV backbone is unlikely to be optimal in terms of eliciting strong and broadly

Downloaded from http://jvi.asm.org/ on September 28, 2020 by guest

reactive T-cell responses against currently circulating H1N1 or H3N2 IAV strains. Rather, our findings suggest that a better approach may be to reengineer the MDV for future LAIVs, such that it contains the internal segments of a more contemporary virus (e.g., Cal/09).

Currently, two distinct lineages of LAIV MDV are licensed for human use: the U.S. AA MDV and the Russian Len MDV. Only the *ts* and *att* mutations of the Russian Len MDV were able to confer a strong *in vitro ts* phenotype and a strong *in vivo att* phenotype to Cal/09. It is still unclear why the mutations responsible for the *ts* and *att* phenotypes of the U.S. AA MDV failed to strongly attenuate Cal/09.

While we have demonstrated that the Len *ts* mutations make Cal/09 highly attenuated in mice, further studies will be required to determine whether a similar level of attenuation is observed in other animal models (e.g., ferrets), while still permitting virus replication at levels capable of inducing robust humoral and cellular immunity. Future experiments in ferrets would also accomplish two additional goals. First, they would test our hypothesis in an animal model that is more genetically outbred than C57/BL6 mice, which is important in terms of the diversity of the influenza-specific $CD8^+$ T-cell response (55, 56). Second, such studies would allow us determine whether our findings can be reproduced in the background of H3N2 subtype viruses, which do not replicate in mice.

Finally, before our findings could be translated into human clinical studies, it will of course be necessary to test the safety and immunogenicity of Cal/09 Len in humans. However, even if Cal/09 Len should unexpectedly fail to demonstrate acceptable levels of attenuation in humans, there are multiple other methods that can be applied to rationally attenuate a more contemporary IAV and to produce an LAIV that elicits a more effective cellular immune response (57–60). Likewise, a similar approach can be used for the development and implementation of a new MDV LAIV for the treatment of IAV in other animals.

In summary, these studies show that the *ts* mutations of the Russian Len MDV LAIV confer a strong *ts* and *att* phenotype on a currently circulating H1N1 IAV strain (Cal/09). They further demonstrate that a Cal/09-based LAIV MDV based on the Len mutations induces superior heterologous protection to a WT Cal/09 challenge compared to a control LAIV containing mismatched internal genes. These findings may have important implications for the development of improved LAIVs for the prevention of influenza viral infections in humans, including the development of universal vaccines, as well as other animal species.

MATERIALS AND METHODS

Cells and viruses. Human embryonic kidney 293T (HEK293T cells, ATCC CRL-3216) and Madin-Darby canine kidney (MDCK; ATCC CCL-34) cells were grown in Dulbecco modified Eagle medium (DMEM) (Mediatech, Inc.) supplemented with 10% fetal bovine serum (FBS; Atlanta Biologicals) and 1% penicillin (100 U/ml)–streptomycin (100 μg/ml)–2 mM L-glutamine (P-S-G; Mediatech, Inc.) at 37°C in air enriched with 5% CO_2. After viral infections, cells were maintained at 37°C in p.i. media: DMEM supplemented with 0.3% bovine serum albumin (Sigma), 1% P-S-G, and TPCK (tolylsulfonyl phenylalanyl chloromethyl ketone)-treated trypsin (2 μg/ml; Sigma).

Recombinant A/California/4_NYICEE3/2009 H1N1 (Cal/09) wild-type (WT) and Cal/09 containing the temperature-sensitive (*ts*) mutations of the A/Ann Arbor/6/60 H2N2 MDV LAIV (Cal/09 AA) have been previously described (38). The recombinant Cal/09 viruses with the *ts*, *ca*, and *att* mutations from A/Leningrad/134/17/57 and the HA and NA from Cal/09 (Cal/09 Len) or PR8 [Cal/09 Len (PR8)] were generated using plasmid-based reverse genetics techniques at 33°C (61).

The recombinant A/Puerto Rico/8/34 H1N1 (PR8) virus containing the *ts*, *ca*, and *att* mutations of the Russian MDV A/Leningrad/134/17/57 MDV (PR8/Len) was generated using previously described plasmid-based reverse techniques (61) and is described elsewhere (39). All viral rescues, stocks, and titrations were conducted at 33°C (LAIV) or 37°C (WT).

Plasmids. Cal/09 Len PB1, PB2, and NS plasmids were generated by site-directed mutagenesis (Agilent) using the Cal/09 ambisense pDZ WT plasmids with the following mutations: PB1 I487L, PB2 K265N and V591I, and NS2 M100I. All plasmids were confirmed by sequencing (ACGT, Inc.). Primers for the generation of the different plasmid constructs are available upon request.

Rescue of recombinant Cal/09 viruses. Recombinant viruses were rescued as previously described, and propagated in cell lines (61). Cocultures (1:1) of HEK293T and MDCK cells in six-well plates were transiently cotransfected in suspension with 1 μg of each of the ambisense plasmids (pDZ-$PB2_{Cal/09\ Len}$, $PB1_{Cal/09\ Len}$, $PA_{Cal/09\ WT}$, $HA_{Cal/09\ WT}$ or $HA_{PR8\ WT}$, $NP_{Cal/09\ WT}$, $NA_{Cal/09\ WT}$ or $NA_{PR8\ WT}$, $M_{Cal/09\ WT}$, and

Downloaded from http://jvi.asm.org/ on September 28, 2020 by guest

$NS_{Cal/09\ Len}$) using Lipofectamine 2000 (Invitrogen). At 12 h posttransfection, the transfection medium was replaced with p.i. medium. At 72 h posttransfection, tissue culture supernatants (TCS) were collected, clarified, and used to infect fresh MDCK cells (1×10^6 cells/well, six-well plate format). At 3 to 4 days p.i., recombinant viruses were plaque purified and propagated in MDCK cells (59). Stocks were titrated by plaque assay (PFU/ml) on MDCK cells as previously described (38). Virus stocks were confirmed by sequencing (ACGT, Inc.) the PB2, PB1, and NS viral segments using purified total RNA (TRIzol reagent; Invitrogen) from infected MDCK cells (1×10^6 cells/well, six-well plate format).

Virus growth kinetics. To determine virus growth kinetics *in vitro*, triplicate wells of confluent monolayers of MDCK cells (1×10^6 cells/well, six-well plate format) were infected at a multiplicity of infection (MOI) of 0.001. After 1 h at room temperature, the cells were overlaid with p.i. medium and incubated at 33, 37, or 39°C. At the indicated times (12, 24, 48, and 72 h p.i.), TCS were collected, and viral titers were determined by tissue culture infectious dose assay ($TCID_{50}$/ml) as described previously (52). Mean values and standard deviations (SD) were calculated using Prism software.

Mouse experiments. All mouse experiments were conducted using female 6- to 8-week-old C57BL/6 mice purchased from Jackson Laboratories and maintained in the animal care facility at the University of Rochester under specific-pathogen-free conditions. All animal protocols were approved by the University of Rochester Committee of Animal Resources and complied with the recommendations in the *Guide for the Care and Use of Laboratory Animals* of the National Research Council (62). To evaluate the *in vivo* attenuation of the different viruses, mice were anesthetized intraperitoneally (i.p.) with 2,2,2-tribromoethanol (Avertin; 240 mg/kg [body weight]) and then inoculated intranasally (i.n.) with 30 μl of a virus preparation containing the indicated doses of virus diluted in PBS. Mice were monitored daily for 13 to 14 days for morbidity (body weight loss) and mortality (survival). Mice showing a 30% loss in initial body weight were considered to have reached the experimental endpoint and were humanely euthanized. The 50% mouse lethal dose (MLD_{50}) was determined using the method of Reed and Muench (63).

For prime-challenge experiments, mice were rested for 21 days between prime and challenge infections, during which time they were also monitored for weight loss and survival. Virus replication was evaluated by determining viral titers in the lungs and nares of infected mice at 3 and 6 days p.i. To that end, three mice in each group were sacrificed, and the lungs and nares were extracted and homogenized. Virus titers were determined by $TCID_{50}$ as indicated above.

Passive serum transfer. Individual serum pools were obtained from mice 3 weeks after infection with 10^5 PFU of the indicated viruses. Each serum pool was then injected i.p. in a volume of 400 μl into naive mice. At 12 h after injection, mice were anesthetized (i.p.) and challenged (i.n.) with 30 μl of the indicated challenge virus. The mice were monitored daily for weight loss and survival as described above.

T-cell depletion. For T-cell depletion, mice were primed with Cal/09 Len (PR8) and rested for 21 days. Groups of mice were then injected i.p. with 200 μg of an anti-CD4 antibody (clone GK1.5; BioXCell), 200 μg of an anti-CD8 antibody (clone 2.43; BioXCell), 200 μg of both anti-CD4 and anti-CD8 antibodies, or 200 μg of an IgG2b isotype antibody control (clone LTF-2; BioXCell). Antibodies were injected every other day three times before viral infection and once at day 2 after infection with Cal/09 WT. After infection, the mice were monitored daily for weight loss and survival as indicated above.

HAI assays. Mouse sera were treated with receptor-destroying enzyme (RDE; Denka Seiken) and heat inactivated for 30 min at 56°C. Sera were then serially 2-fold diluted (starting dilution, 1:8) in 96-well V-bottom plates and mixed 1:1 with four hemagglutinating units of either Cal/09 WT or PR8 WT virus for 60 min at room temperature. HAI titers were determined by adding 0.5% turkey red blood cells (RBCs) to the virus-antibody mixtures for 30 min on ice, as previously described (59).

Flow cytometry. On day 8 after infection with Cal/09 WT, lungs, mesenteric lymph nodes (MLNs), and spleens were collected and processed to obtain cellular preparations. Lungs were perfused with PBS, surgically removed, and dissociated in C tubes by the GentleMACS (Miltenyi Biotec) using the Lung01 program. Samples were then incubated in 5 ml (2 μg/ml) of collagenase II in RPMI medium containing 8% FBS for 30 min at 37°C with gentle shaking. After digestion, the samples were further dissociated using the Heart01 program. Cell suspensions were filtered through 100-μm filters prior to 75:40 Percoll (GE Healthcare) discontinuous gradient separation. The top layer, containing fat and other debris, was removed by aspiration. The cell layer was harvested and washed prior to counting and staining. Single-cell suspensions were prepared from collected spleens and MLNs by disruption in RPMI plus 8% FBS. Counting was achieved through trypan blue exclusion on a hemocytometer.

To prepare samples for flow cytometry analysis, single-cell suspensions in PBS were stained with purified CD16/32 (clone 2.4G2), the fixable viability dye Live Dead Aqua (Invitrogen), and the following antibodies: TCRβ-Brilliant Violet 786 (clone H57-597), CD8α-PE (clone 53-6.7), and CD4-APC (clone RM4-5). All antibodies were obtained from BD Biosciences or BioLegend. Cells were analyzed by an LSRII (BD Biosciences) in the University of Rochester Flow Cytometry core facility and analyzed by using FlowJo software (Tree Star).

ACKNOWLEDGMENTS

We are grateful for funding support from DOD W81XWH-17-1-0168 (to S.D.), DOD W81XWH-18-1-0460 to (L.M.S.), and NIH T32GM068411 and T32GM007356 (to A.S.), as well as the New York Influenza Center of Excellence, a member of the National Institute of Allergy and Infectious Diseases (NIAID), National Institutes of Health (NIH), Department of Health and Human Services, Centers of Excellence for Influenza Research and Surveillance (CEIRS) contract no. HHSN272201400005C.

Downloaded from http://jvi.asm.org/ on September 28, 2020 by guest

REFERENCES

1. Centers for Disease Control and Prevention. 2010. Estimates of deaths associated with seasonal influenza—United States, 1976–2007. MMWR Morb Mortal Wkly Rep 59:1057–1062.
2. Mullooly JP, Bridges CB, Thompson WW, Chen J, Weintraub E, Jackson LA, Black S, Shay DK. 2007. Influenza- and RSV-associated hospitalizations among adults. Vaccine 25:846–855. https://doi.org/10.1016/j.vaccine.2006.09.041.
3. Centers for Disease Control and Prevention. 2018. Summary of the 2017–2018 influenza season. Centers for Disease Control and Prevention, Atlanta, GA. https://www.cdc.gov/flu/about/season/flu-season-2017-2018.htm. Accessed 9 February 2019.
4. Centers for Disease Control and Prevention. 2018. Estimated influenza illnesses, medical visits, hospitalizations, and deaths in the United States: 2017–2018 influenza season. Centers for Disease Control and Prevention, Atlanta, GA. https://www.cdc.gov/flu/about/burden/estimates.htm. Accessed 9 February 2019.
5. Centers for Disease Control and Prevention. 2018. June 2018 ACIP minutes. Centers for Disease Control and Prevention, Atlanta, GA. https://www.cdc.gov/vaccines/acip/meetings/index.html. Accessed 9 February 2019.
6. World Health Organization. 2016. Consultation and information meeting on the composition of influenza virus vaccines for use in the 2017 southern hemisphere influenza season. World Health Organization, Geneva, Switzerland. https://www.who.int/influenza/vaccines/virus/recommendations/consultation201609/en/. Accessed 9 February 2019.
7. Centers for Disease Control and Prevention. 2018. Influenza vaccine effectiveness. Centers for Disease Control and Prevention, Atlanta, GA. https://www.cdc.gov/flu/about/qa/vaccineeffect.htm. Accessed 9 February 2019.
8. Centers for Disease Control and Prevention. 2018. GRADE evidence tables: recommendations in MMWR. Centers for Disease Control and Prevention, Atlanta, GA. https://www.cdc.gov/vaccines/acip/recs/grade/table-refs.html. Accessed 9 February 2019.
9. Dutta A, Huang CT, Lin CY, Chen TC, Lin YC, Chang CS, He YC. 2016. Sterilizing immunity to influenza virus infection requires local antigen-specific T cell response in the lungs. Sci Rep 6:32973. https://doi.org/10.1038/srep32973.
10. Sridhar S, Begom S, Bermingham A, Hoschler K, Adamson W, Carman W, Bean T, Barclay W, Deeks JJ, Lalvani A. 2013. Cellular immune correlates of protection against symptomatic pandemic influenza. Nat Med 19:1305–1312. https://doi.org/10.1038/nm.3350.
11. Gilchuk P, Hill TM, Guy C, McMaster SR, Boyd KL, Rabacal WA, Lu P, Shyr Y, Kohlmeier JE, Sebzda E, Green DR, Joyce S. 2016. A distinct lung-interstitium-resident memory CD8$^+$ T cell subset confers enhanced protection to lower respiratory tract infection. Cell Rep 16:1800–1809. https://doi.org/10.1016/j.celrep.2016.07.037.
12. Wu T, Hu Y, Lee YT, Bouchard KR, Benechet A, Khanna K, Cauley LS. 2014. Lung-resident memory CD8 T cells (TRM) are indispensable for optimal cross-protection against pulmonary virus infection. J Leukoc Biol 95:215–224. https://doi.org/10.1189/jlb.0313180.
13. Zens KD, Chen JK, Farber DL. 2016. Vaccine-generated lung tissue-resident memory T cells provide heterosubtypic protection to influenza infection. JCI Insight 1:85832.
14. Slutter B, Van Braeckel-Budimir N, Abboud G, Varga SM, Salek-Ardakani S, Harty JT. 2017. Dynamics of influenza-induced lung-resident memory T cells underlie waning heterosubtypic immunity. Sci Immunol 2:eaag2031. https://doi.org/10.1126/sciimmunol.aag2031.
15. Pizzolla A, Nguyen THO, Smith JM, Brooks AG, Kedzieska K, Heath WR, Reading PC, Wakim LM. 2017. Resident memory CD8$^+$ T cells in the upper respiratory tract prevent pulmonary influenza virus infection. Sci Immunol 2:eaam6970. https://doi.org/10.1126/sciimmunol.aam6970.
16. Van Braeckel-Budimir N, Varga SM, Badovinac VP, Harty JT. 2018. Repeated antigen exposure extends the durability of influenza-specific lung-resident memory CD8$^+$ T cells and heterosubtypic immunity. Cell Rep 24:3374–3382. https://doi.org/10.1016/j.celrep.2018.08.073.
17. Amorij JP, Hinrichs W, Frijlink HW, Wilschut JC, Huckriede A. 2010. Needle-free influenza vaccination. Lancet Infect Dis 10:699–711. https://doi.org/10.1016/S1473-3099(10)70157-2.
18. Belshe RB, Gruber WC, Mendelman PM, Cho I, Reisinger K, Block SL, Wittes J, Iacuzio D, Piedra P, Treanor J, King J, Kotloff K, Bernstein DI, Hayden FG, Zangwill K, Yan L, Wolff M. 2000. Efficacy of vaccination with live attenuated, cold-adapted, trivalent, intranasal influenza virus vaccine against a variant (A/Sydney) not contained in the vaccine. J Pediatr 136:168–175. https://doi.org/10.1016/S0022-3476(00)70097-7.
19. Belshe RB, Gruber WC, Mendelman PM, Mehta HB, Mahmood K, Reisinger K, Treanor J, Zangwill K, Hayden FG, Bernstein DI, Kotloff K, King J, Piedra PA, Block SL, Yan L, Wolff M. 2000. Correlates of immune protection induced by live, attenuated, cold-adapted, trivalent, intranasal influenza virus vaccine. J Infect Dis 181:1133–1137. https://doi.org/10.1086/315323.
20. Cox RJ, Brokstad KA, Ogra P. 2004. Influenza virus: immunity and vaccination strategies. Comparison of the immune response to inactivated and live, attenuated influenza vaccines. Scand J Immunol 59:1–15. https://doi.org/10.1111/j.0300-9475.2004.01382.x.
21. Forrest BD, Pride MW, Dunning AJ, Capeding MR, Chotpitayasunondh T, Tam JS, Rappaport R, Eldridge JH, Gruber WC. 2008. Correlation of cellular immune responses with protection against culture-confirmed influenza virus in young children. Clin Vaccine Immunol 15:1042–1053. https://doi.org/10.1128/CVI.00397-07.
22. He XS, Holmes TH, Zhang C, Mahmood K, Kemble GW, Lewis DB, Dekker CL, Greenberg HB, Arvin AM. 2006. Cellular immune responses in children and adults receiving inactivated or live attenuated influenza vaccines. J Virol 80:11756–11766. https://doi.org/10.1128/JVI.01460-06.
23. Hoft DF, Babusis E, Worku S, Spencer CT, Lottenbach K, Truscott SM, Abate G, Sakala IG, Edwards KM, Creech CB, Gerber MA, Bernstein DI, Newman F, Graham I, Anderson EL, Belshe RB. 2011. Live and inactivated influenza vaccines induce similar humoral responses, but only live vaccines induce diverse T-cell responses in young children. J Infect Dis 204:845–853. https://doi.org/10.1093/infdis/jir436.
24. Centers for Disease Control and Prevention. 2019. Advisory Committee on Immunization Practices meeting minutes archive. Centers for Disease Control and Prevention, Atlanta, GA. https://www.cdc.gov/vaccines/acip/meetings/minutes-archive.html. Accessed 9 February 2019.
25. Rudenko LG, Lonskaya NI, Klimov AI, Vasilieva RI, Ramirez A. 1996. Clinical and epidemiological evaluation of a live, cold-adapted influenza vaccine for 3–14-year-olds. Bull World Health Organ 74:77–84.
26. Palese P. 2004. Influenza: old and new threats. Nat Med 10:S82–S87. https://doi.org/10.1038/nm1141.
27. Wu C, Zanker D, Valkenburg S, Tan B, Kedzierska K, Zou QM, Doherty PC, Chen W. 2011. Systematic identification of immunodominant CD8$^+$ T-cell responses to influenza A virus in HLA-A2 individuals. Proc Natl Acad Sci U S A 108:9178–9183. https://doi.org/10.1073/pnas.1105624108.
28. Chan W, Zhou H, Kemble G, Jin H. 2008. The cold adapted and temperature sensitive influenza A/Ann Arbor/6/60 virus, the master donor virus for live attenuated influenza vaccines, has multiple defects in replication at the restrictive temperature. Virology 380:304–311. https://doi.org/10.1016/j.virol.2008.07.027.
29. Isakova-Sivak I, Chen LM, Matsuoka Y, Voeten JT, Kiseleva I, Heldens JG, den Bosch H, Klimov A, Rudenko L, Cox NJ, Donis RO. 2011. Genetic bases of the temperature-sensitive phenotype of a master donor virus used in live attenuated influenza vaccines: A/Leningrad/134/17/57 (H2N2). Virology 412:297–305. https://doi.org/10.1016/j.virol.2011.01.004.
30. Cox A, Baker SF, Nogales A, Martinez-Sobrido L, Dewhurst S. 2015. Development of a mouse-adapted live attenuated influenza virus that permits *in vivo* analysis of enhancements to the safety of live attenuated influenza virus vaccine. J Virol 89:3421–3426. https://doi.org/10.1128/JVI.02636-14.
31. Jin H, Zhou H, Lu B, Kemble G. 2004. Imparting temperature sensitivity and attenuation in ferrets to A/Puerto Rico/8/34 influenza virus by transferring the genetic signature for temperature sensitivity from cold-adapted A/Ann Arbor/6/60. J Virol 78:995–998. https://doi.org/10.1128/jvi.78.2.995-998.2004.
32. Suguitan AL, Jr, McAuliffe J, Mills KL, Jin H, Duke G, Lu B, Luke CJ, Murphy B, Swayne DE, Kemble G, Subbarao K. 2006. Live, attenuated influenza A H5N1 candidate vaccines provide broad cross-protection in mice and ferrets. PLoS Med 3:e360. https://doi.org/10.1371/journal.pmed.0030360.
33. Zhou B, Li Y, Speer SD, Subba A, Lin X, Wentworth DE. 2012. Engineering temperature-sensitive live attenuated influenza vaccines from emerging

Downloaded from http://jvi.asm.org/ on September 28, 2020 by guest

viruses. Vaccine 30:3691–3702. https://doi.org/10.1016/j.vaccine.2012.03.025.
34. Nogales A, Rodriguez L, Chauche C, Huang K, Reilly EC, Topham DJ, Murcia PR, Parrish CR, Martinez-Sobrido L. 2017. Temperature-sensitive live-attenuated canine influenza virus H3N8 vaccine. J Virol 91:e02211-16.
35. Rodriguez L, Nogales A, Murcia PR, Parrish CR, Martinez-Sobrido L. 2017. A bivalent live-attenuated influenza vaccine for the control and prevention of H3N8 and H3N2 canine influenza viruses. Vaccine 35:4374–4381. https://doi.org/10.1016/j.vaccine.2017.06.060.
36. Rodriguez L, Nogales A, Reilly EC, Topham DJ, Murcia PR, Parrish CR, Martinez Sobrido L. 2017. A live-attenuated influenza vaccine for H3N2 canine influenza virus. Virology 504:96–106. https://doi.org/10.1016/j.virol.2017.01.020.
37. Rodriguez L, Reedy S, Nogales A, Murcia PR, Chambers TM, Martinez-Sobrido L. 2018. Development of a novel equine influenza virus live-attenuated vaccine. Virology 516:76–85. https://doi.org/10.1016/j.virol.2018.01.005.
38. Nogales A, Rodriguez L, DeDiego ML, Topham DJ, Martinez-Sobrido L. 2017. Interplay of PA-X and NS1 proteins in replication and pathogenesis of a temperature-sensitive 2009 pandemic H1N1 influenza A virus. J Virol 91:e00720-17.
39. Rodriguez L, Blanco-Lobo P, Reilly EC, Maehigashi T, Nogales A, Smith A, Topham DJ, Dewhurst S, Kim B, Martínez-Sobrido L. 2019. Comparative study of the temperature sensitive, cold adapted and attenuated mutations present in the master donor viruses of the two commercial human live attenuated influenza vaccines. Viruses 11:928. https://doi.org/10.3390/v11100928.
40. Hobson D, Curry RL, Beare AS, Ward-Gardner A. 1972. The role of serum haemagglutination-inhibiting antibody in protection against challenge infection with influenza A2 and B viruses. J Hyg (Lond) 70:767–777. https://doi.org/10.1017/s0022172400022610.
41. Guo H, Santiago F, Lambert K, Takimoto T, Topham DJ. 2011. T cell-mediated protection against lethal 2009 pandemic H1N1 influenza virus infection in a mouse model. J Virol 85:448–455. https://doi.org/10.1128/JVI.01812-10.
42. Belz GT, Xie W, Altman JD, Doherty PC. 2000. A previously unrecognized H-2D(b)-restricted peptide prominent in the primary influenza A virus-specific CD8$^+$ T-cell response is much less apparent following secondary challenge. J Virol 74:3486–3493. https://doi.org/10.1128/jvi.74.8.3486-3493.2000.
43. Townsend AR, Rothbard J, Gotch FM, Bahadur G, Wraith D, McMichael AJ. 1986. The epitopes of influenza nucleoprotein recognized by cytotoxic T lymphocytes can be defined with short synthetic peptides. Cell 44:959–968. https://doi.org/10.1016/0092-8674(86)90019-x.
44. Erbelding EJ, Post DJ, Stemmy EJ, Roberts PC, Augustine AD, Ferguson S, Paules CI, Graham BS, Fauci AS. 2018. A universal influenza vaccine: the strategic plan for the National Institute of Allergy and Infectious Diseases. J Infect Dis 218:347–354. https://doi.org/10.1093/infdis/jiy103.
45. Korenkov D, Nguyen THO, Isakova-Sivak I, Smolonogina T, Brown LE, Kedzierska K, Rudenko L. 2018. Live attenuated influenza vaccines engineered to express the nucleoprotein of a recent isolate stimulate human influenza CD8$^+$ T cells more relevant to current infections. Hum Vaccin Immunother 14:941–946. https://doi.org/10.1080/21645515.2017.1417713.
46. Korenkov DA, Laurie KL, Reading PC, Carolan LA, Chan KF, Isakova S, II, Smolonogina TA, Subbarao K, Barr IG, Villanueva J, Shcherbik S, Bousse T, Rudenko LG. 2018. Safety, immunogenicity and protection of A(H3N2) live attenuated influenza vaccines containing wild-type nucleoprotein in a ferret model. Infect Genet Evol 64:95–104. https://doi.org/10.1016/j.meegid.2018.06.019.
47. Pérez-Girón JV, Belicha-Villanueva A, Hassan E, Gómez-Medina S, Cruz JLG, Lüdtke A, Ruibal P, Albrecht RA, García-Sastre A, Muñoz-Fontela C. 2014. Mucosal polyinosinic-polycytidylic acid improves protection elicited by replicating influenza vaccines via enhanced dendritic cell function and T cell immunity. J Immunol 193:1324–1332. https://doi.org/10.4049/jimmunol.1400222.
48. Zhang J, Fan HY, Zhang Z, Zhang J, Zhang J, Huang JN, Ye Y, Liao M. 2016. Recombinant baculovirus vaccine containing multiple M2e and adjuvant LTB induces T cell dependent, cross-clade protection against H5N1 influenza virus in mice. Vaccine 34:622–629. https://doi.org/10.1016/j.vaccine.2015.12.039.
49. Ekiert DC, Kashyap AK, Steel J, Rubrum A, Bhabha G, Khayat R, Lee JH, Dillon MA, O'Neil RE, Faynboym AM, Horowitz M, Horowitz L, Ward AB, Palese P, Webby R, Lerner RA, Bhatt RR, Wilson IA. 2012. Cross-neutralization of influenza A viruses mediated by a single antibody loop. Nature 489:526–532. https://doi.org/10.1038/nature11414.
50. Krammer F, Palese P. 2015. Advances in the development of influenza virus vaccines. Nat Rev Drug Discov 14:167–182. https://doi.org/10.1038/nrd4529.
51. Song H, Nieto GR, Perez DR. 2007. A new generation of modified live-attenuated avian influenza viruses using a two-strategy combination as potential vaccine candidates. J Virol 81:9238–9248. https://doi.org/10.1128/JVI.00893-07.
52. Cox A, Dewhurst S. 2015. A single mutation at PB1 residue 319 dramatically increases the safety of PR8 live attenuated influenza vaccine in a murine model without compromising vaccine efficacy. J Virol 90:2702–2705. https://doi.org/10.1128/JVI.02723-15.
53. Pena L, Vincent AL, Ye J, Ciacci-Zanella JR, Angel M, Lorusso A, Gauger PC, Janke BH, Loving CL, Perez DR. 2011. Modifications in the polymerase genes of a swine-like triple-reassortant influenza virus to generate live attenuated vaccines against 2009 pandemic H1N1 viruses. J Virol 85:456–469. https://doi.org/10.1128/JVI.01503-10.
54. Solorzano A, Ye J, Perez DR. 2010. Alternative live-attenuated influenza vaccines based on modifications in the polymerase genes protect against epidemic and pandemic flu. J Virol 84:4587–4596. https://doi.org/10.1128/JVI.00101-10.
55. Gustin KM, Belser JA, Katz JM, Tumpey TM, Maines TR. 2012. Innovations in modeling influenza virus infections in the laboratory. Trends Microbiol 20:275–281. https://doi.org/10.1016/j.tim.2012.03.006.
56. Thangavel RR, Bouvier NM. 2014. Animal models for influenza virus pathogenesis, transmission, and immunology. J Immunol Methods 410:60–79. https://doi.org/10.1016/j.jim.2014.03.023.
57. Du Y, Xin L, Shi Y, Zhang TH, Wu NC, Dai L, Gong D, Brar G, Shu S, Luo J, Reiley W, Tseng YW, Bai H, Wu TT, Wang J, Shu Y, Sun R. 2018. Genome-wide identification of interferon-sensitive mutations enables influenza vaccine design. Science 359:290–296. https://doi.org/10.1126/science.aan8806.
58. Moratorio G, Henningsson R, Barbezange C, Carrau L, Borderia AV, Blanc H, Beaucourt S, Poirier EZ, Vallet T, Boussier J, Mounce BC, Fontes M, Vignuzzi M. 2017. Attenuation of RNA viruses by redirecting their evolution in sequence space. Nat Microbiol 2:17088. https://doi.org/10.1038/nmicrobiol.2017.88.
59. Nogales A, Baker SF, Ortiz-Riaño E, Dewhurst S, Topham DJ, Martínez-Sobrido L. 2014. Influenza A virus attenuation by codon deoptimization of the NS gene for vaccine development. J Virol 88:10525–10540. https://doi.org/10.1128/JVI.01565-14.
60. Nogales A, DeDiego ML, Topham DJ, Martinez-Sobrido L. 2016. Rearrangement of influenza virus spliced segments for the development of live-attenuated vaccines. J Virol 90:6291–6302. https://doi.org/10.1128/JVI.00410-16.
61. Martinez-Sobrido L, Garcia-Sastre A. 2010. Generation of recombinant influenza virus from plasmid DNA. J Vis Exp 2010:2057. https://doi.org/10.3791/2057.
62. National Research Council. 2011. Guide for the care and use of laboratory animals, 8th ed. National Academies Press, Washington, DC.
63. Reed LJ, Muench H. 1938. A simple method of estimating fifty percent endpoints. Am J Hyg 27:493–497. https://doi.org/10.1093/oxfordjournals.aje.a118408.

Downloaded from http://jvi.asm.org/ on September 28, 2020 by guest